Development of an *in vitro* 3D microfluidic system for maintaining PHH over long time and its possible use for drug testing

Inaugural-Dissertation
zur Erlangung des Doktorgrades
der Humanwissenschaften

der Medizinische Fakultät
der Eberhard Karls Universität
zu Tübingen

vorgelegt von
Juan José Martínez Sánchez
aus
Elda, Alicante, Spanien
2015

Dekan: Professor Dr. I. B. Autenrieth

1. Berichterstatter: Professor Dr. A. K. Nüssler

2. Berichterstatter: Professor Dr. Dr. P. Ruth

Table of Contents

List of Figures

List of Tables

List of Abbreviations

Abbreviations	Description
4-MU	4-Methylumbelliferone
5-CFDA	5,6-Carboxyfluorescein Diacetate
5-CFSE	5-Carboxyfluorescein succinimidyl ester
7-EC	7-Ethoxycoumarin
7-ER	7-Ethoxyresorufin
ABC	ATP-binding cassette
AHMC	3-(2-(N,N-diethylamino)ethyl)-7-hydroxy-4-methyl-coumarin
ALT	Alanine aminotransferase
AMMC	3-(2-N, N-diethyl-N-methylaminoethyl)-7-methoxy-4-methylcoumari
APA	Acetaminophen
AST	Aspartate aminotransferase
BCRP	Breast cancer resistance protein
BFC	7-Benzyloxy-4(trifluormethyl)coumarin
bp	Base pare
BSA	Bovine serum albumin
BSEP	Bile salt export pump
cDNA	Complementary DNA
CHC	3-cyano-7-hydroxicoumarin
Cou	Coumarin
CYP 1A1	Cytochrome P450 1A1
CYP 1A2	Cytochrome P450 1A2
CYP 2A1	Cytochrome P450 2A1
CYP 2A6	Cytochrome P450 2A6
CYP 2B6	Cytochrome P450 2B6
CYP 2C8	Cytochrome P450 2C8
CYP 2C9	Cytochrome P450 2C9
CYP 2D6	Cytochrome P450 2D6
CYP 2E1	Cytochrome P450 2E1
CYP 3A4	Cytochrome P450 3A4

DBF	Dibenzylfluoresceine
DMEM	Dulbecco's Modified Eagle's Medium
DMSO	Dimethyl sulfoxide
DNA	Deoxyribonucleic acid
dNTP	Desoxynukleotidtriphosphat
DPBS	Dulbeccos's Phosphate Buffered Saline
DPEC	Diethylpyrocarbonat
ECM	Extracellular matrix
EDTA	Ethylendiamintetraessigsäure
EFC	7-Ethoxy-4(trifluoromethyl)coumarin
EU	European Union
FCS	Fetal Calf Serum
FL	Fluorescein
g	Gramm
g	Multiple of the acceleration of gravity (x 9,81 m/s^2)
GAPDH	Glyceraldehyde 3-phosphate dehydrogenase
GSH	Glutathione conjugate
h	Hour
HC	7-Hydroxycoumarin
HFC	7-Hydroxy-4(trifluoromethyl)coumarin
LDH	Lactate dehydrogenase
M	Molar
MCB	Monochlorobimane
MDR1	Multidrug resistance protein 1
MDR2	Multidrug resistance protein 2
MDR3	Multidrug resistance protein 3
MFC	7-Methoxy-4(trifluoromethyl)coumarin
mg	Milligramm
min	Minute
ml	Milliliter
mM	Millimolar
MRP1	Multidrug resistance associate protein 1
MRP2	Multidrug resistance associate protein 2

MRP3	Multidrug resistance associate protein 3
MRP4	Multidrug resistance associate protein 4
MRP5	Multidrug resistance associate protein 5
MRP6	Multidrug resistance associate protein 6
m/z	Mass-to-charge ratio
NH_4	Ammonium
nM	Nanomolar
NTCP	Sodium/Taurocholate Co-transporting Polypeptide
OCT1	Organic cation transporter 1
PCR	Polymerase chain reaction
Pen/Strep	Penicillin/Streptomycin
PHH	Primary human Hepatocyte
pM	Picomolar
Res	Resorufin
RNA	Ribonucleic acid
RT	Room temperature
SD	Standard deviation
SEM	Standard Error of the Mean
SOP	Standard Operating Procedure
UGT	Uridine diphosphate glucoronosyltransferase
V	Volt
µg	Microgram
µl	Microliter
µM	Micromolar

1. Introduction

Toxicology is a multidisciplinary field involving biology, chemistry and medicine which investigates the interaction of chemicals with living organisms [1]. As toxicological studies are performed on new drugs (medicines), pesticides and food additives, toxicology plays a key role in our daily life. From a toxicological point of view, almost all substances that we ingest may cause damage to our organism. If a substance is toxic or non-toxic largely depends on the ingested quantity and the time of exposure. For instance, certain medicines have beneficial effects at lower doses, while others have no visible effects. However, an increase of the dose and the exposure time to some of these substances may lead to a negative response of an organism. For instance, acetaminophen is a worldwide used analgesic and it is safe a low doses [2], however, an acetaminophen overdose causes acute liver failure [3]. The liver plays a crucial role in the natural (non-specific) defense against chemical injuries [4]. Liver injury has been linked to nearly 1000 drugs and is the single most frequent reason to withdraw previously approved medications from the market [5].

Pharmaceutical toxicology tries to identify the effectiveness, the pathways of actions, and the risk assessment of the active chemicals of the compounds of medicines [6].

1.2. Drug toxicity studies

During the development of new medicaments, pharmaceutical companies perform toxicity tests in order to determine the acute, subchronic and chronic toxicity of the compounds. First, acute toxicity tests are performed and the toxicity is a single or brief exposure. Meanwhile, subchronic and chronic toxicity tests determine the effects and side-effects of a substance after repeated administration ranging from 1 to 2 weeks up to 1 to 2 years respectively [7].

In the pharmaceutical industry, laboratory animals are used for traditional toxicity tests in order to prevent possible damage in human organism, *e.g.* cancer, birth defects [8]. Moreover, the development of genetically modified animals which allow for the study of specific health disorders, as for instance

cancer, has led to an increase of the number of animals in research [9]. In the European Union (EU), there are two documents that regulate the use of animals in research; the Convention for the Protection of Vertebrate Animals used for Experimental and other Scientific Purposes (ETS 123) of the Council of Europe (1985) and the Directive for the Protection of Vertebrate Animals used for Experimental and other Scientific Purposes (86/609/EEC) (1986). Both directives control the use of vertebrate animals in experiments that can cause pain, suffering and stress, provide welfare for the animals, and regulate the necessary training of researchers and animal staff, the use of anesthesia and euthanasia, the generation of statistics on animal experimentation as well as the supply of animals. However, animal testing presents some major drawbacks, like *e.g.* high costs (accommodation and maintenance of animals), ethical problems (the right to use animals) and lack of reliability (animals have different physiology and metabolism than humans and therefore, which is difficult to translate into man) [8].

1.1.2. Alternative methods

In 2001, the EU created the REACH (Registration, Evaluation and Authorization of Chemicals) program system to quantify the toxicity of existing and new chemical substances [10]. In the framework of the 7th revision to the EU Cosmetics Directive, an agreement to prohibit animal testing for cosmetic products which are already on the market after 2013 was reached [11]. Therefore, REACH favors the development of alternative methods to animal testing, which are regulated by the European Centre for the Validation of Alternative Methods (ECVAM) in Ispra, Italy [12]. In 2011, the EU through the ECVAM started the SEURAT-1 Research Initiative ('Safety Evaluation Ultimately Replacing Animal Testing') in order to establish a safe long-term chemical research strategy for humans which consists in repeated dose systemic toxicity testing of chemicals integrated in different projects, like *e.g*. SCR & Tox, HeMiBio, ESNATS, DETECTIVE, COSMOS, NOTOX, ToxBank and COACH [13].

SCR & Tox ('Stem Cells for Relevant efficient extended and normalized TOXicology')

HeMiBio (‘Hepatic Microfluidic Bioreactor’)
ESNATS **(‘**Embryonic Stem cell-based Novel Alternative Testing Strategies’).
DETECTIVE (‘Detection of endpoints and biomarkers for repeated dose toxicity using *in vitro* systems’)
COSMOS (‘Integrated *In Silico* Models for the prediction of Human Repeated Dose Toxicity of COSMetics to Optimase Safety’)
NOTOX (‘Predicting long-term toxic effects using computer models based on systems characterization of organotypic cultures’)
ToxBank (‘Supporting Integrated Data Analysis and Servicing of Alternative Testing Methods in Toxicology’)
COACH (‘Coordination of projects on new approaches to replace current repeated dose systemic toxicity testing of cosmetics and chemicals’)

1.2. Liver

The liver is a vital and complex organ which is located on the right side of the abdominal cavity. The liver plays an important role in the regulation of the metabolism of the human body. It is responsible for many vital tasks, such as glycogen storage, bile production and excretion, fat metabolism, plasma protein synthesis, as well as the endo- and xenobiotic metabolism [1, 14]. The liver is constituted by different types of cells which can be divided into two subgroups: parenchymal and non-parenchymal cells. The non-parenchymal cells include sinusoidal endothelial cells, Kupffer cells, hepatic stellate cells (Ito or fat-storing cells), pit cells (NK cells), hepatic dendritic cells, natural killer T cells (NKT) and biliary epithelial cells. The parenchymal cells are mainly consisting of hepatocytes [4].

1.2.1. Liver architecture

The smallest structural unit of the liver is the lobule (Figure 1.1). The lobule has a hexagonal shape. At its corners are located the portal triads which are comprised of the bile duct, the hepatic artery and the portal vein. Blood enters the liver through the hepatic arteries and the portal veins and circulates among the sinusoidal vessels to the central vein which is located in the centre of the lobule. Hepatocytes are organized in plates consisting of 15-25 cells and their thickness differs the central vein and the borders of the lobule [4, 15, 16].

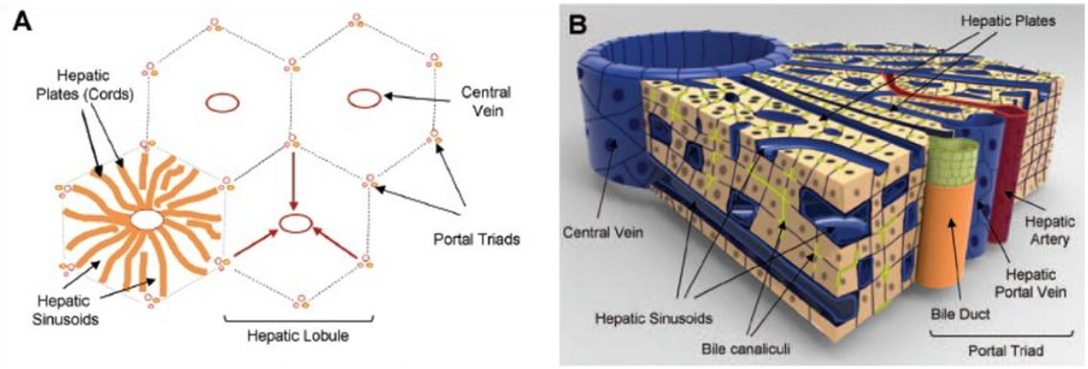

Figure 1. 1 Basic representation of the physiology of the liver. **(A)** Schematic representation of the lobule and the hepatic plates. **(B)** Figure of the three-dimensional architecture of the liver between a portal triad and the central vein [15].

1.3. Hepatocytes

Hepatocytes are functional cells of the liver and constitute 70-80% of the tissue volume of the whole organ [4]. Hepatocytes are responsible for the majority of the most important liver functions. To be functional, a different kind of cell, the endothelial cell are bordered as apical membrane, hepatocytes are limited by an apical and basal lateral membrane [17]. The apical membrane faces the bile canaliculi while the basal lateral membrane faces the sinusoidal vessels (Figure 1.2.).

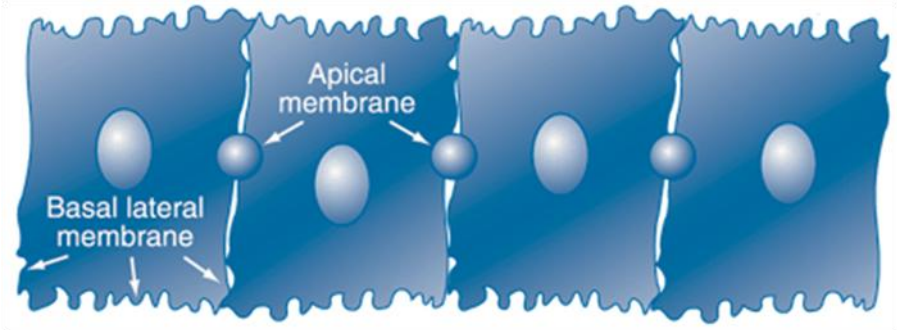

Figure 1. 2 Schematic representation of hepatocytes with their respective apical and basal lateral membranes [18].

1.3.1. Glucose production in hepatocytes

The liver balances the blood glucose levels by controlling the absorption, storage and release of glucose. Excessive glucose in the liver is stored as glycogen and used as a long-term energy storage [19]. For fasting periods of more than one day, or intense exercise, glucose must be synthesized from non-carbohydrate precursors, such as pyruvate, lactate, oxaloacetate, and amino acids via gluconeogenesis (Figure 1.3.).

Gluconeogenesis takes places in three different compartments of the hepatocytes: the mitochondria, the cytosol and the endoplasmic reticulum. Pyruvate and oxaloacetate are produced from the partial breakdown of amino acids. In the mitochondria, oxaloacetate is formed by the carboxylation of the pyruvate. Oxaloacetate is reduced to malate by NADH which will be transported out of the mitochondria. Then, NAD^+ triggers and oxidizes and oxaloacetate is transformed into phosphoenolpyruvate by phosphoenolpyruvate carboxykinase. Until the completion of the formation of glucose-6-phosphate, the following reactions take place in the cytosol. The formation of glucose takes place in the lumen of endoplasmic reticulum where glucose-6-phosphate is hydrolyzed by glucose-6-phosphatase. Finally, glucose is released to the cytosol by glucose transporters [20].

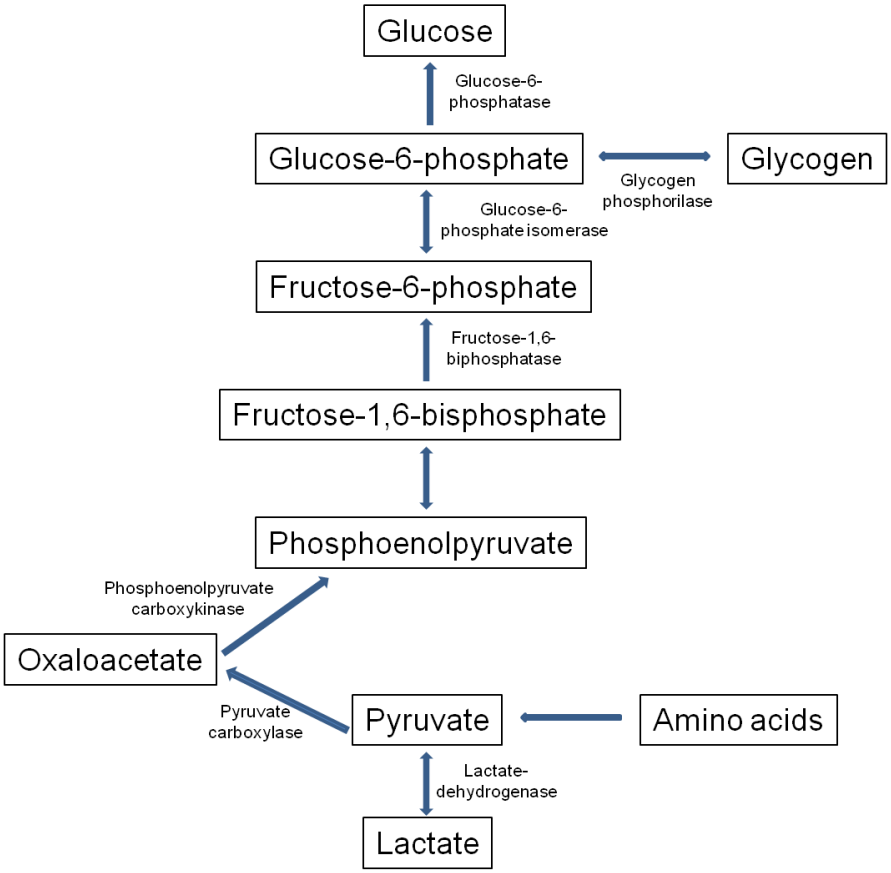

Figure 1. 3 Schematic description of gluconeogenesis from lactate and pyruvate [21].

1.3.2. Ammonia detoxification in hepatocytes

Ammonia is biosynthesized during the metabolism of amino acids. Hepatocytes are responsible for the detoxification of ammonia via ureagenesis. Thereby, they prevent the organism from suffering from hyperammonia and hepatic encephalopathy [22]. Ammonia is excreted as urea via the urea cycle (Figure 1.4.) [23]. Then, aminotransferases convert amino acids into ammonia, before the amine group of glutamate is removed by glutamate dehydrogenase and glutaminase. Then, ammonia is converted into urea through the urea cycle by carbamoyl-phosphate-synthetase I, ornithine transcarbamylase, arginosuccinate synthetase, arginosuccinate lyase and arginase I [23].

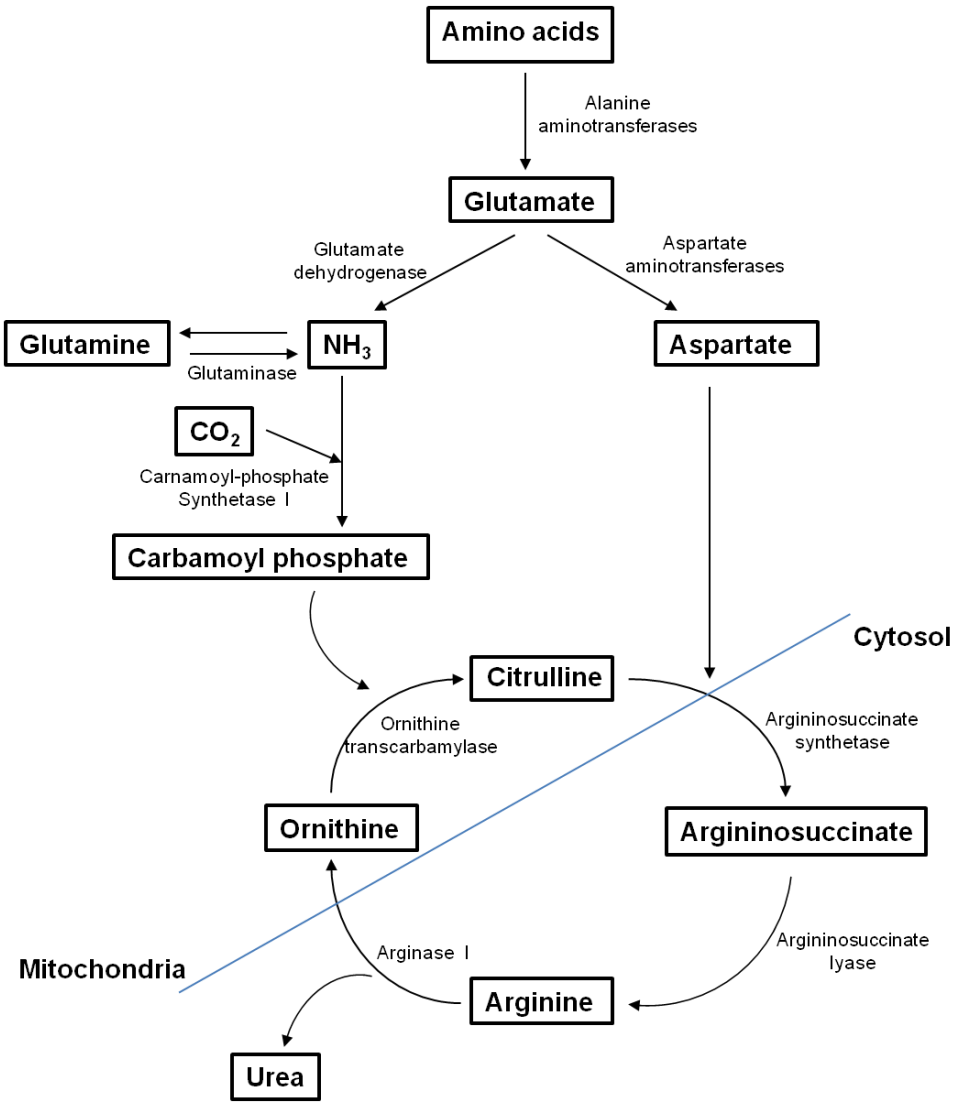

Figure 1. 4 Schematic representation of the ureagenesis pathway [23].

1.3.3. Biotransformation of drugs

Hepatocytes are responsible for the metabolism of xenobiotic and endobiotic substances. The metabolism of these substances consists of three different phases. Phase I reactions include hydrolyses, reductions and oxidations [24]. Oxidative reactions are performed by the cytochrome P450 (CYP) enzyme family, which comprises thirty five different CYPs that are grouped in different subfamilies. The eighteen CYPs which make up the subfamilies 1-3 mainly participate in the metabolism of xenobiotic and endobiotic substances, like *e.g.* CYP3A4 (52%), CYP2D6 (30%), 2C9/10/19 (11%), CYP1A2 (4%) and CYP2E1 (2%) [25, 26]. Phase II reactions are performed by transferases which conjugate the metabolic products from phase I. These reactions facilitate the modification

and conjugation of the xenobiotic substances and, in some cases, the conjugated metabolites can be substrates for specific transport proteins in order to facilitate the excretion [27]. Finally, phase III involves the elimination of conjugated metabolites via elution by transporter proteins located at the apical and at the basolateral membranes. The transporter proteins involving in the elution of the metabolism products are part of the ATP-binding cassette (ABC) family which is divided into several subfamilies, *e.g.*; ABCA, ABCB, ABCC, ABCD, ABCE, ABCG and ABCG [28, 29].

1.4. Hepatocyte culture

Since the approval of the Directive for the Protection of Vertebrate Animals used for Experimental and other Scientific Purposes (86/609/EEC) in 1986 researchers have focused on the establishment of long-term cultures of PHH in order to reduce animal testing [30]. Compared to animal models, hepatocytes dispose several advantages for the investigation of liver functions, such as controlled experimental conditions, reduction of material needed, easier analysis of the results, high throughput screening test can be performed, and a comparison of different species can be performed [31]. As mentioned before in the section 1.3, hepatocytes are limited by an apical and basal lateral membrane in their functional state [17]. However, hepatocytes have been traditionally cultured on monolayer (2D) cultures, which have been used to study drug metabolism and hepatotoxicity, spread losing their cuboidal shape generating a epithelial-mesenchymal transition during which the hepatocytes lose their polarity and architecture, lose many liver specific functions, and decrease cell viability during the time of culture (Fig. 1.5) [31, 32]. In order to improve hepatocytes attachment, culture plates are coated with an ECM protein. Several proteins have been used, for instance fibronectin which increases cell attachment and enables the organization of hepatocytes in cord-like structures [33]; however, collagen type I is the most commonly used [34]. In addition, fetal calf serum and formulations containing several hormones added to the medium culture have proved to influence on the cell survival of hepatocytes in culture [30]. Despite all these advances in hepatocyte culturing, long-term cultures of primary hepatocytes are needed in order to investigate drug metabolism and hepatotoxicity, which reduces the use of animals testing in drug development

[30] and allows the possibility of studying subchronic or even chronic toxicity [35]. In order to maintain hepatocytes polarity in long-term cultures, hepatocytes must be cultured in three dimensions (3D) which mimics the *in vivo* situation. Previous studies, have reported the importance of culturing cells in 3D compared to 2D [36]. In addition, hepatocytes cultured in 2D de-differentiate over the time. This de-differentiation state can be reversible by re-plating them in 3D [37]. Hepatocytes cultured in a sandwich disposition using two layers of hydrogels have shown a delay in the loss of hepatic architecture and polarization, and consequently hepatic dedifferentiation (Fig. 1.5). Collagen and Matrigel® are the most common gels used [30]. The second layer of gel allows the hepatocytes to form aggregates maintaining their cuboidal shape for a longer time, and consequently hepatocytes dedifferentiation is at least delayed [38, 39]. This means that hepatocytes maintain their hepatocytic phenotype and consequently their liver specific functions longer permitting long-term cultures.

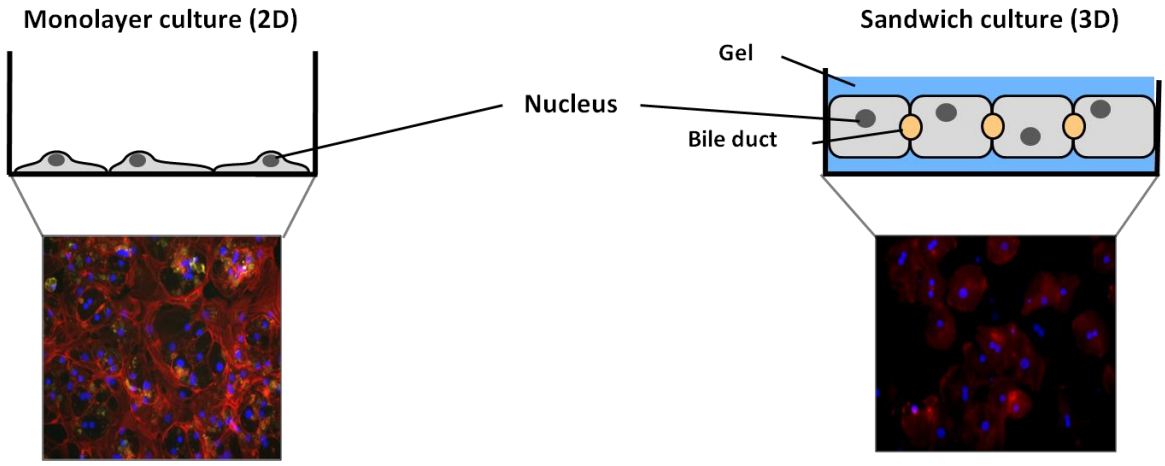

Figure 1.5 Schematic representation of PHH culture in 2D and 3D over 7 days and their respective fluorescence micrographs; where nuclei are in blue, actin fibers in red and dead cells are in green (autofluorescence).

1.5. Tissue engineering

Tissue engineering has been defined as 'an interdisciplinary field that applies the principles of engineering and the life sciences towards the development of biological substitutes that restore, maintain, or improve tissue function' [40]. The principle of tissue engineering is illustrated below (Figure 1.6), where primary cells are isolated from a human tissue and cultured *in vitro* until they proliferate

and seeded onto a carrier [41]. Then, the material containing the cells is implanted into the same patient in order to restore the damaged tissue. The carriers that are used in tissue engineering, are hydrogels, scaffolds, and bioreactors which enable the three-dimensional growth of the cells just like in the *in vivo* situation [15, 42]. PHH do not proliferate *in vitro*, nevertheless hydrogels, scaffolds, and bioreactors mimic the organotypic environmental conditions which allow preserving hepatocytic functions/phenotype during the time of culture.

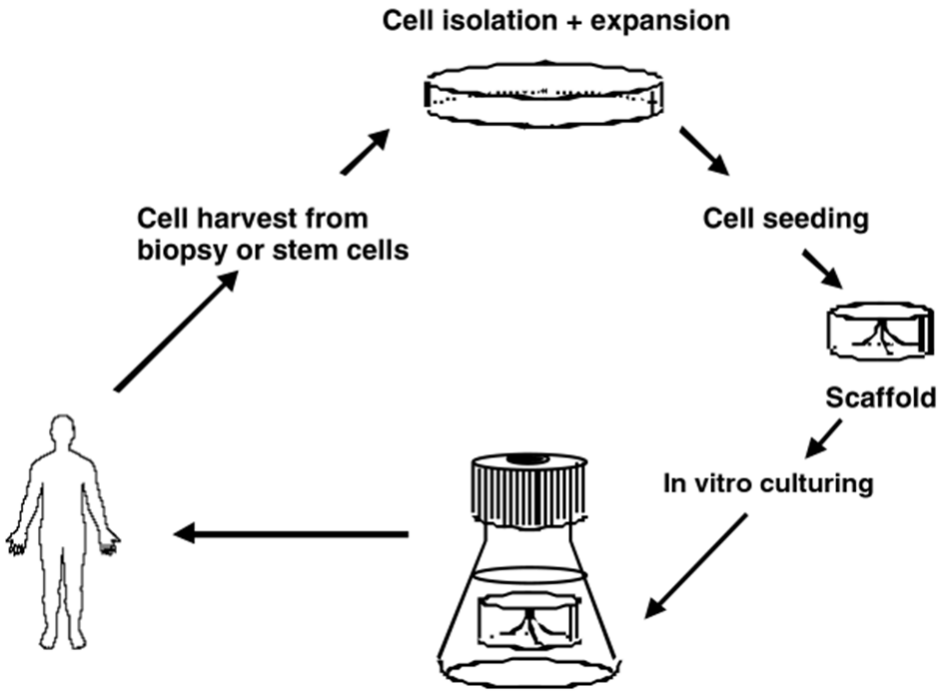

Figure 1. 6 Schematic representation of the basic principles of tissue engineering [41].

1.5.1. Hydrogels

Hydrogels are hydrophilic, water-swollen polymers which form a network which can be modified concerning their nature and physical properties in order to mimic the extracellular matrix [43]. Therefore, several physical and biological properties based on degradation of the material, as well as mechanical and chemical properties, cell adhesion and biocompatibility must be taken into consideration during the design and selection of hydrogels [44]. Mechanical properties, such as porosity, must allow for the transport of signaling molecules, nutrients and metabolic products while maintaining the mechanical integrity of

the gels. Chemical properties are able to direct morphological cell changes by releasing specific signaling molecules or by degrading the matrix over time [45]. Based on their composition, hydrogels can be subdivided into natural and synthetic hydrogels (Table 1.1.).

Table 1. 1 Overview of natural and synthetic hydrogels for the culture of PHH [33, 46, 47].

Polymer	**Observed benefits**
Natural hydrogels	
Collagen	High biocompatibility, maintenance of viability and biotransformation capacity over 6 weeks
Gelatin + Co-polymers	High biocompatibility, maintenance of hepatocytes functions for 3 weeks
Matrigel®	Maintenance of viability and hepatocytes functions for 3 weeks
Laminin	High biocompatibility, maintenance of hepatic morphology and albumin secretion for 3 weeks
Alginate	Maintenance of cell polarity, high albumin production over 4 days
Synthetic hydrogels	
PEG	High reproducibility, high diffusion of liquids and particles
+ PGLA	Increase of urea synthesis and CYP3A4 activity compared to PEG hydrogel alone for 1 week
+ Heparin	High production of albumin and urea synthesis over 3 weeks
+ RGD	Formation of spheroids, maintenance of albumin and urea production over 4 weeks
RAD16-I	Maintenance of hepatic morphology, bile canaliculi formation, albumin secretion for 1 week

Natural hydrogels are obtained from natural compounds, like *e.g.*; collagen, gelatin, Matrigel® (BD Biosciences, Billerica, MA, USA), laminin, fibronectin, and alginate. The major advantages of these hydrogels are their non-toxicity and their high biocompatibility as they are comprised of proteins and other ECM components, which present multiple membrane receptor sites [48]. Furthermore, hepatocytes cultured in hydrogels maintain their hepatic-specific functions and, in comparison to monolayer cultures, their hepatocyte dedifferentiation is at least delayed [38, 39, 49]. For instance, alginate beads are used in xenotransplantation as a cell therapy to bridge patients with acute liver failure until a suitable liver is available [50], and in bioreactors [51]. PHH cultured in

alginate beads have shown to delay the loss of hepatocytic activity over the time of culture in comparison to 2D cultures. Other hydrogel like laminin rich-gel maintains hepatocytes morphology and albumin secretion levels stable for 3 weeks [47].

As mentioned above, collagen and Matrigel® are the most commonly used gels [30]. Matrigel® is a gelatinous mixture of ECM components secreted by Engelbreth-Holm-Swarm sarcoma cells. On the other hand, collagen is the most common fibrous protein in the extracellular matrix and in the connective tissue in mammals. In humans, 16 different types of collagen can be found, but collagen type I, II, and III already form 80-90% of the total collagen in the body [52]. Traditionally, hepatocytes have been cultured between two layers of collagen (sandwich) [53, 54] (Figure 1.7 B). More recently, they have been re-suspended in collagen gels [55, 56] (Figure 1.7 C), which allow for a reduction of the number of cells. The collagen that is used in cell cultures is either synthesized collagen type I or a collagen mixture mainly isolated from rat tails. It has been proved that collagen type III contributes to the hepatocytes spreading and maintenance of the phenotypic expression of the hepatocytes [57]. Therefore, rat tail collagen which is a mixture of collagens (I-III) [58] is widely used in hepatocyte cultures. Despite the advantages of culturing hepatocytes in rat tail collagen and Matrigel® these matrices present batch-to-batch differences.

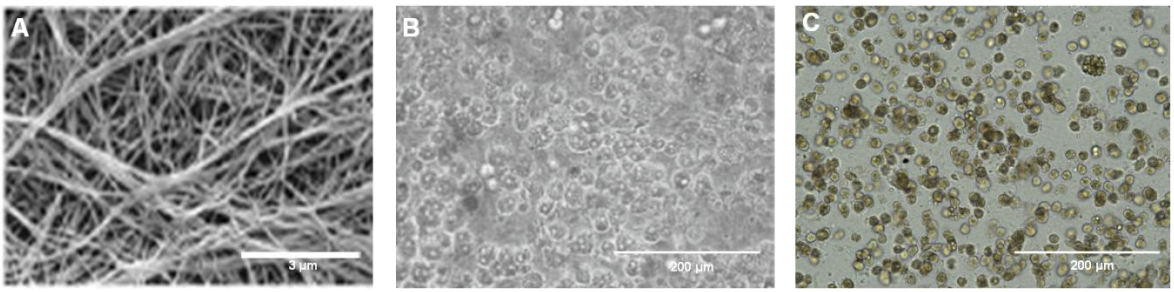

Figure 1. 7 Micrographs of collagen gel. **(A)** Scanning electron microscopy image of rat tail collagen fibers [59]. **(B)** PHH in collagen sandwich culture. **(C)** PHH in collagen gel culture.

Synthetic hydrogels overcome batch-to-batch differences as they have a clearly defined composition. Therefore, the interest in synthetic hydrogels has increased in the last years. Furthermore, they can be customized to mimic the liver ECM by controlling the chain length and the density of the polymers and by

adding degradable linkages, adhesive peptide moieties, and other active factors [60, 61]. Polyethylene glycol (PEG) hydrogels have been extensively used in PHH culture enhancing hepatic functions related to monolayer cultures [62]. In addition, PEG gels can be combined with poly(lactic-coglycolic) acid (PLGA) or with biologically active entities from the hepatic ECM in order to benefit from cell adhesion and to improve hepatic-specific functions [63, 64]. Self-assembling peptides, like *e.g.* Puramatrix™ (3-D Matrix Inc., Waltham, MA, USA) are a category of peptides which undergo spontaneous assembling into ordered nanostructures which biochemical properties are similar to those of hepatic ECM. PHH cultures in self-assembling peptides maintain their activity over 3 weeks [65, 66].

In this research two synthetic hydrogels: 3D-Life Hydrogel (Dextran-PEG-Hydrogel) (Cellendes GmbH, Reutlingen, Germany) and PEG hydrogels (Tecnalia, San Sebastián, Spain), which had not been tested for the culture of PHH beforehand were tested in comparison to collagen gel. However, both gel types were excluded as they did not allow for a homogeneous flow in the μ-slide channel.

1.5.2. Scaffolds

Scaffolds are porous solid biocompatible 3D materials which enable an interaction between the cells and the biomaterial, cell adhesion, ECM deposition, transport of nutrients and metabolic products [67]. Like hydrogels, scaffolds can be divided into natural and synthetic scaffolds as recently summarized by our group (Table 1.2.).

Table 1. 2 Overview of natural and synthetic scaffolds for the culture of PHH [46].

Polymer	**Observed benefits**
Natural scaffolds	
Alginate	Cell-matrix interaction, high albumin and urea synthesis, CYP activities stable for 1 week
Chitosan + Heparin/Collagen/Galactose	Improved cell attachment, maintenance of hepatocytes morphology, albumin and urea secretion
Synthetic scaffolds	
Polyvinyl alcohol	Improved cell attachment, higher viability, albumin and urea synthesis over 3 weeks
Polylactic acid	Improved cell attachment, permeation of proteins and maintenance of hepatic functions
Polystyrene	Maintenance of hepatic morphology, bile canaliculi formation, albumin synthesis over 3 weeks. Better prediction of drug-induced toxicity

Natural scaffolds favor cell-matrix communications and thereby enhance the biological performance of the cells over the time of culture [67]. These scaffolds are made up of proteins, polysaccharides or the combination of both such as chitin, alginate, chitosan/alginate (Figure 1.8), chitosan/heparin, chitosan/gelatin, etc. Hepatocytes that are cultured on these matrices maintain their metabolic activities over 15 days [68-70].

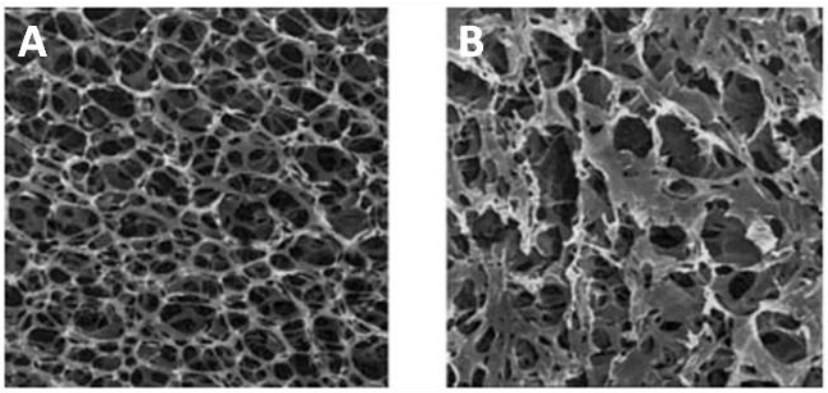

Figure 1. 8 Image of porous chitosan and porous chitosan/alginate. **(A)** Chitosan scaffold (x100 magnification). **(B)** Chitosan/alginate scaffold (x100 magnification) [68].

Synthetic scaffolds are very common in research as they present a clearly defined composition and their properties can be modified according to the required functions [67]. In addition, depending on their fabrication and their use,

synthetic polymers are able to build foam disks (Figure 1.9 A) or fiber membranes (Figure 1.9 B) [71]. Polyvinyl alcohol (PVA) scaffolds allow for the formation of spheroid aggregates of hepatocytes favoring the production of albumin and urea over 3 weeks [72]. Due to its biodegradability, polylactic acid (PLA) is another common material for scaffolds. PLA scaffolds maintain their metabolic activities for 2 weeks [73]. Recently, a new scaffold which consists of polystyrene used in conventional tissue culture plates has been commercialized by Alvetex® (Reinnervate Ltd., Durham, UK). Hepatocytes that are cultured on these scaffolds preserve bile canaliculi morphology, metabolic activity and sensitivity to acetaminophen stimulation over 3 weeks [74].

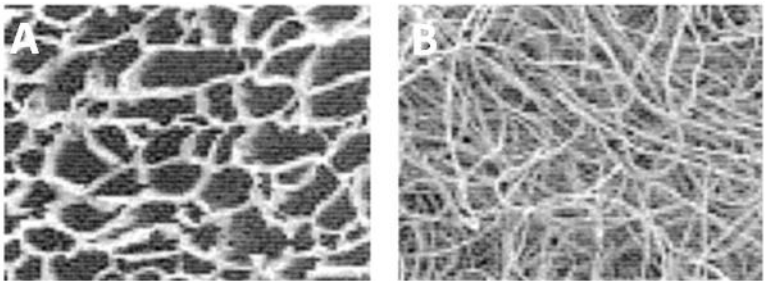

Figure 1. 9 Scanning electron microscopy images of foam and fibrous scaffolds. **(A)** PLA foam scaffold. **(B)** fibrous scaffold [71].

1.5.3. Bioreactors

Liver tissue is one of the most irrigated tissues in the body. This high blood perfusion allows for the transport of nutrients, oxygen, endobiotic and xenobiotic substances and excreted metabolites by the hepatocytes [15, 75]. Traditional 2D and 3D cultures present cells in static media differing from the *in vivo* condition [15]. In the last years, more and more sophisticated types of hepatocytes cultures, especially bioreactors, have been developed in order to create flow culture systems that mimic the *in vivo* conditions (Table 1.3).

Table 1. 3 Benefits and drawbacks of bioreactors and microfluidic devices applied for the culture of PHH [46].

Approach	**Cell No. (million)**	**Demonstrated benefits**	**Drawbacks**	**Group**
Sartorius-Stedim Biostat® Q-Plus bioreactor	15-30	Maintenance of hepatic differentiation for more than 4 weeks Protection from shear stress	High cell number Costly equipment	Animal Cell Technology, [51]
Hollow-fiber bioreactor	~ 100	Maintenance of CYP enzyme and transport protein expression and activity for up to 3 weeks Formation of bile canaliculi	High cell number Low throughput Non-microscopable Costly equipment	Biochemical Engineering Institute, University of Saarland, [76]
Multicompartment modular bioreactor	< 1	Expression of detoxifying genes stimulated by medium flow	Low throughput Non-microscopable	Centro Interdipartimentale di Ricerca, University of Pisa, [77]
Perfused multi-well plate	< 1	*In vivo*-like testosterone metabolism and hepatic clerance High throughput	Not commercially available	Massachusetts Institute of Technology, [78]
KITChip bioreactor	< 10	Improvement of hepatic phenotype and up-regulation of hepatic marker genes in HepG2 cells Homogeneous medium flow and oxigen supply	High cell number Low throughput	Karlsruhe Institute of Technology and Institute for Biological Interfaces -1, [79]
HepaChip®	< 1	Maintenance of CYP activities and albumin secretion compared to hepatocyte monolayers Formation of bile canaliculi, cell-cell interaction	Costly equipment Low throughput	Naturwissenchaft-liches und Medizinisches, University of Tübingen, [80]

Bioreactors are 'devices which biological and biochemical process develop under closely monitored and tightly controlled environmental and operating conditions (*e.g.*; pH, temperature, oxygenation, pressure, nutrient supply and waste removal)' [81]. These devices create artificial culture conditions which are similar to the normal and pathological *in vivo* situation, and which enable a more realistic study of the cell-cell and cell-environment interactions [82]. Therefore bioreactors are excellent tools for long-time hepatic cultures, as PHH dedifferentiate by losing hepatic-specific functions after one week of culture [83]. The first commercially available bioreactors required large volumes and large numbers of PHH. Bioreactors with alginate-encapsulated hepatocytes (Figure 1.10 A & B), in which alginate beads protect the hepatocytes from shear stress and maintain the hepatocytes alive over 4 weeks [51]. Another large-scale

bioreactor is the 3D hollow-fiber bioreactor (Figure 1.10 C) consists of three interwoven hollow-fibers which supply medium and gas to the cells [76]. This bioreactor maintains the hepatocytes alive for 3 weeks and enables the formation of bile canaliculi [76]. The major limitations of these systems are the high number of required cells, the high costs of the equipment, and the low number of laboratories in which they can be tested.

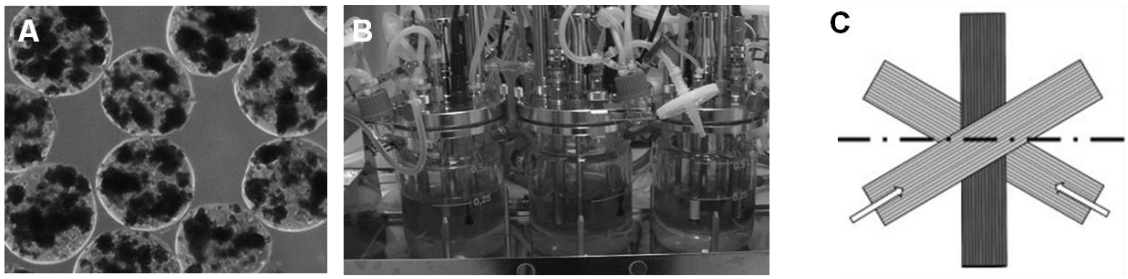

Figure 1. 10 Images of different bioreactors. **(A)** Hepatocyte aggregates encapsulated in alginate beads. **(B)** Sartorius-Stedim Biostat® Q-Plus Bioreactor system [51]. **(C)** Disposition of hollow fibers within the 3D bioreactor; light grey, medium capillaries; dark grey, gas capillaries [76].

Over the last decade, many efforts have been made in order to create new micofluidic systems which enable a reduction of the number of required cells and an increase of the throughput. One of these novel systems is the multichamber modular bioreactor which recreates different organs that can be used for the study of different diseases. This bioreactor has been commercialized under the name of Quasi-Vivo® (Kirkstall Ltd, UK). Hepatocytes are cultured on hydrogels or scaffolds in silicon chambers which induce the expression of metabolizing genes [77]. Another commercialized microfluidic system which is based on multi-well plates is the LiverChip (Zyoxel, Oxfordshire, UK). With this system, the hepatocytes are cultured on scaffolds in modified culture plates under continuous medium flow. This system allows for the implementation of high-throughput screening assays [78]. HepaChip® and KITChip are two microfluidic systems in which the cells are cultured in the cavities of the chips under continuous medium flow (Figure 1.11 A). HepaChip® recreates the liver sinusoid and allows for an active positioning of hepatocytes [80]. On the other hand, the KITChip system maintains high CYP activities for 10 days (Figure 1.11 B) [79].

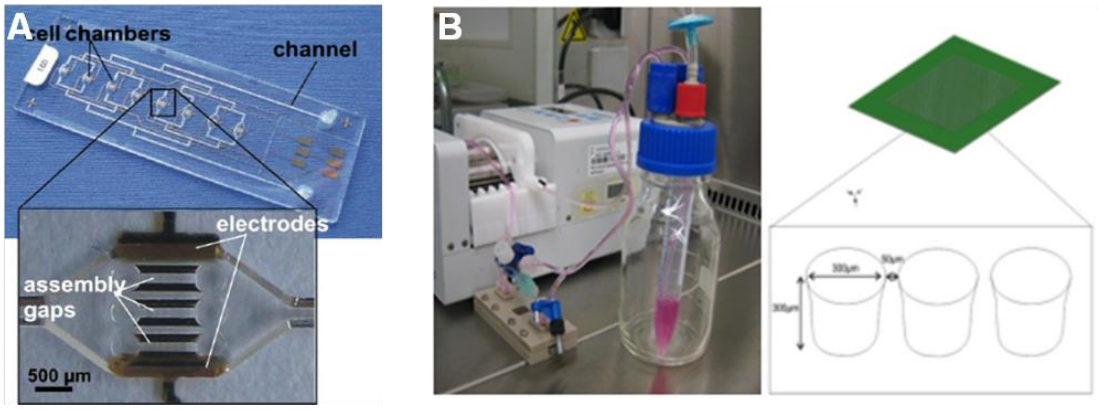

Figure 1. 5 Images of different microfluidic systems. **(A)** HepaChip® with detail view of one chamber, showing the three assembly gaps and the electrodes required for dielectrophoresis [80]. **(B)** KITChip with round cavities and experimental setup for culture of primary hepatocytes in the KITChip bioreactor [79].

1.6. µ-slide microfluidic system

PHH present a short life span when they are cultured in monolayer cultures. In this culture dispositon PHH lose their hepatocytic phenotype and become flat during the time of culture [31, 32] (Figure 1.12).

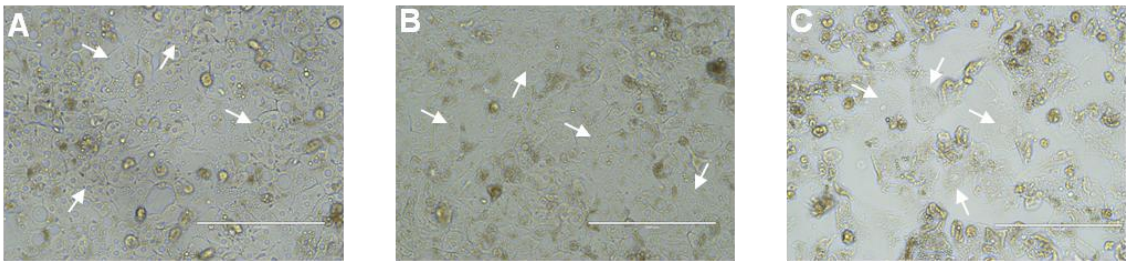

Figure 1.12 Transmitted light micrograph of PHH on monolayer cultures: day 1 **(A)**, day 7 **(B)**, and day 14 **(C)**. PHH are indicated by white arrows.

In the last decades many efforts have been made in order to preserve hepatocyte phenotype in *in vitro* conditions by the development of hydrogels, scaffolds, and later bioreactors. Despite the fact that the bioreactors described in the previous point preserve hepatic differentiation by the expression of detoxifying genes, CYPs and transporter proteins, formation of bile canaliculi, and high albumin production, bioreactors are sophisticated and expensive devices difficult to handle and in many cases present low throughput compared to traditional cultures in 96-well plates [46]. Moreover, bioreactors are limited to

a small number of laboratories. Therefore, there is a need to create a simple microfluidic system which can be used by any laboratory. In this study we present a microfluidic system which uses a µ-slide (ibidi®, Munich, Germany) as a platform for culturing cells. The µ-slide is a commercially available plate for the culture of cells under a continuous flow. The µ-slide VI$^{0.4}$ contains six channels and allows for the simultaneous creation of different flow cultures (Figure 1.13). The continuous flow system is relatively simple as only a conventional syringe pump is needed. The µ-slide is relatively small (30 µl/channel), so, it only requires a low cell number (< 0.2*10^6 cells/channel). Moreover, it can be combined with different hydrogels depending on the study requirements and it is suitable for live cell imaging. Due to the small height of the channels, 3D cultures can only be performed by re-suspending cells in gels. This new conformation implies the previous characterization of the cells in static condition in order to have an adequate comparison.

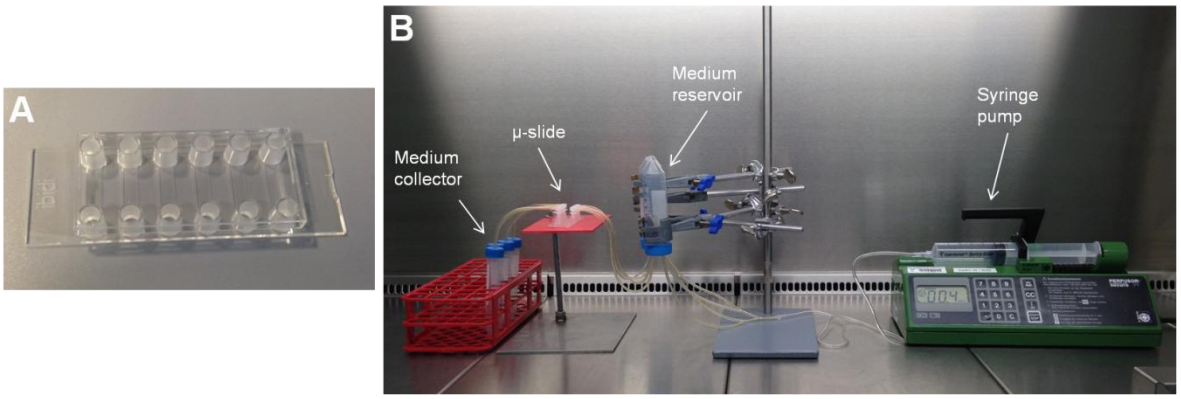

Figure 1. 13 Photograph of the µ-slide and the microfluidic culture. **(A)** ibidi® µ-slide and **(B)** microfluidic culture system.

1.7. Aim

This study investigates the behavior of PHH culture in different matrices under static and fluidic conditions. The precise aims of this research were:

i. Analysis of MRP1 and MDR1/P-gp transporter membrane activity in 2D and 3D cultures.
ii. Adaptation cell number in collagen gel cultures for down-screening purposes.
iii. Characterization of PHH in static cultures, monolayer and 3D, over 28 days of culture.
iv. Reproduction of similar biological culturing conditions in a µ-slide which permit the maintenance of the differentiated state of primary human hepatocytes for seven days.
v. Characterization of PHH in the microfluidic system.

2. Materials and Methods

2.1. Materials

2.1.1. Equipment

Table 2. 1 Equipment

Device	Company
Auto sampler	Thermo Fisher Scientific, Dreieich, Germany
Balance KERN ABJ	Kern & Sohn GmbH, Balingen, Germany
Balance KERN PCB	Kern & Sohn GmbH, Balingen, Germany
Centrifuge Megafuge 40R	Thermo Fisher Scientific GmbH, Osterode, Germany
Clean Bench Safe 2020	Thermo Fisher Scientific GmbH, Langenselbold, Germany
Digital Monochrome Printer P93DW	Mitsubishi Electric SDN. BHD, Senai, Malaysia
Fluorescence Microscope EVOS-fl	Peqlab Biosysteme GmbH, Erlangen, Germany
FLUOstar Omega	BMG Labtech, Offenburg, Germany
LVis Plate	BMG Labtech, Offenburg, Germany
Gel Stick Imager	Imaging Instruments GmbH, Chemnitz, Germany
Hot plate IKA® RH basic 2	IKA®, Staufen, Germany
Incubator BINDER	BINDER GmbH, Tuttlingen, Germany
Perfusor® secura FT pum	B-Braun Melsungen AG, Melsungen, Germany
Ligth Microscope Primo Vert	Carl Zeiss MicroImaging GmbH, Gottingen, Germany
Microcentrifuge Fresco 17	Thermo Fisher Scientific GmbH, Osterode, Germany
IPC peristaltic pump	IDEX Health & Science GmbH, Wertheim, Germany

Power Pack HC	Bio-Rad Laboratories GmbH, München, Germany
Shaker DRS-12	LTF Labortechnik GmbH & Co. KG, Wasserburg, Germany
Syringe Pump Perfusor Secura	B-Braun Melsungen AG, Melsungen, Germany
Thermal Cycler Block ARKTIK	Thermo Fisher Scientific Oy, Vantaa, Finland
Thermal Cycler Block Veriti®	Applied Biosystems (Life Technologies ™), Darmstadt, Germany
Thermostat Lauda Alpha	Lauda Dr. R. Wobser GmbH & Co. KG, Lauda-Königshofen, Germany
TSQ Quantum Discovery Max	Thermo Fisher Scientific, Dreieich, Germany
Vortex mixer LSE™	Corning Incorporated, Corning, USA
Water bath Aqualine AL25	Lauda Dr. R. Wobser GmbH & CO. KG, Lauda-Königshofen, Germany

2.1.2. Consumables

Table 2. 2 Consumables

Product	Company
Cellstart® Cell Culture Flasks 25, 75 and 175 cm^2	Greiner Bio-One GmbH, Frickenhausen, Germany
Cellstart® Cell Culture Plates 24 and 96 wells	Greiner Bio-One GmbH, Frickenhausen, Germany
Falcon® Cell Culture Plates 6 wells	Becton, Dickinson & Co. Ltd, Franklin Lakes, USA
Cellstart® Tubes 15 and 50 ml	Greiner Bio-One GmbH, Frickenhausen Germany
Costar® Stripette 5, 10 and 25 ml	Corning Incorporated, Corning, USA
Cryo Tube™ vials	Nunc, Roslkilde, Denmark
Elbow Luer Connector	ibidi, Munich, Germany

Feather® Scalpel	Feather Safety Razor Co. Ltd, Osaka, Japan
Fixo gum	Marabu GmbH & Co. KG, Bietigheim-Bissingen, Germany
Infusion	Oriplast, Neunkirchen-Saar, Germany
Injection needles BD Microlance™ 3	Becton, Dickinson & Co. Ltd, S. Agustin del Guadix, Spain
Injectomat®-Syringe 50 ml	Fresenius Kabi AG, Bad-Homburg, Germany
Injection syringe 2, 10 and 20 ml	B-Braun Melsungen AG, Melsungen, Germany
Kinetex PFP analytical column	Phenomenex, Aschaffenburg, Germany
Micro Tube 0.5 ml	Sarstedt Aktiengesellschaft & Co., Nümbrecht, Germany
Multiply-Pro cup 0.2 ml	Sarstedt Aktiengesellschaft & Co., Nümbrecht, Germany
Multiwell™ 6 wells	Becton, Dickinson & Co. Ltd., Franklin Lakes, USA
Pasteur Pipettes 150 mm and 230 mm, glass	Carl Roth GmbH & Co. KG, Karlsruhe, Germany
pH indicator Pehanon	Macherey-Nagel, Düren, Germany
Pipette Tips 10 µl	Biozym Scientific GmbH, Oldendorf, Germany
Pipette Tips 200 µl	Sarstedt Aktiengesellschaft & Co., Nümbrecht, Germany
Ratiolab® Pipette Tips 1000 µl	Ratiolab GmbH, Dreieich, Germany
Rotilabo®-microcentrifuge tubes 1.5 ml	Carl Roth GmbH & Co. KG, Karlsruhe, Germany
Safe-Lock Tubes 2.0 ml	Eppendorf AG, Hamburg, Germany
Sterile Filter Millex® GP	Merck Millipore Ltd., Cork, Ireland
Tygon® R3603	Carl Roth GmbH & Co. KG, Karlsruhe, Germany
µ-slide VI$^{0.4}$	ibidi, München, Germany

2.1.3. Chemicals

Table 2. 3 Chemicals

Chemical	Company
3-(2-(N,N-diethylamino)ethyl)-7-hydroxy-4-methylcoumarin	Sigma Aldrich Chemie GmbH, Steinheim, Germany
3-(2-N,N-diethyl-N-methylaminoethyl)-7-methoxy-4-methylcoumarin	Sigma Aldrich Chemie GmbH, Steinheim, Germany
3-Cyano-7-hydroxycoumarin	Sigma Aldrich Chemie GmbH, Steinheim,Germany
4-Methylumbelliferone	Sigma Aldrich Chemie GmbH, Steinheim,Germany
5-Carboxyfluorescein	Sigma Aldrich Chemie GmbH, Steinheim, Germany
5(6)-Carboxy-2',7'-dichlorofluorescein diacetate	Sigma Aldrich Chemie GmbH, Steinheim,Germany
7-Benzyloxy-4(trifluoromethyl)coumarin	Sigma Aldrich Chemie GmbH, Steinheim,Germany
7-Ethoxycoumarin	Fluka Chemie GmbH, Steinheim, Germany
7-Ethoxy-4(trifluoromethyl)coumarin	Sigma Aldrich Chemie GmbH, Steinheim,Germany
7-Hydroxycoumarin	Sigma Aldrich Chemie GmbH, Steinheim,Germany
7-Hydroxy-4(trifluoromethyl)coumarin	Sigma Aldrich Chemie GmbH, Steinheim,Germany
7-Methoxy-4(trifluoromethyl)coumarin	Sigma Aldrich Chemie GmbH, Steinheim,Germany
Acetaminophen	Sigma Aldrich Chemie GmbH, Steinheim,Germany
Acetic acid	Carl Roth GmbH & Co. KG, Karlsruhe, Germany
Acetonitrile	Carl Roth GmbH & Co. KG, Karlsruhe, Germany

Agarose	Carl Roth GmbH & Co. KG, Karlsruhe, Germany
Ammonium chloride	Carl Roth GmbH & Co. KG, Karlsruhe, Germany
Boric acid	Carl Roth GmbH & Co. KG, Karlsruhe, Germany
Bovine Serum Albumin (BSA)	Carl Roth GmbH & Co. KG, Karlsruhe, Germany
Brij 35	Carl Roth GmbH & Co. KG, Karlsruhe, Germany
Bromophenol Blue sodium salt	Carl Roth GmbH & Co. KG, Karlsruhe, Germany
Calcium chloride	Carl Roth GmbH & Co. KG, Karlsruhe, Germany
Chloroform	Carl Roth GmbH & Co. KG, Karlsruhe, Germany
Collagenase P	Roche Diagnostics Deutschland GmbH, Mannheim, Germany
Copper (II) sulphate	Carl Roth GmbH & Co. KG, Karlsruhe, Germany
Coumarin	Fluka Chemie GmbH, Steinheim, Germany
D-(+)-glucose	Sigma Aldrich Chemie GmbH, Steinheim,Germany
Deoxyribonucleoside (dNTPs)	Axon, Kaiserslautern, Germany
Diethylpyrocarbonate (DEPC)	Carl Roth GmbH & Co. KG, Karlsruhe, Germany
Dibenzylfluorescein	Sigma Aldrich Chemie GmbH, Steinheim,Germany
Diclofenac	Sigma Aldrich Chemie GmbH, Steinheim,Germany
Dimethylsufoxide (DMSO)	Carl Roth GmbH & Co. KG, Karlsruhe, Germany
DMEM (10x)	Biochrom AG, Berlin, Germany

Easycoll Separating Solution	Biochrom AG, Berlin, Germany
EGTA	Carl Roth GmbH & Co. KG, Karlsruhe, Germany
Ethanol	Carl Roth GmbH & Co. KG, Karlsruhe, Germany
Ethidium bromide	Carl Roth GmbH & Co. KG, Karlsruhe, Germany
Ethylendiamine tetraacetic acid disodium salt dehydrate	Carl Roth GmbH & Co. KG, Karlsruhe, Germany
Folin & Ciocalteu's phenol reagent	Sigma Aldrich Chemie GmbH, Steinheim,Germany
Fluorescein	Sigma Aldrich Chemie GmbH, Steinheim,Germany
Glucose oxidase	Sigma Aldrich Chemie GmbH, Steinheim,Germany
Glycerol	Carl Roth GmbH & Co. KG, Karlsruhe, Germany
Griseofulvin	Sigma Aldrich Chemie GmbH, Steinheim,Germany
Hydrochloric acid	Carl Roth GmbH & Co. KG, Karlsruhe, Germany
Isopropanol	VWR, Leuven, Belgium
Magnesium chloride	Carl Roth GmbH & Co. KG, Karlsruhe, Germany
Magnesium chloride 25 μM	Axon, Kaiserslautern, Germany
Monochlorobimane	Sigma Aldrich Chemie GmbH, Steinheim,Germany
Na-K Tartrate	Sigma Aldrich Chemie GmbH, Steinheim,Germany
N-Acetyl-L-Cysteine	Carl Roth GmbH & Co. KG, Karlsruhe, Germany
N-(1-naphthyl)ethylenediamine dihydrochloride	Sigma Aldrich Chemie GmbH, Steinheim,Germany

O-Dianisidine	Sigma Aldrich Chemie GmbH, Steinheim,Germany
O-Phthalaldehyde	Sigma Aldrich Chemie GmbH, Steinheim,Germany
Ornithine	Sigma Aldrich Chemie GmbH, Steinheim,Germany
Peroxidase	Sigma Aldrich Chemie GmbH, Steinheim,Germany
Potassium chloride	Carl Roth GmbH & Co. KG, Karlsruhe, Germany
Probenecid	Sigma Aldrich Chemie GmbH, Steinheim,Germany
pUC 19	Carl Roth GmbH & Co. KG, Karlsruhe, Germany
Reaction buffer BD	Axon, Kaiserslautern, Germany
Resazurin sodium salt	Sigma Aldrich Chemie GmbH, Steinheim,Germany
Resorufin sodium salt	Sigma Aldrich Chemie GmbH, Steinheim,Germany
Rhodamine 123	Sigma Aldrich Chemie GmbH, Steinheim,Germany
Salicylamide	Fluka Chemie GmbH, Steinheim, Germany
Sodium carbonate	Carl Roth GmbH & Co. KG, Karlsruhe, Germany
Sodium chloride	VWR, Leuven, Belgium
Sodium hydroxide	Carl Roth GmbH & Co. KG, Karlsruhe, Germany
Sodium-L-lactate	Sigma Aldrich Chemie GmbH, Steinheim,Germany
Sodium pyruvate	Sigma Aldrich Chemie GmbH, Steinheim,Germany
Sulfuric acid	Carl Roth GmbH & Co. KG, Karlsruhe, Germany

Taq DNA Polymerase, 1000U	Axon, Kaiserslautern, Germany
Tissue glue (Histoacryl)	B-Braun Melsungen AG, Melsungen, Germany
peqGOLD TriFast™	Peqlab Biosysteme GmbH, Erlangen, Germany
TRIS(hydroxymethyl)aminomethane	Applichem GmbH, Darmstadt, Germany
Trypan Blue 0,5%	Carl Roth GmbH & Co. KG, Karlsruhe, Germany
Urea	Carl Roth GmbH & Co. KG, Karlsruhe, Germany

2.1.4. Culture media and supplements

Table 2. 4 Culture media and supplements

Culture media and suplements	Company
Amino acids	PAA Lab. GmbH, Traun, Austria
DMEM high glucose, 4.5 g/L	PAA Lab. GmbH, Traun, Austria
FCS	Gibco, Paisley, UK
HEPES	PAA Lab. GmbH, Traun, Austria
Hydrocortisone	Pfizer, Berlin, Germany
Insulin (100E/ml)	Novo Nordisk, Bagsvaerd, Denmark
L-Glutamine	PAA Lab. GmbH, Traun, Austria
PBS	PAA Lab. GmbH, Traun, Austria
Penicillin / streptomycin	PAA Lab. GmbH, Traun, Austria
Sodium pyruvate	PAA Lab. GmbH, Traun, Austria
Trypsin / EDTA	PAA Lab. GmbH, Traun, Austria
Williams medium E	Sigma Aldrich Chemie GmbH, Steinheim, Germany

2.1.5. Items used (Kits)

Table 2. 5 Kits

Kit	Company
First Strand cDNA Synthesis	Thermo Fisher Scientific GmbH, Schwerte, Germany
Fluitest® LDH-L	Analyticon Biotechnologies AG, Lichtenfels, Germany
Fluitest® GOT AST	Analyticon Biotechnologies AG, Lichtenfels, Germany
Fluitest® GPT ALT	Analyticon Biotechnologies AG, Lichtenfels, Germany

2.1.6. Software

Table 2. 6 Software

Program	Company
EndNote X5	Japone / Team LnDL, Thomas Reuters, San Francisco, USA
Graph Pad Prism 5.01	GraphPad Software Inc., San Diego, USA
ImageJ 1.45s	National Institute of Health, Maryland, USA
Intas Image software	Imaging Instruments GmbH, Göttingen, Germany
OMEGA software for FLUOstar, V1.10	BMG Labtech, Offenburg, Germany
Xcalibur 2.0.7. software	Thermo Fisher Scientific, Dreieich, Germany

2.2. Methods

2.2.1. Isolation of primary human hepatocytes

The hepatocytes were isolated from resected liver capsules of tumor patients. Every patient had signed a consent form according to the ethical guidelines (368/2012BO2) of the Medical faculty of the Eberhard-Karls University Tübingen beforehand. PHH were isolated from resected livers by a two-step collagenase P perfusion technique (Figure 2.1.).

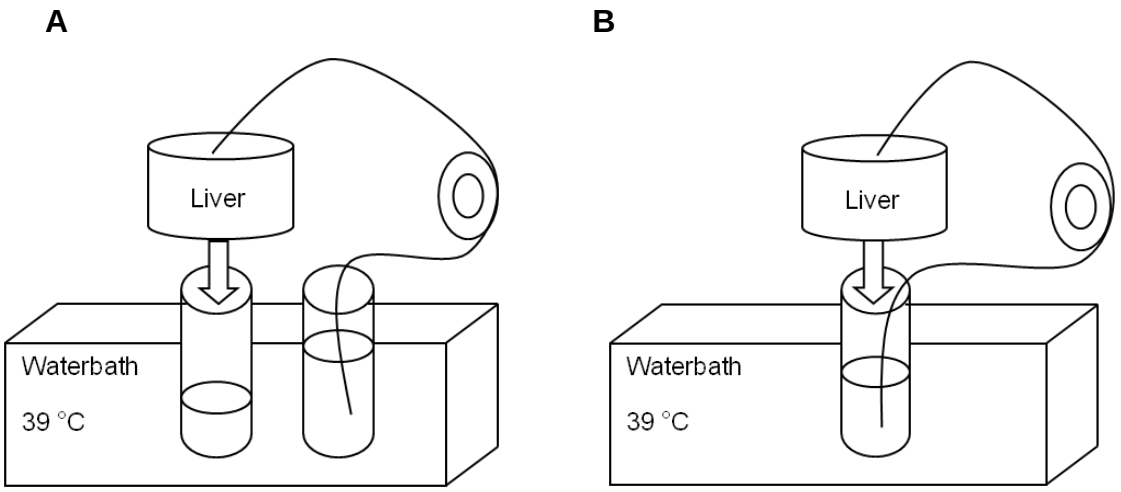

Figure 2. 1 Schematic representation of the two-step perfusion technique. **(A)** Step 1: Perfusion solution I was used to remove residual blood from the vessels and to warm up the tissue **(B)** Step 2: Perfusion solution II containing collagenase P was recirculated to digest the liver tissue structure [84].

Perfusion solution I (142 mM NaCl, 6.7 mM KCl, 10 mM Hepes, 240 mM EGTA, 500 mM N-Acetyl-L-cysteine, pH = 7.4) was used to rinse the resected liver in order to eliminate the residual blood. In addition, it warmed up the liver tissue in order to facilitate the digestion of the tissue by the collagenase P. Then, perfusion solution II (67 mM NaCl, 6.7 mMl KCl, 100 mM HEPES, 0.5% albumin, 4.8 mM $CaCl{\cdot}2H_2O$, pH = 7.6) containing collagenase P was recirculated in order to facilitate the digestion of the liver tissue structure by releasing the hepatocytes. The digested tissue was treated with ice-cold DPBS containing 20% FCS to stop the over-digestion of the tissue by the collagenase P. The hepatocytes that had been suspended in DPBS (20% FCS) were filtrated with a plastic funnel containing aseptic gauze to separate tissue debris. Finally, an

additional washing step was performed and the hepatocytes were re-suspended in DPBS. Cell viability was determined by Trypan blue exclusion using a Neubauer hematocytometer. If the cell viability was below 70%, the living cells were separated from the dead cells by density gradient centrifugation with Percoll® [75, 85].

2.2.2. Isolation of collagen from rat tails

Collagen for cell culture was isolated from rat tails. The collagen tendons were isolated by breaking the skinned tails between every vertebra and pulling the tendons out. Then, the collagen fibers were air-dried and sterilized under UV radiation; 4.2 g of dried collagen fibers were stirred for 48 h in 500 ml of 1% acetic acid solution in order to solubilize the collagen. The protein concentration was determined by Lowry assay [86].

2.2.3. Optimization of the number of PHH in 3D

Cells that are cultured in collagen gel dispose of a greater surface area than those cultured in monolayer. The optimization of the cell number was performed with Huh-7 cells, as their size is comparable to that of PHH. The optimal cell density was determined by seeding different cell numbers, from $100*10^3$ cells to $250*10^3$ cells, in a 96-well plate. Then, resazurin conversion was performed in order to determine the highest viability among the different cell numbers.

2.2.4. Cultivation of PHH

In monolayer cultures, isolated hepatocytes were cultured in Williams' medium E (10% FCS, 1 µM insulin, 15 mM HEPES, 0.8 µg/ml hydrocortisone, 100 U/ml penicillin and 100 µg/ml streptomycin, 1% L-glutamine, 1% non-essential amino acids, 1 mM sodium pyruvate) overnight on collagen-coated culture plates with a density of $1.5*10^5$ cells/cm^2 in monolayer cultures. Afterwards, the cells were washed with DPBS and the medium was replaced. In collagen sandwich cultures, 1:10 volume of 10× DMEM with phenol red and 1:100 volume of penicillin and streptomycin were dissolved in collagen stock solution. The pH was neutralized to 7.2-7.3 with NaOH. Each step was conducted on ice under

agitation in order to avoid collagen polymerization. The final collagen concentration was 2 mg/ml; 400 µl of collagen solution was spread into 10 cm^2 wells (6-well plates). After the polymerization of the gel, the PHH were seeded onto 6-well plates that have been prepared as described above. The cell density has to ensure cell confluence, $1.5*10^5$ cells/cm^2, as lower cell number favors the synthesis of nitric oxide [87]. Following the cell attachment, a second layer of collagen was added. In contrast to sandwich cultures, hepatocytes were re-suspended at $5*10^3$ cells/µl of collagen and 30 µl of PHH re-suspended in collagen was loaded in 96-well plates. After collagen polymerization, Williams' medium E was added in both 3D cultures [88].

2.2.5. Static cultures

2.2.5.1. Collagen sandwich

PHH are used in *in vitro* toxicity tests, however, monolayer cultures (2D) have limitations and several drug toxicities observed *in vivo* cannot be reproduced in 2D *in vitro* models, like *e.g.* acetaminophen. Acetaminophen is a worldwide drug used due its therapeutic properties [2, 89], but an overdose can cause acute liver failure [3]. PHH were stimulated with acetaminophen over 72 h because it has been proved that hepatocytes can metabolize and show toxicity after the administration of acetaminophen during 72 h [74]. Therefore, PHH were cultured in monolayer and in collagen sandwich (3D) in order to investigate molecular differences during acetaminophen stimulation.

2.2.5.1.1. Cell morphologies

PHH were cultured over 11 days. Cell morphology was investigated by taking light micrographs with a microscope of PHH at different days, like *e.g.* day 1, day 3, and day 11.

2.2.5.1.2. Acetaminophen toxicity

Primary human hepatocytes in 2D or 3D culture were treated with different concentrations acetaminophen (APA), like *e.g.*, 0 mM, 0.25 mM, 0.5 mM, 1mM, 5 mM and 10 mM, for 72 h.

2.2.5.1.2.1. Live/Dead staining

Calcein AM is a cell-permeable non-fluorescent dye which is converted into green fluorescent calcein by cytosolic esterases [90] in the cell cytoplasm at an excitation wavelength of λ = 485 nm and at an emission wavelength of λ = 530 nm. In contrast, ethidium homodimer-1 can only enter cells with damaged membranes and produces a bright red fluorescent light when it interacts with the cell DNA at an excitation wavelength of λ = 530 nm and at an emission wavelength of λ = 645 nm. PHH were washed three times with DPBS. Then, the cells were stained with calcein AM (2µM) ethidium homodimer (4 µM) solution for 30 min and stored in a dark place. After the incubation time, the cells were washed three times with DPBS and pictures were taken with a fluorescence microscope [66, 91].

2.2.5.1.2.2. LDH, AST and ALT

Cellular damage was investigated by measuring lactate dehydrogenase (LDH) [92], aspartate aminotransferase (AST) [93], and alanine aminotransferase (ALT) [94] leakage in the culture supernatants with a commercially available reaction kit (Analyticon Biotechnologies, Lichtenfels, Germany). For reference purposes, absorbance was measured at 570 and 690 nm with a plate reader.

2.2.5.1.3. Gene expression of CYP2E1 and superoxide dismutase 1 (SOD1)

PHH RNA was isolated by using TriFast reagent, a ready-to-use reagent for the separation of RNA from most DNA and protein in 2D cultures. In collagen gel cultures (3D), a collagen digestion was performed previously by incubating the cells for 10 min at 37 ºC, 5% CO_2 with collagenase P (3 mg/ml) in DPBS. The quantity and the purity of RNA were determined by photometry which had been

obtained at 260 nm and 280 nm. The integrity of the RNA was checked by gel electrophoresis. Subsequently, the transcription of RNA to complementary DNA (cDNA) was performed with the First Strand cDNA Synthesis Kit (Fermentas). Then, reverse transcriptase PCR (RT-PCR) was performed. PCR is used to amplify a specific region of a DNA strand (the DNA target). It is based on thermal cycling and consists of cycles of repeated heating and cooling of the reaction in order to trigger DNA melting and the enzymatic replication of the DNA (see below).

Figure 2. 2 Representation of the PCR cycle. **(A)** Denaturation (95 ºC); separation of parent strands in order to prepare of new strand synthesis. **(B)** Annealing (52-65 ºC); the primers bind to the parent strands. **(C)** Extension (72 ºC); addition of nucleotides to the growing end of the DNA strand (3' end) by the Taq polymerase using the present strand as the template (http://users.ugent.be/~avierstr/principles/pcr.htm [30.05.2014l]).

All cDNA samples were diluted to a final concentration of 10 ng/µl. The composition of the master mix was prepared as follows:

Reaction Buffer B 10x (Mg^{2+} free)	2.0 µl (1x)
$MgCl_2$	2.0 µl
dNTP mix	0.5 µl
Taq DNA polymerase	0.1 µl
Forward Primer	1.0 µl
Reverse Primer	1.0 µl
Template	*Variable
H_2O PCR Grade	*Variable
Total volume	20 µl

Finally, the PCR tubes were sealed and placed in the thermal cycler and the respective thermal cycle conditions were set. In general, PCR consists of a succession of 20-40 repeated temperature changes, named cycles (Fig. 2.3) PCR cycle consists of a denaturation, an annealing and an elongation step. The

temperatures and the time of each step vary according to the melting temperature of the used primers and polymerase. Before cycling, an initialization step at high temperature (> 90 ºC) is performed. A final elongation step followed by a hold step is performed after the cycling. [95].

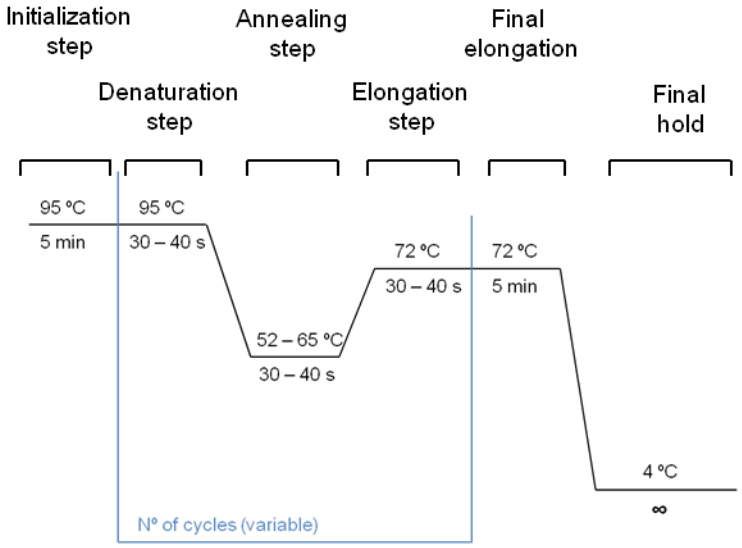

Figure 2. 3 Schematic representation of a program of the PCR cycle.

In table 2.7 (see below), all used primers are listed with their respective size and annealing temperature. The primer annealing temperatures, number of cycles and the amount of used cDNA were optimized by testing various conditions. All generated PCR products were separated by electrophoresis gel stained with ethidium bromide. Gene expression was quantified by the ImageJ 1.45 software (National Institute of Health, Maryland, USA).

Table 2. 7 Primer sequences used in RT-PCR.

Gen	Forward / Reverse primer 5'→3'	Annealing ºC	bp
CYP 2E1	GAC TGT GGC CGA CCT GTT	59	297
	AC ACG ACT GTG CCC TGG G		
SOD1	AAGGCCGTGTGCGTGCTGAA	62	243
	GTCTCCAACATGCCTCTCTTCATCC		
GAPDH	GTC AGT GGT GGA CCT GAC CT	56	420
	AGG GGT CTA CAT GGC AAC TG		

2.2.5.1.4. Protein expression of CYP2E1 and Superoxide Dismutase 1 (SOD1)

Western blot analysis, cells were collected by centrifugation and lysed in 0.5% Nonidet P40, 100 mM NaCl, 0.5% Deoxycholic acid, 10 mM EDTA and 10 mM Tris–HCl (pH 7.5) with the Complete Protease Inhibitor Cocktail (Roche, Mannheim, Germany) for 30 min in 2D cultures. In collagen gel cultures (3D), a collagen digestion was performed previously by incubating the cells for 10 min at 37 ºC, 5% CO_2 with collagenase P (3 mg/ml) in DPBS. Lysates were centrifuged at 10,000 × *g* for 10 min at 4 °C. Protein concentration was determined by micro-Lowry [86]. The proteins were separated by SDS-PAGE and transferred to nitrocellulose membranes (Carl Roth, Karlsruhe, Germany). Membranes were blocked for 1 h with 5% semi-skimmed milk in 0.1% Tween-20/PBS and incubated overnight with a primary antibody against SOD1 (mouse monoclonal antibody, Santa Cruz, Heidelberg, Germany), CYP2E1 and GAPDH (both rabbit polyclonal antibodies, Santa Cruz, Heidelberg, Germany). Proteins were visualized by secondary antibodies conjugated to horseradish peroxidase. Membranes were exposed to X-ray films and developed in a Curix 60 Developing processor (Agfa, Cologne, Germany). All primary antibodies were diluted at a ratio of 1:1,000, and all secondary antibodies at a ratio of 1:5,000 in 1% semi-skimmed milk in 0.1% Tween-20/PBS. Proteins were visualized using secondary antibodies conjugated to horseradish peroxidase. Membranes were exposed to X-ray films and developed in a Curix 60 Developing processor (Agfa, Cologne, Germany). The quantification was carried out with the ImageJ 1.45 software (National Institute of Health, Maryland, USA).

Table 2. 8 First antibody used in Western blot

Antibody	Isotype	Dilution	Size [KD]	Company
CYP 2E1	Rabbit IgG_1	1:1000	57	Santa Cruz, Heidelberg, Germany
SOD1	Mouse IgG_1	1:1000	24	Santa Cruz, Heidelberg, Germany
GAPDH	Rabbit IgG_1	1:1000	37	Santa Cruz, Heidelberg, Germany

Table 2. 9 Secondary antibody used in western blot

Antibody	Dilution	Company
Goat anti rabbit IgG1	1:5000	Santa Cruz, Heidelberg, Germany
Goat anti mouse IgG1	1:5000	Santa Cruz, Heidelberg, Germany

2.2.5.1.4. MRPs gene expression

The isolation, quantification, and purity check of RNA, as well as RT-PCR were performed as CYP2E1 and SOD1 gene expression (Section 2.2.5.1.3). In table 2.10. (see below), all the primers that were used in these experiments are listed with their respective size and annealing temperature. Gene expression was quantify by the ImageJ 1.45 software (National Institute of Health, Maryland, USA).

Table 2. 10 Primer sequences used for the RT-PCR.

Gen	Forward / Reverse primer 5'→3'	Annealing ºC	bp
MRP1	TTG GAT GAG GCC ACG GCA GC	58	247
	CTG GGG CTC ACA CCA AGC CG		
MRP2	AGA CGC AGT CCA GGA ATC ATG C	61	171
	CAC GTG GAG AAG CTG CCA GGG		
MRP3	CTG CCC CAG TTA ATC AGC AAC CTG	60	405
	GCG CTT GGG GTT CAG GGC TTT		
MRP4	TGA TCA CAG CCA GCC GCG TG	60	307
	ACG GGG CCG ACC ACA GCT AA		

2.2.5.1.5. MRP1 transporter activity assay

Multidrug resistance-associated protein 1 (MRP1) transport activity was investigated by using a modified carboxyfluorescein efflux assay [96]. Cells were seeded in 96-well plates; washed 3 times with DPBS and incubated with 4 µM of 5(6)-carboxy-2′,7′-dichlorofluorescein diacetate (5-CFDA) for 30 min. Wells without cells were used as background subtraction for 2D and 3D cultures.

The cells were washed 3 times with DPBS and a fluorescence measurement was conducted in order to determine the amount of 5-CFDA that had been taken up and metabolized to 5-carboxyfluorescein succinimidyl ester (5-CFSE) by the hepatocytes. Next, the cells were re-incubated with DPBS containing 11 mM glucose for 60 min. Supernatants were collected 5, 10, 20, 30, and 60 min after the incubation and transferred to a new 96-well plate in order to determine the amount of 5-CFSE that is eluted by the hepatocytes. The quantification was carried out by using a linear calibration curve of the linear standard curve (Fig. 2.4).

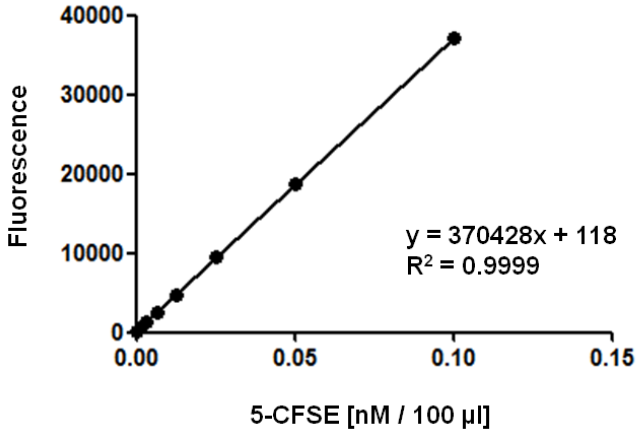

Figure 2. 4 Standard curve of 5-CFSE.

2.2.5.1.6. Quantification of Acetaminophen

The quantification of remaining acetaminophen was performed by LC/MS analysis. The samples were precipitated with twice the volume of acetonitrile supplemented with the internal standard (1 µM griseofulvin). After vigorous shaking (10 sec) and centrifugation for 5 min with 5000 g at RT, the particle-free supernatants were subjected to LC–MS/MS. The HPLC system consisted of an LC Plus pump and an auto sampler. Mass spectrometry was performed on a TSQ Quantum Discovery Max triple quadrupole mass spectrometer equipped with an electrospray interface and connected to a PC with the Xcalibur 2.0.7 standard software (Thermo Fisher Scientific, Dreieich, Germany). The flow rate of the HPLC pump was set to 600 µl/min and the compounds were separated

on a Kinetex PFP, 2.6 µm, 50 × 2.1 mm analytical column with Krudkatcher. The analytes were separated by gradient elution with acetonitrile/0.1% formic acid as the organic phase (A) and 10 mM ammonium acetate / 0.1% formic acid as the aqueous phase (B) (%A (t (min), 0 (0–0.2)–97 (0.8–1.8)–0 (2.0–4.0)). The MS–MS identification of characteristic fragment ions was performed using the following set of parameters: ion source temperature: 350 °C, capillary voltage: 3.8 kV, collision gas: 0.8 mbar argon, spray and sheath gas: 20 and 8 (arbitrary units), respectively. The stable product ions with the highest S/N ratio were used to quantify the test item in the selected reaction monitoring mode (SRM). The transitions used for the analysis were *m*/*z* 152.1 to *m*/*z* 65.0 and *m*/*z* 93.0 (acetaminophen) and *m*/*z* 353.0 to *m*/*z* 215.0 (griseofulvin, internal standard).

2.2.5.2. Collagen gels

One of the major problems to culture PHH is the short life span in 2D cultures

2.2.5.2.1. Cell morphology studies

PHH were cultured over 28 days. Cell morphology was investigated by taking light micrographs with a microscope of PHH at different days, like *e.g.* day 1, day 7, day 14, day 21, and day 28.

2.2.5.2.2. Cell viability

2.2.5.2.2.1. Live/Dead staining

Live/dead staining was performed as described in the section 2.2.5.1.2.1.

2.2.5.2.2.2. Resazurin conversion

Resazurin conversion is a fluorescence assay which can be used to measure proliferation, viability and toxicity (indirectly) in cells. The assay is based on the ability of living cells to convert a redox dye (resazurin) into an end product (resorufin). This conversion involves a colorimetric change which can be measured with fluorescence-based measuring instruments [97, 98].

Fluorescence was monitored at an excitation wavelength of 530-560 nm and an emission wavelength of 590 nm.

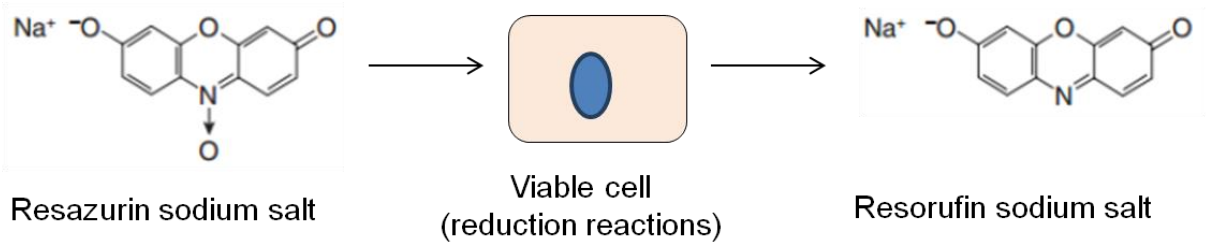

Figure 2. 5 Chemical structure of resazurin sodium salt and resorufin sodium salt.

The culture mediums were removed from the cells and washed twice with DPBS. Then the cells were incubated with 1:10 resazurin stock solution in plain medium (0.025%) in an incubator at 37 °C, 5% CO_2 for 2 h. Wells without cells were used as background subtraction for 2D and 3D cultures. The fluorescence was measured at an excitation wavelength of λ = 544 nm and at an emission wavelength of λ = 590-610 nm. The average background was subtracted from the other data [99].

2.2.5.2.3. Glucose production

Glucose production was studied through the gluconeogenesis process which takes mainly place in the liver and is based on the production of glucose from pyruvate.

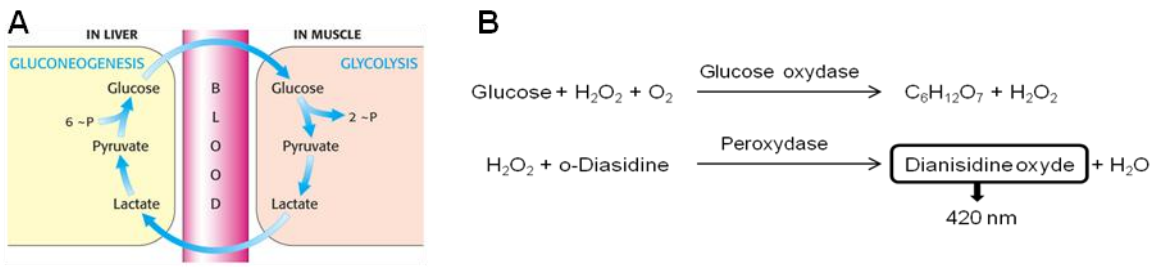

Figure 2. 6 Glucose cycle. **(A)** Schematic representation of the glucose cycle (http://www.uv.es/marcof/Tema17.pdf [28.10.2013]). **(B)** Glucose detection in the supernatant.

PHH were washed three times with DPBS. Then, one part of the cells was incubated with 150 µl (96-well plate) reaction buffer (1 mM $MgCl_2$ and 1 mM

sodium pyruvate in DPBS), while the other part was incubated with 150 µl of 11 mM L-lactate reaction buffer for 24 h at 37 ºC, 5% CO_2. Wells without cells were used as background subtraction for 2D and 3D cultures. After 24 h, 100 µl of culture supernatants were transferred to a new 96-well plate for glucose quantification. Simultaneously, a glucose standard curve was prepared in the same 96-well plate. Then, 150 µl of GLOX solution (250 mM TRIS, 0.2 mM EDTA, 0.04% glucose oxidase, 0.01% o-Dianisidine, 0.007% peroxidase, pH = 8.0) was added in every well and incubated for 2 h at 37 ºC, 5% CO_2. After the incubation time, the absorption was measured at a wavelength of λ = 425 nm with a plate reader [100].

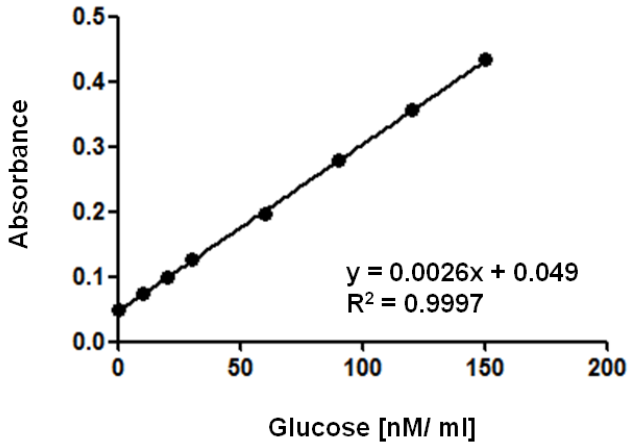

Figure 2. 7 Glucose standard curve.

2.2.5.2.4. Ammonia detoxification

The urea production was measured by the photometric determination of urea, a decomposition product of ammonia in PHH. PHH were washed three times with DPBS. Then, the cells were incubated with 100 µl (96-well plate) of 300 mM NH_4Cl in reaction buffer (1 mM MgCl2 and 1 mM sodium pyruvate in DPBS) for 24 h at 37 ºC, 5% CO_2. Wells without cells were used as background subtraction for 2D and 3D cultures. After 24 h, 80 µl of culture supernatant were transferred to a new 96-well plate for urea quantification. Simultaneously, a urea standard curve was prepared in the same 96-well plate. Then, 60 µl of o-

Phthalaldehyde solution (1.5 mM o-Phthalaldehyde, 4 mM Brij-35, 0.75 M H_2SO_4) and 60 µl of NED's reagent (2.3 mM N-(1-naphthyl) ethylenediaminedihydrochloride, 0.08 M boric acid, 4 mM Brij-35, 2.25 M H_2SO_4) were added in each per well and incubated for 2 h at 37 ºC, 5% CO_2. After the incubation time, the absorption was measured at a wavelength of λ = 460 nm with a plate reader [101, 102].

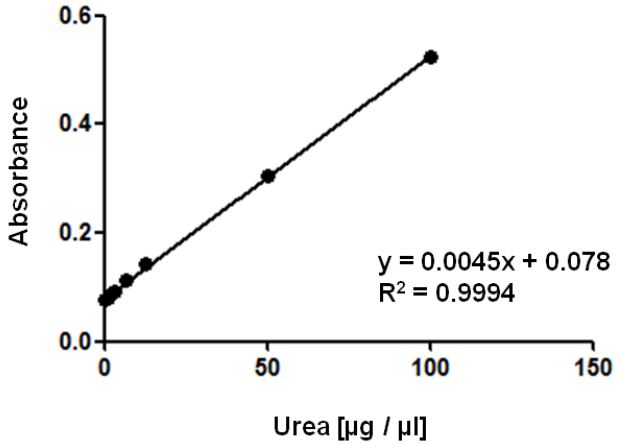

Figure 2. 8 Urea standard curve.

2.2.5.2.5. Enzymatic activity of Cytochrome P450

2.2.5.2.5.1. Cytochrome P450 gene expression

The isolation, quantification and purity check of RNA, as well as RT-PCR were performed as CYP2E1 and SOD1 gene expression (Section 2.2.5.1.3). In table 2.11. (see below), all the primers that were used in these experiments are listed with their respective size and annealing temperature. Gene expression was quantified by the ImageJ 1.45 software (National Institute of Health, Maryland, USA).

Table 2. 11 Primer sequences used in RT-PCR.

Gen	Forward / Reverse primer 5'→3'	Annealing ºC	bp
CYP 1A1	TTC GTC CCC TTC ACC ATC	55	302
	CTG AAT TCC ACC CGT TGC		
CYP 1A2	TCG ACC CTT ACA ATC AGG TGG	60	254
	GCA GGT AGC GAA GGA TGG G		
CYP 2A6	CAA CCA GCG CAC GCT GGA TC	60	423
	CCA GCA TAG GGT ACA CTT CG		
CYP 2B6	ATG GGG CAC TGA AAA AGA CTG A	62	283
	AGA GGC GGG GAC ACT GAA TGA C		
CYP 2C8	CAT TAC TGA CTT CCG TGC TAC AT	60	147
	CTC CTG CAC AAA TTC GTT TTC		
CYP 2C9	CTG GAT GAA GGT GGC AAT TT	59	308
	AGA TGG ATA ATG CCC CAG AG		
CYP 2D6	CTT TCG CCC CAA CGG TCT C	59	222
	TTT TGG AAG CGT AGG ACC TTG		
CYP 2E1	GAC TGT GGC CGA CCT GTT	59	297
	AC ACG ACT GTG CCC TGG G		
CYP 3A4	ATT CAG CAA CAA GAA CAA GGA CA	64	314
	TGG TGT TCT CAG GCA CAG AT		
GAPDH	GTC AGT GGT GGA CCT GAC CT	56	420
	AGG GGT CTA CAT GGC AAC TG		

2.2.5.2.5.2. Phase I (CYPs) and phase II enzymatic activity

The enzymatic activity was analyzed with a modified fluorescence-based method [103, 104]. PHH were incubated for 2 h at 37 ºC with different substrates diluted in plain medium (Tables 2.12. and 2.13.). The cells converted to a metabolite. These conversions produced a change in fluorescence which was measured with a plate reader. Moreover, in the phase I substrates, 15 µl/ml salicylamide buffer (100 µM in DMSO), 10 µl/ml probenecid buffer (200 mM in

DMSO) and 1 µl/ml buffer dicoumarol buffer (10 mM in DMSO) were added to prevent spontaneous fluorescence decay. Wells without cells were used as background subtraction for 2D and 3D cultures.

Table 2. 12 Substrates used during the study of phase I.

Reaction	Substrate	Substrate conc.	Metabolite	Excitation/Emission
CYP 1A1/2	7-EC	25 µM	HC	355 nm/460 nm
CYP 2A1	7-ER	7.5 µM	Res	544 nm/590 nm
CYP 2A6	Cou	50 µM	HC	355 nm/460 nm
CYP 2B6	EFC	30 µM	HFC	355 nm/520 nm
CYP 2C8/9	DBF	12.5 µM	FL	485 nm/520 nm
CYP 2D6	AMMC	10 µM	AHMC	355 nm/460 nm
CYP 2E1	MFC	5 µM	HFC	355 nm/520 nm
CYP 3A4	BFC	5 µM	HFC	355 nm/520 nm

Table 2. 13 Substrates used during the study of phase II.

Reaction	Substrate	Substrate conc.	Excitation / Emission
Resorufin conjugation	Res	25 µM	355 nm/460 nm
GSH conjugation	MCB	7.5 µM	544 nm/590 nm
UGT activity	4-MU	50 µM	355 nm/460 nm
HC conjugation	HC	30 µM	355 nm/520 nm
HFC conjugation	HFC	12.5 µM	485 nm/520 nm
FL conjugation	FL	10 µM	355 nm/460 nm
AHMC conjugation	AHMC	5 µM	355 nm/520 nm
CHC conjugation	CHC	5 µM	355 nm/520 nm

The measured values were quantified by using their respective standard curves.

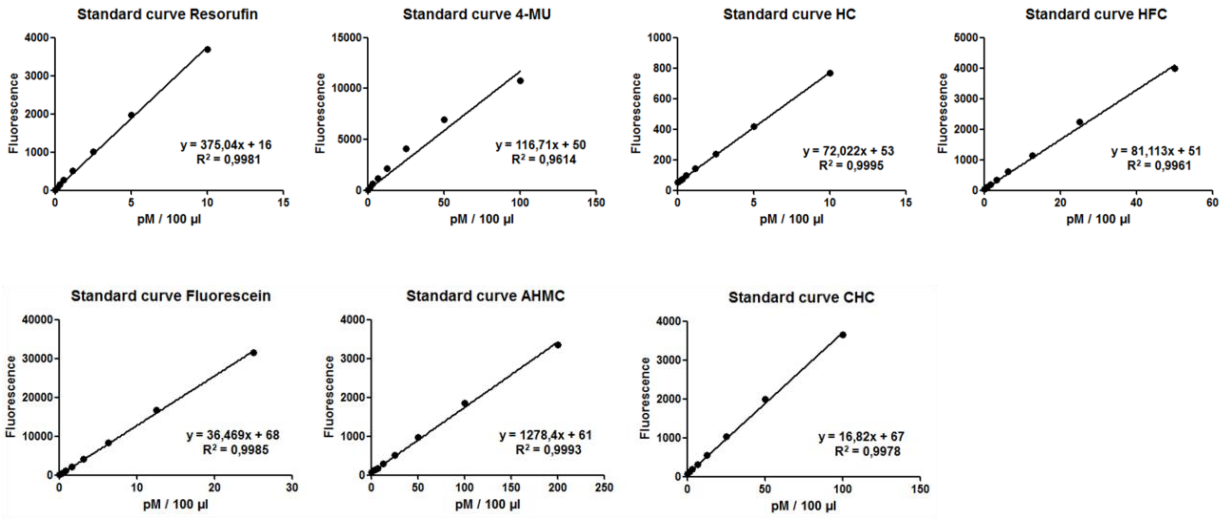

Figure 2. 9 Standard curves of the studied enzymatic products.

2.2.5.2.6. Efflux assays

2.2.5.2.6.1. Gene expression of the transporter channels

The isolation, quantification and purity check of RNA, as well as RT-PCR were performed as CYP2E1 and SOD1 gene expression (Section 2.2.5.1.3). In table 2.14 (see below), all the primers that were used in these experiments are listed with their respective size and annealing temperature. Gene expression was quantified by the ImageJ 1.45 software (National Institute of Health, Maryland, USA).

Table 2. 14 Primer sequences used for the RT-PCR.

Gen	Forward / Reverse primer 5'→3'	Annealing ºC	bp
NTCP	CCC TCA CGG CCT TTG TGC TGG	60	394
	ACT GTG ACG GCC ACA CTG CAC		
OCT1	CTG GTC GAA ATC CCG GGG GC	60	363
	CAG GCC CAA CAC CGC AAA CAA		
MDR1	ATC CGG GCC GGG AGC AGT CA	61	252
	ATT CCG ACC TCG CGC TCC TTG		
MDR2	GGA ATT GGT GAC AAG GTT GG	61	395
	ATA CCA GAA GGC CAG TGC AT		
MDR3	TGG CCA GGC TGC CCC ATG TA	61	245
	CAA CCA GGG CCA CCG TCT GC		
MRP1	TTG GAT GAG GCC ACG GCA GC	58	247
	CTG GGG CTC ACA CCA AGC CG		
MRP2	AGA CGC AGT CCA GGA ATC ATG C	61	171
	CAC GTG GAG AAG CTG CCA GGG		
MRP3	CTG CCC CAG TTA ATC AGC AAC CTG	60	405
	GCG CTT GGG GTT CAG GGC TTT		
MRP4	TGA TCA CAG CCA GCC GCG TG	60	307
	ACG GGG CCG ACC ACA GCT AA		
MRP5	GGG CCA GAC GCT GCT TCC CT	61	228
	AAG CGA CCA AGA CCG CAC GAT		
MRP6	TTG GAA AAT CCA ACA GGG AAC GCC	62	190
	CTG CTG GGC AGC GTT GGT AGC		
BSEP	GGT CGT TGG CTG TGG GTT GC	61	266
	AGC ACG CCT GGC TGG GCT AT		
BCRP	CTC CGA GCG CAC GCA TCC TG	61	153
	AGC TGT CGC GGG GAA GCC AT		
GAPDH	GTC AGT GGT GGA CCT GAC CT	56	420
	AGG GGT CTA CAT GGC AAC TG		

2.2.5.2.6.2. Transporter channel activity

2.2.5.2.6.2.1. Multidrug resistance-associated protein-1

MRP1 transport activity was investigated as described in the section 2.2.5.1.5.

2.2.5.2.6.2.2. Multidrug resistance P-glycoprotein

Multidrug resistance P-glycoprotein (MDR1/P-gp) transport activity was investigated by using a modified rhodamine 123 efflux assay [96]. Cells were seeded in 96-well plates, washed 3 times with DPBS, and incubated with 3 µM of rhodamine 123 for 30 min. Wells without cells were used as background subtraction for 2D and 3D cultures. The cells were washed 3 times with PBS and a fluorescence measurement was conducted in order to determine the amount of rhodamine 123 that had been taken up by the hepatocytes. The cells were re-incubated in DPBS containing 11 mM glucose for 60 min. Supernatants were collected 5, 10, 20, 30, and 60 min after the incubation and transferred to a new 96-well plate in order to determine the amount of rhodamine 123 eluted by the hepatocytes. The quantification was carried out by using a linear calibration curve of the linear standard curve.

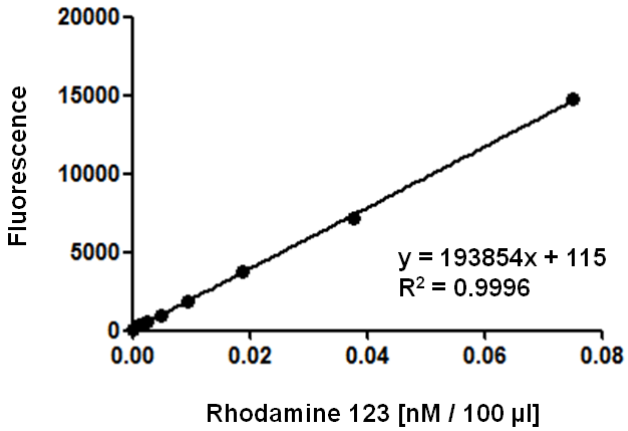

Figure 2. 10 Standard curve of Rhodamine 123.

2.2.5.7. Drug toxicity

PHH that were seeded in 96-well plates were washed twice with DPBS. Then, they were stimulated for 72 h with various concentrations of acetaminophen (0-10 mM in medium) and diclofenac (0-1 mM in medium). Wells without cells were used as background subtraction for 2D and 3D cultures. The experimental set up was as follows:

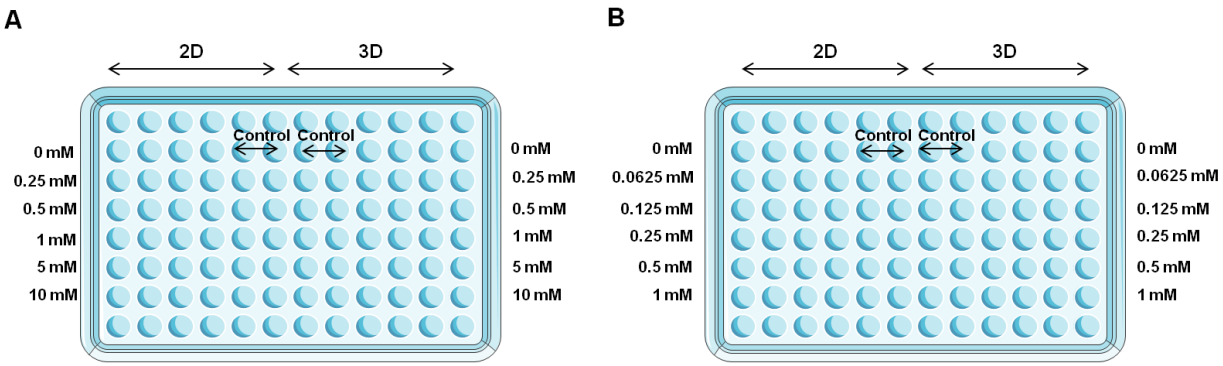

Figure 2. 11 Representation of the experimental set-up. **(A)** Acetaminophen, **(B)** Diclofenac.

After the stimulation, the cell supernatants were removed. The viability of the cells was measured as described in section 2.2.5.2.2.2 (resazurin conversion) and the results were indicated as % of the untreated control.

2.2.6. Flow culture

2.2.6.1. Perfusion assays

Perfusion assays were performed in order to determine an appropriate flow rate which allows for a homogeneous diffusion of the medium in the µ-slide channels. Collagen gel (2 mg/ml; Section 2.2.2) was loaded into the µ-slide channels, first without cells, and then with cells. Resazurin sodium salt in DPBS (0.025%) was pumped through the channels by using a syringe pump with different flow rates: 100 µl/h, 800 µl/h, 2 ml/h.

2.2.6.2. Cell culture

Isolated PHH were resuspended in collagen gel (2 mg/ml) with a density of $5*10^3$ cells/µl. The µ-slide channels and the 96-well plate were loaded with 30 µl of collagen gel containing PHH. After the collagen polymerization, µ-slide system was set up. The microfluidic system has the following components (Fig. 2.12):

- µ-slide; used as a cell culture platform and fixed at the height of 14.5 cm.
- Falcon tubes (50 ml); used as medium reservoirs and fixed at the height of 11 cm.
- Luer connectors which connect the µ-slide with the tubing.
- Y connectors which connect the tubing.
- Tubing.
- Syringe pump; used as flow supplier.
- Falcon tubes (15 ml); used to collect the eluted medium.

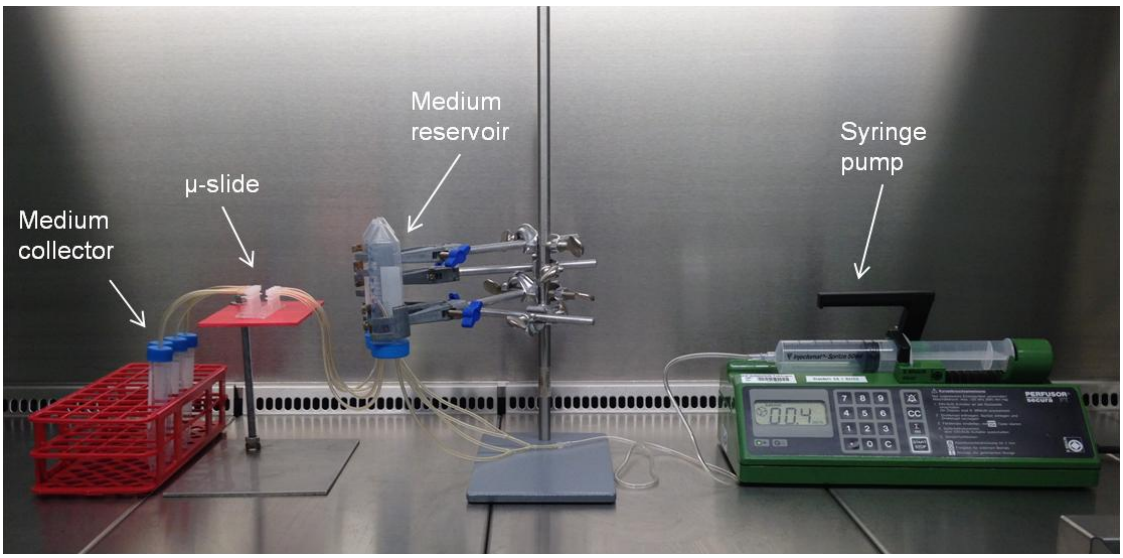

Figure 2. 12 µ-slide flow system.

2.2.6.3. Cell morphology studies

PHH were cultured over 7 days. Cell morphology was investigated by taking light micrographs with a microscope of PHH at day 1 and day 7.

2.2.6.4. Cell viability

2.2.6.4.1. Live/Dead staining

After day 1 and day 7 of culture, the µ-slide was removed from the µ-slide system. Then, collagen gels containing PHH were removed from the µ-slide and placed in a 24-well plate. Live/dead staining was performed as described in the section 2.2.5.1.2.1.

2.2.6.4.2. Resazurin conversion

After day 1 and day 7 of culture, the µ-slide was removed from the system. Then, collagen gels containing PHH were removed from the µ-slide and placed in a 96-well plate in order to make a proper comparison with the static cultures. Resazurin conversion was measured as described in the section 2.2.5.2.2.2.

2.2.6.5. Glucose production

After day 1 and day 7 of culture, the µ-slide was removed from the system. Then, collagen gels containing PHH were removed from the µ-slide and placed in a 96-well plate in order to make a proper comparison with the static cultures. Glucose production was measured as described in the section 2.2.5.2.3.

2.2.6.6. Enzymatic activity of CYP2E1 and CYP3A4

After day 1 and day 7 of culture, the µ-slide was removed from the system. Then, collagen gels containing PHH were removed from the µ-slide and placed in a 96-well plate in order to make a proper comparison with the static cultures. CYP2E1 was investigated by stimulating the hepatocytes with 100 µM of acetaminophen and CYP3A4 with 10 µM of diclofenac. The quantification of the remaining acetaminophen and diclofenac; as well as of their respective

products acetaminophen-sulfate and hydroxydiclofenac were performed by LC/MS analysis as described in the section 2.2.5.1.6.

2.2.6.7. Drug toxicity

After day 1 and day 7 of culture, the µ-slide was removed from the µ-slide system. Then, collagen gels containing PHH were removed from the µ-slide and placed in a 96-well plate in order to make a proper comparison with the static cultures. Hepatocytes were stimulated for 72 h with various concentrations of acetaminophen (0-10 mM in medium) and diclofenac (0-1 mM in medium). Wells without cells were used as background subtraction for 2D and 3D cultures. The viability of the cells was measured as described in section 2.2.5.2.2.2 (resazurin conversion) and the results were shown as % of the untreated control.

2.2.7. Statistics

All results were expressed as mean ± SD. For statistical analysis, the GraphPad Prism software was used. When two test conditions were analyzed, a t-test for spot checks was carried out. When three or more test conditions were observed, the statistical analysis was carried out by one-way analysis of variance (ANOVA) and by Bonferroni's multiple t test, followed by a multiple comparison test. The GraphPad Prism software was used to perform statistical analysis, $p < 0.05$ was set as a threshold for statistical significance.

3. Results

3.1. Static cultures

3.1.1. Collagen sandwich

3.1.1.1. Cell morphology studies

PHH morphology was investigated by observing the cells under the microscope (Fig. 3.1). PHH that were cultured with the 3D collagen sandwich technique maintained a hexagonal shape over the time of culture. However, PHH in 2D cultures gained a planar and fibroblast-like appearance after having been cultured for several days. In addition, after day 11 of culture, hepatocytes in 2D died and detached from the plate.

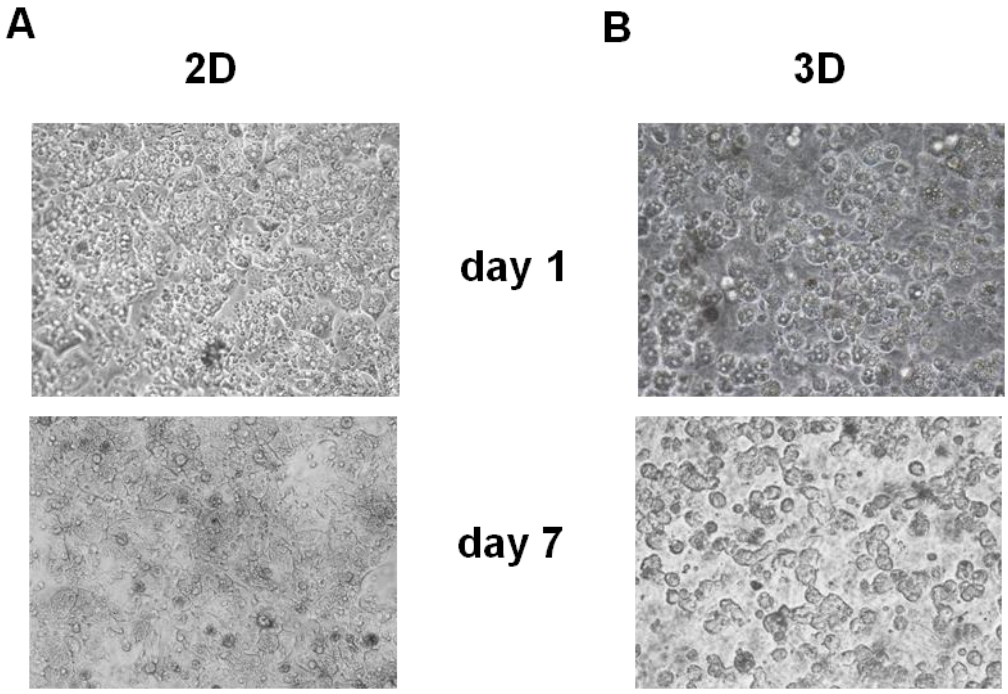

Figure 3. 1 PHH preserve their morphology over the cell culture period in collagen gel, day 1, day 3 and day 11 (x100 magnification). **(A)** 2D culture; **(B)** 3D sandwich culture [105].

3.1.1.2. Acetaminophen toxicity

3.1.1.2.1. Live/Dead staining

PHH cultures on collagen monolayer and collagen sandwich were stimulated with different concentrations of APA for 72 h. An increased number of dead cells were observed in 3D, but not in 2D cultures (Fig. 3.2 A). The quantification of the fluorescence signal revealed that the drug sensitivity was concentration-dependent (Fig. 3.2 B). The treatment with 1 mM, 5 mM and 10 mM acetaminophen led to a significant increase of the fluorescence intensity (**$p < 0.01$; *$p < 0.001$) (up to 40%, 40% and 50%, respectively). This corresponded to an increase of dead cells in comparison to the untreated cells. Even at 10 mM acetaminophen, no increase in the number of dead cells was detectable in the standard 2D culture. The untreated control in each culture condition was set to 1.

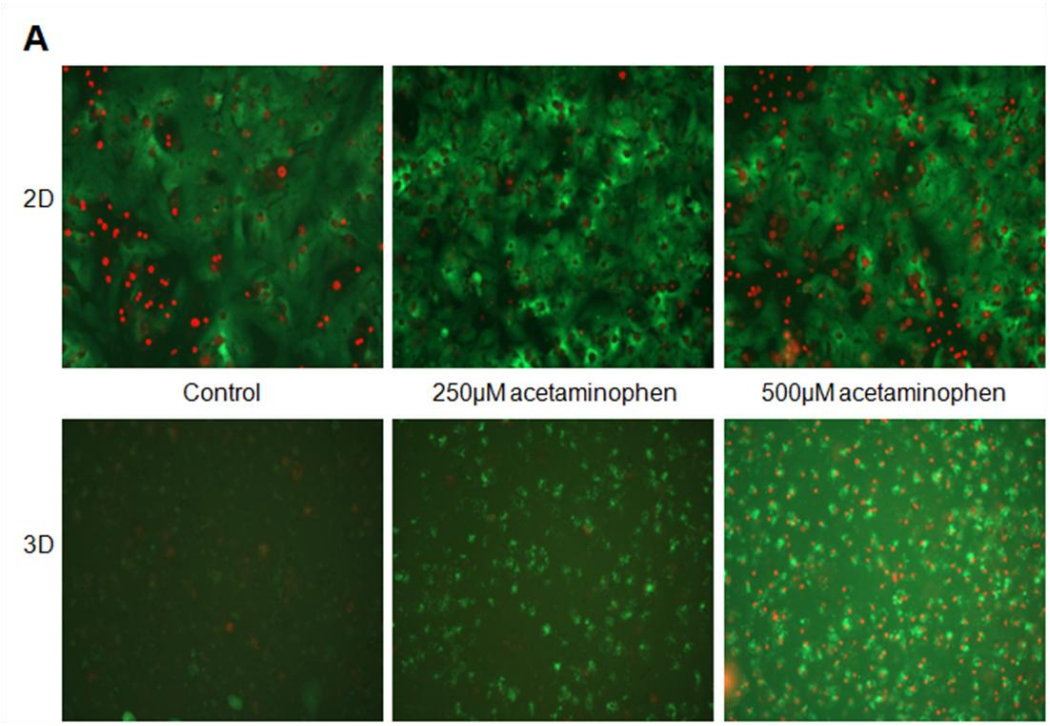

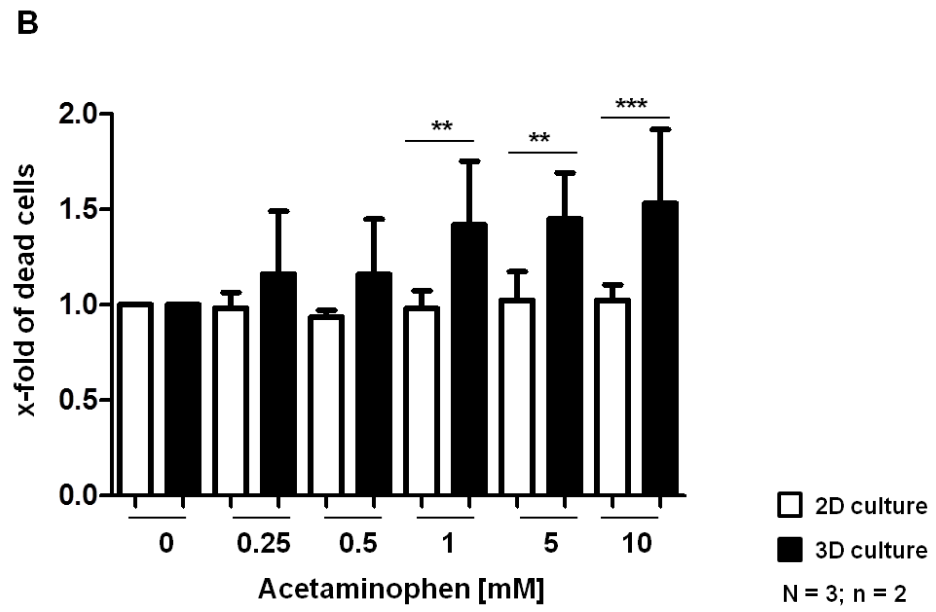

Figure 3. 2 Microscopic observation of PHH in standard 2D and in 3D sandwich cultures after the treatment with varying concentrations of acetaminophen for 72 h **(A)**. Quantification of dead cells stained by a fluorescent dye in each culture condition, the untreated control in each culture condition was set to 1 **(B)**. **p < 0.01; *p < 0.001, N=3, n=2 [105].

3.1.1.2.2. LDH, AST and ALT

Concentration-dependent release of LDH (Fig. 3.3.A), AST (Fig. 3.3.B), and ALT (Fig.3.3.C) was detected in 3D cultures treated with acetaminophen. The incubation with acetaminophen in 3D cultures led to a dose-dependent, but statistically insignificant increase of LDH, AST, and ALT levels at 72 h compared to 2D cultures. The release of LDH**,** AST, and ALT was measured in a fluorescence reader. In each culture condition, the untreated control was set to 1.

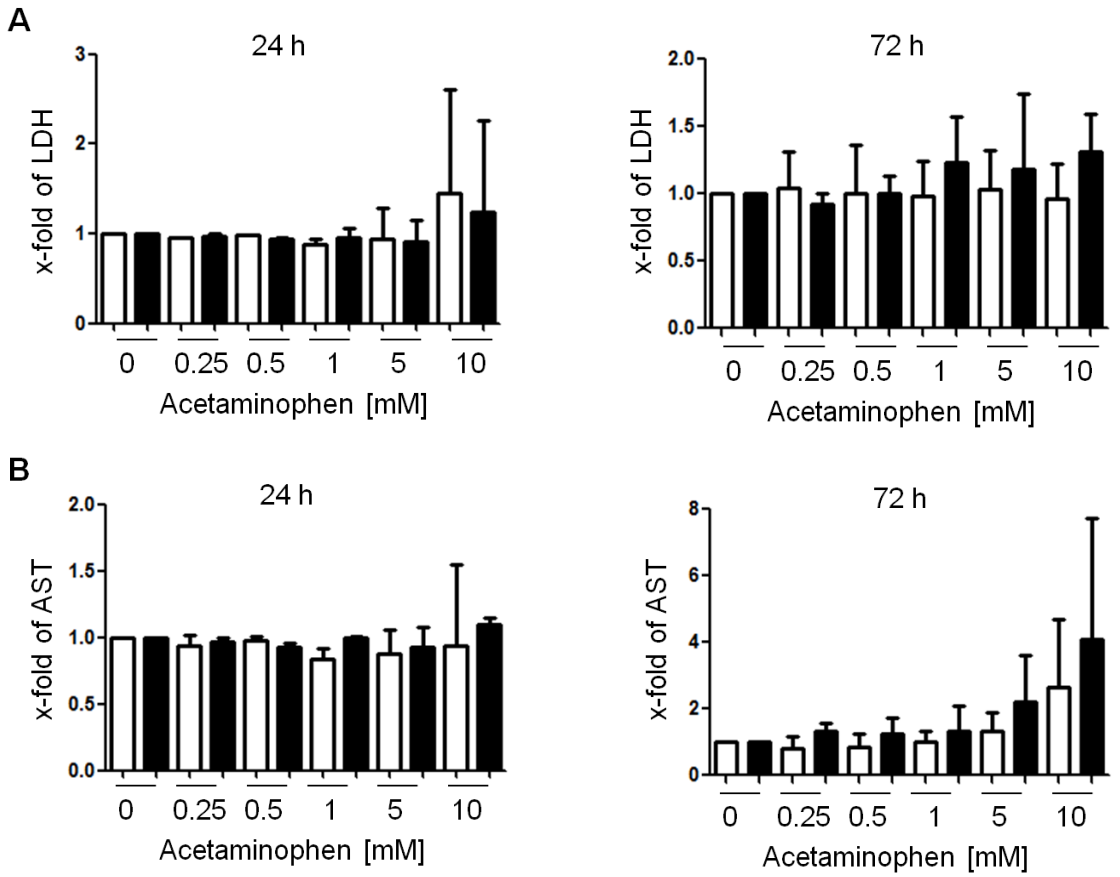

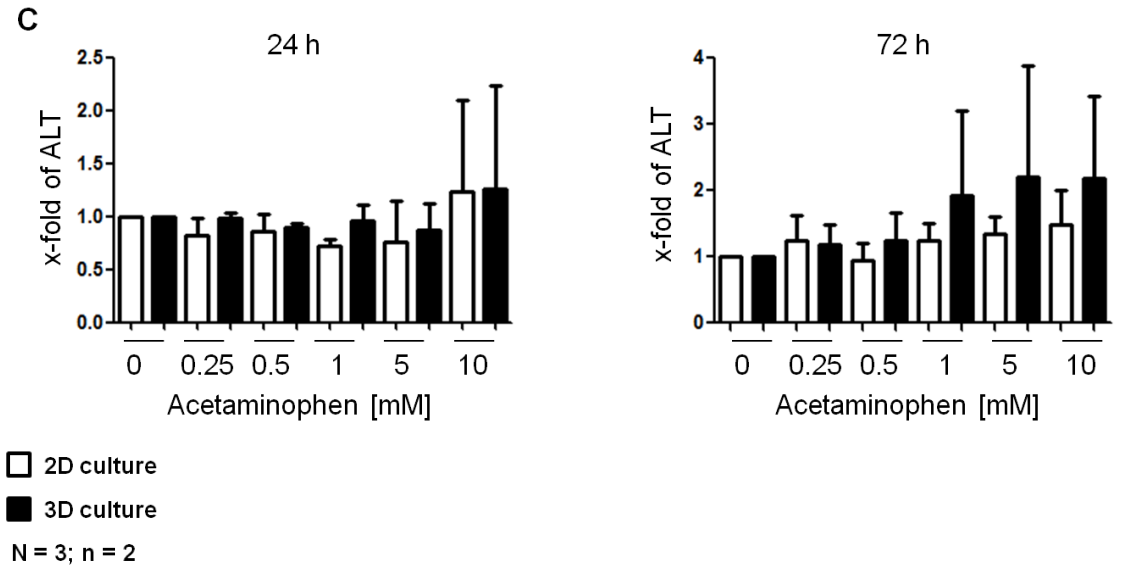

Figure 3. 3 Comparison of amount of LDH, AST, and ALT released by PHH after the treatment with acetaminophen for 24 h and 72 h in 2D and 3D cultures. The release of LDH **(A)**, AST **(B)** and ALT **(C)** was measured in a fluorescence reader. The untreated control was set to 1 [105].

3.1.1.3. Gene and protein expression of CYP2E1 and SOD1

CYP2E1 is involved in the formation of NAPQI, the reactive intermediate of acetaminophen. Therefore, the gene and protein expression of the CYP2E1 after the treatment with acetaminophen were compared between both culture models. No differences between 2D and 3D cultures were detected in the gene expression of CYP2E1 (Fig. 3.4 A and 3.4 B). At protein level, a concentration-dependent increase of the CYP2E1 was only observed in the 3D culture (Fig. 3.4 C). The quantification of the Western blot revealed a significant increase (*$p < 0.05$, **$p < 0.01$) in the expression of CYP2E1 after 72 h of up to 230%, 260%, and 310% in the presence of 1 mM, 5 mM and 10 mM acetaminophen in 3D cultures, while the protein expression remained unaffected in 2D (Fig. 3.4.D). Like CYP2E1, the antioxidant enzyme SOD1 gene expression indicated no difference between 2D and 3D cultures (Fig. 3.4 E and 3.4 F). However, the SOD1 protein expression gradually decreased after the treatment with acetaminophen and was undetectable after a treatment of 24 h with 10 mM acetaminophen in 3D cultures. In 2D cultures however, the SOD expression remained unaffected by the treatment with acetaminophen.

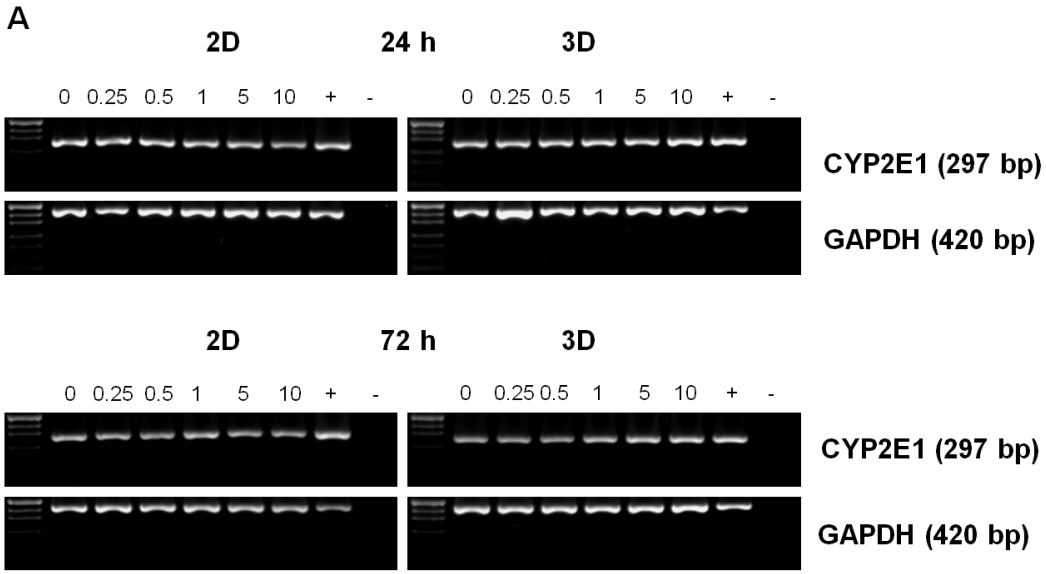
A
2D
24 h
3D
0 0.25 0.5 1 5 10 + -
0 0.25 0.5 1 5 10 + -
CYP2E1 (297 bp)
GAPDH (420 bp)
2D
72 h
3D
0 0.25 0.5 1 5 10 + -
0 0.25 0.5 1 5 10 + -
CYP2E1 (297 bp)
GAPDH (420 bp)

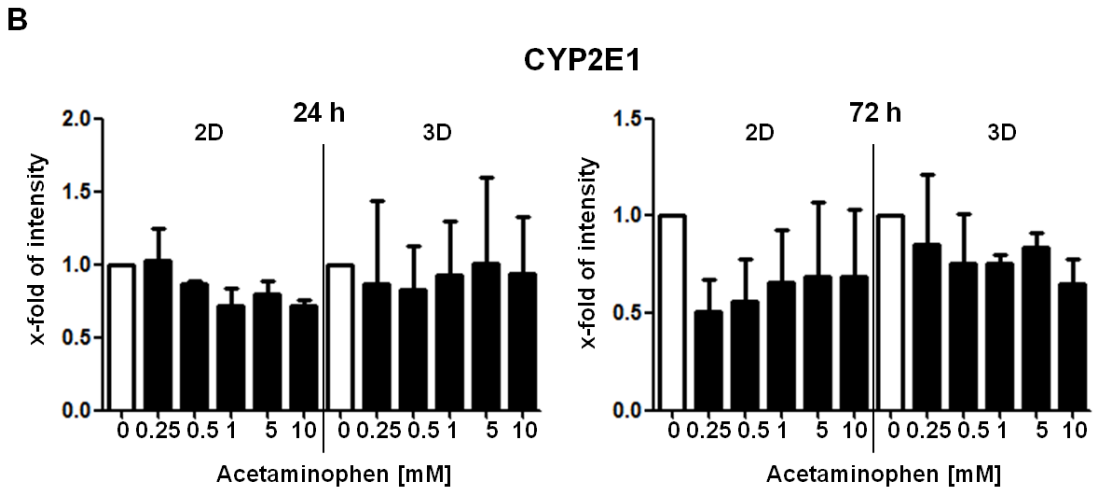
B
CYP2E1
24 h
2D
3D
x-fold of intensity
2.0
1.5
1.0
0.5
0.0
0 0.25 0.5 1 5 10 0 0.25 0.5 1 5 10
Acetaminophen [mM]
72 h
2D
3D
x-fold of intensity
1.5
1.0
0.5
0.0
0 0.25 0.5 1 5 10 0 0.25 0.5 1 5 10
Acetaminophen [mM]

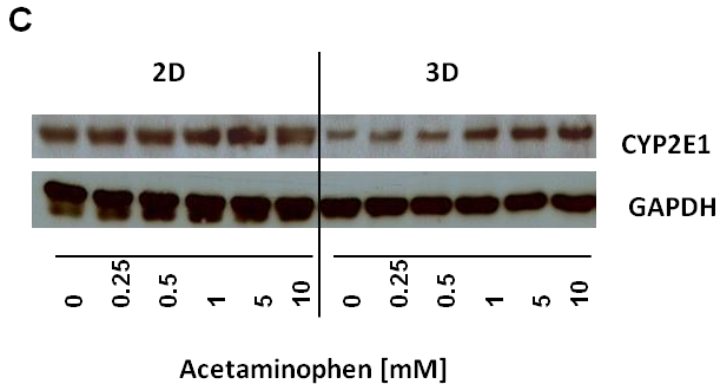
C
2D
3D
CYP2E1
GAPDH
0 0.25 0.5 1 5 10 0 0.25 0.5 1 5 10
Acetaminophen [mM]

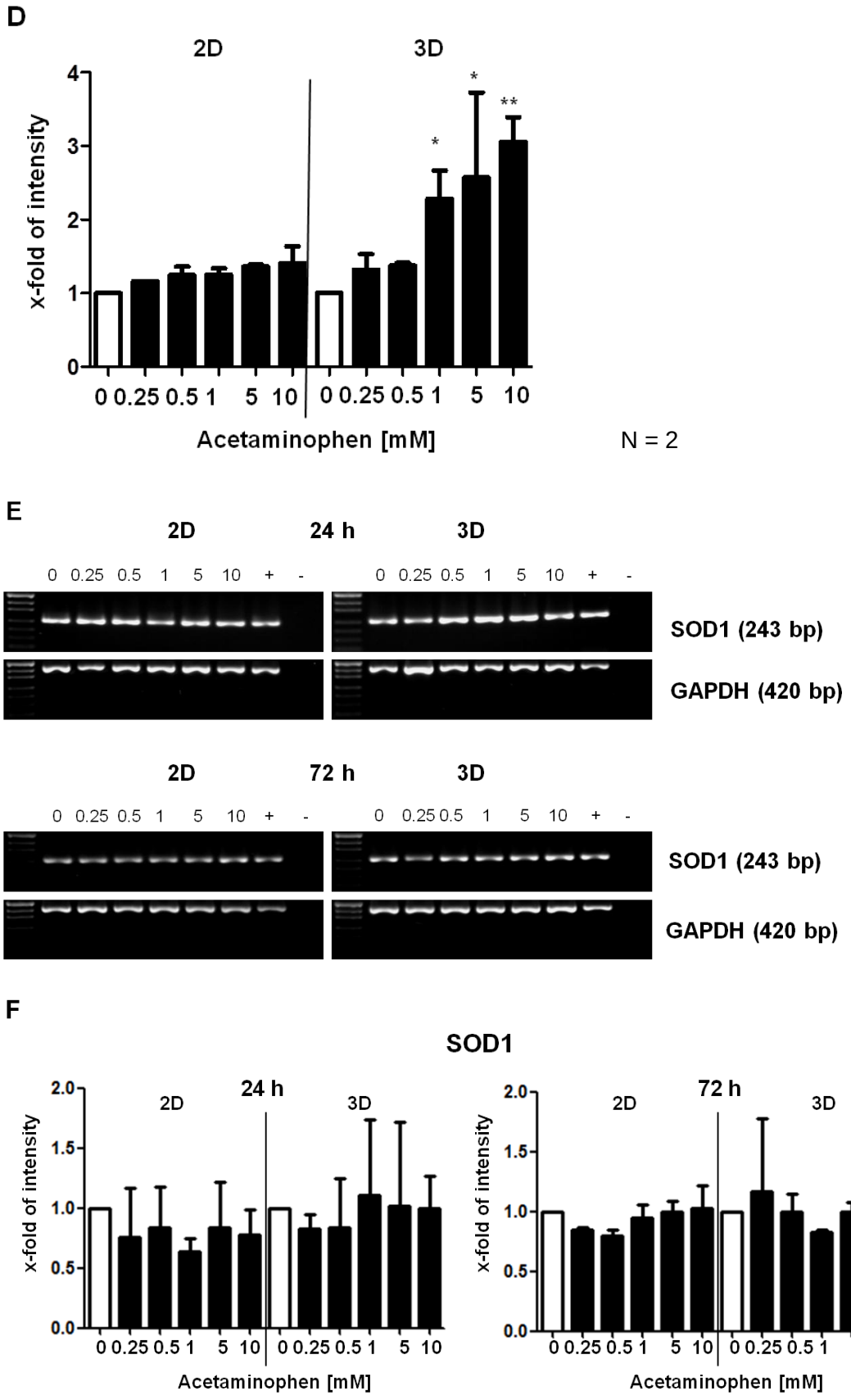
D
2D
3D
x-fold of intensity
0 0.25 0.5 1 5 10 0 0.25 0.5 1 5 10
Acetaminophen [mM]
N = 2
E
2D
24 h
3D
0 0.25 0.5 1 5 10 + -
SOD1 (243 bp)
GAPDH (420 bp)
2D
72 h
3D
SOD1 (243 bp)
GAPDH (420 bp)
F
SOD1
24 h
72 h
2D
3D
x-fold of intensity
Acetaminophen [mM]

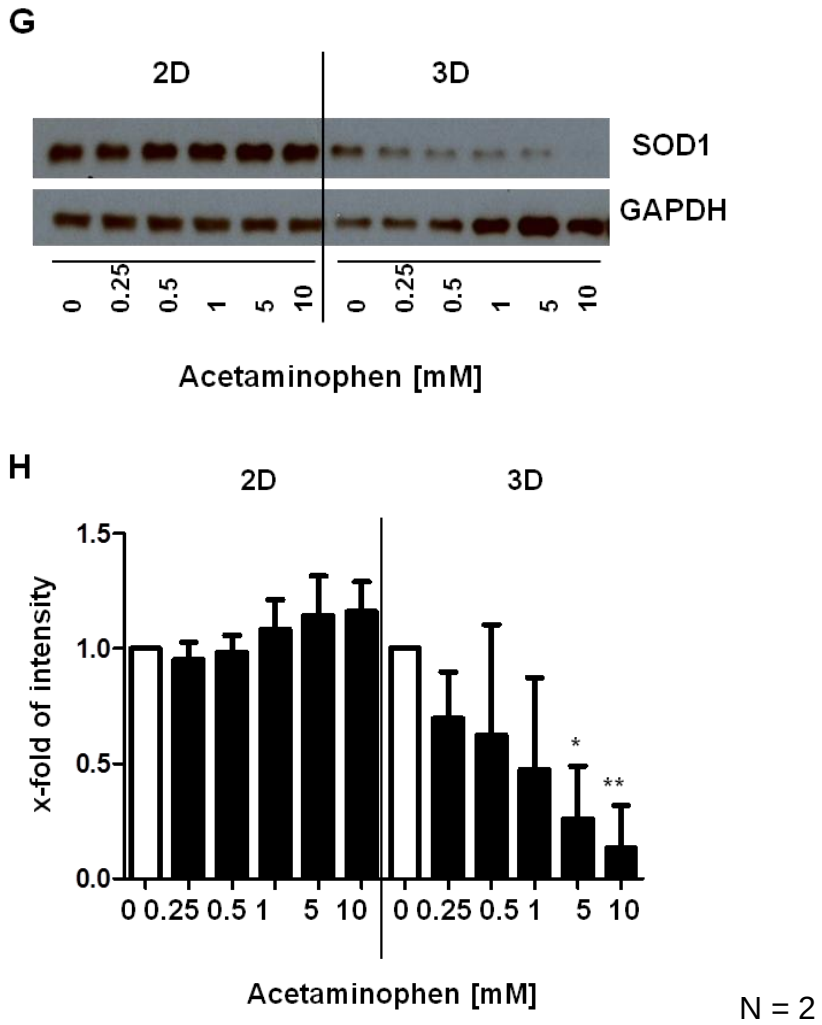

Figure 3. 4 Gene and protein level expression of CYP2E1 and SOD1. Semi-quantitative PCR blots of CYP2E1 **(A, B)** and SOD1 **(E, F)** after acetaminophen stimulation were compared to their respective control in 2D and 3D cultures. Data are shown as x-fold of control normalized to GAPDH; one-way ANOVA, *p < 0.05. Representative blots from two different experiments at 72 h were detected by Western blot. Protein levels of CYP2E1 **(C, D)** and of SOD1 **(G, H)** after the treatment with acetaminophen were compared to their respective control in 2D and 3D cultures. Data are shown as x-fold of control normalized to GAPDH; one-way ANOVA, *p < 0.05, **p < 0.01. Gene and protein levels were quantified by using the ImageJ software [105].

3.1.1.5. MRPs gene expression

Gene expression of MRP1, MRP2, MRP3 and MRP4 hepatocytes treated with acetaminophen exhibited no statistical differences at the intensity expression after 24 and 72 h of acetaminophen stimulation (Fig. 3.5 C, D & E) with the exception of MRP1 at 72 h which was up-regulated (Fig. 3.5 B). Furthermore, 2D cultures exhibited a higher increase of MRP1 expression than 3D cultures. This higher increase could be due to the fact that more cells die in 3D cultures

than in 2D cultures. Therefore, more RNA can be collected from the cells that have been cultivated in 2D.

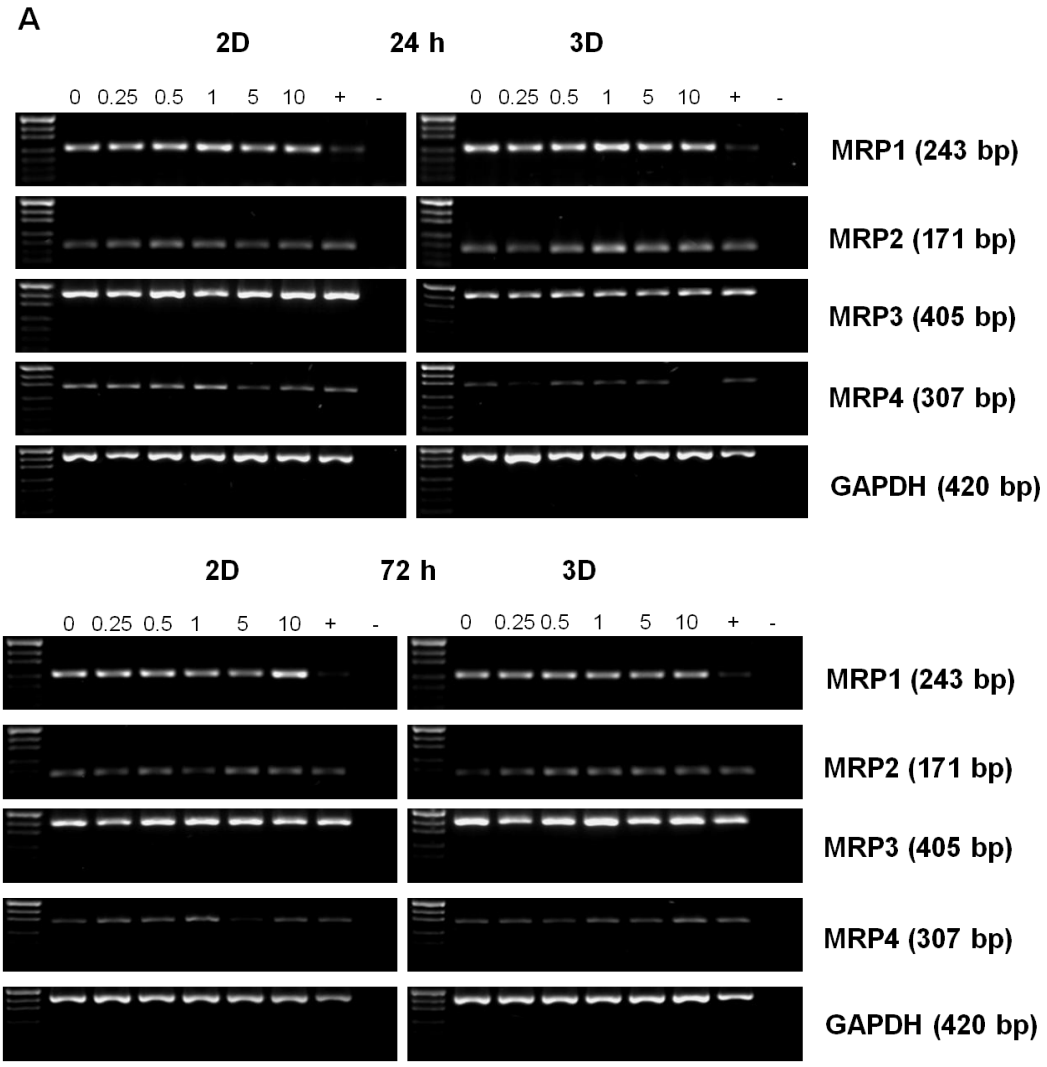

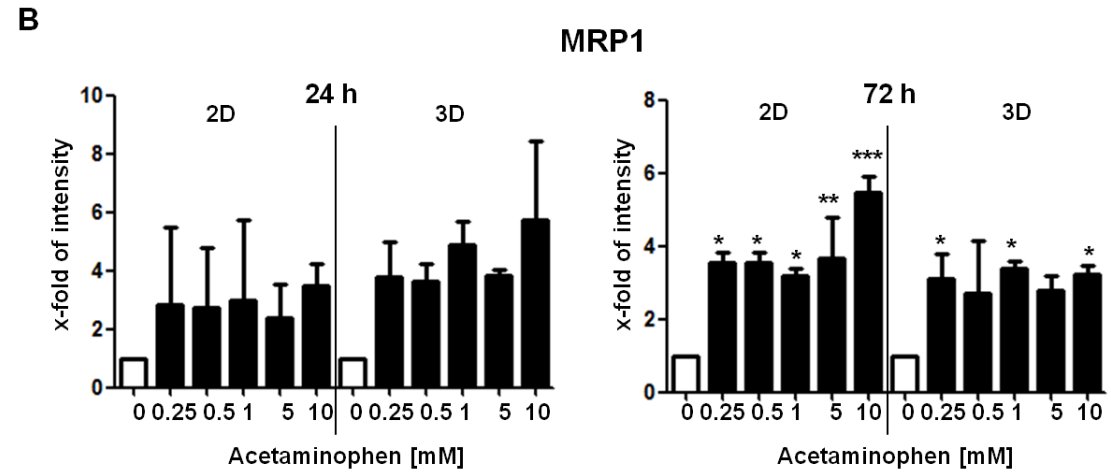

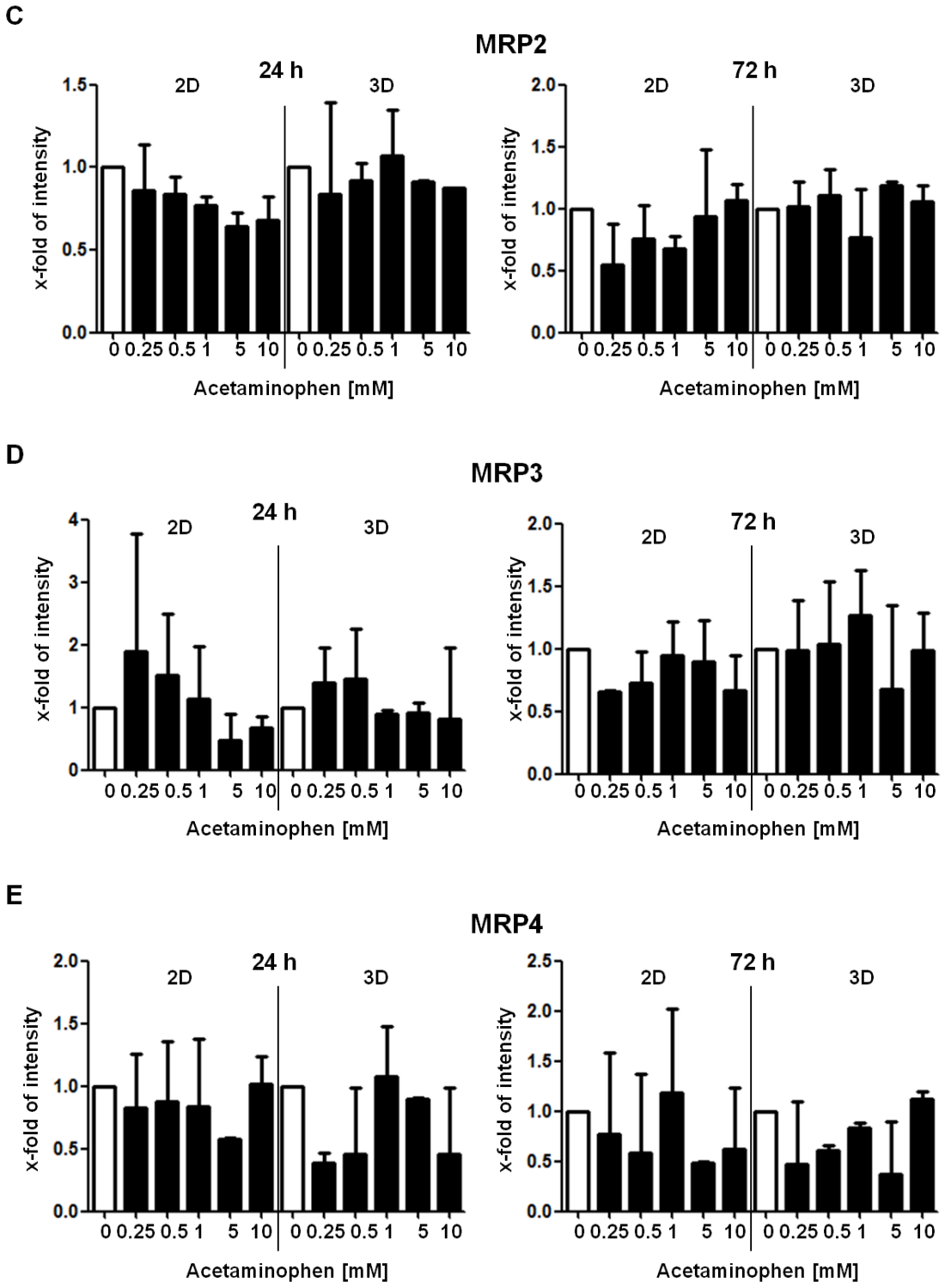

Figure 3. 5 Gene level expression of MRPs. **(A)** Semi-quantitative PCR blots of different MRP transporter channels after acetaminophen stimulation were compared to their respective control in 2D and 3D cultures. The gene expression of **(B)** MRP1, **(C)** MRP2, **(D)** MRP3, and **(E)** MRP4 are displayed. Values are expressed as x-fold of control. Gene levels were quantified by using the ImageJ software and were normalized to GAPDH; *p < 0.05, **p < 0.01, *** p < 0.001 [105].

3.1.1.6. MRP1 transporter activity

Hepatocytes were incubated with 4 µM of 5-CFDA for 30 min. 5-CFDA diffuses into the cells where it is cleaved by esterases into caboxyfluorescein succinimidyl ester (CFSE). In hepatocytes, CFSE is exported into the cell culture supernatant by the activity of hepatic transporters [106]. Finally, the elution of 5-CFSE was quantified by collecting the supernatants at different time points. Figure 3.6 A shows the concentrations of diffused 5-CFDA and metabolized into 5-CFSE by hepatic esterases. Interestingly, the amount of 5-CFDA diffused and metabolized into 5-CFSE by hepatocytes in 3D was 260% higher than in hepatocytes cultured in 2D (****p < 0.0001) after 24 h. After 72 h, no statistically significant difference was observed between 2D and 3D, even though the amount of 5-CFDA diffused and metabolized by hepatocytes into 5-CFSE was higher in 3D cultures than in 2D cultures. As depicted in Figure 3.6 B, 2D and 3D cultures reached the peak of the 5-CFSE efflux after 30 min. After 24 h, the efflux was 350% higher in 3D cultures than in their 2D counterparts. However, after 72 h, no efflux was observed in 2D cultures. In 3D cultures, MRP1 exhibited a different behavior after 72 h than after 24 h reached the peak of 5-CF efflux 20 min after incubation.

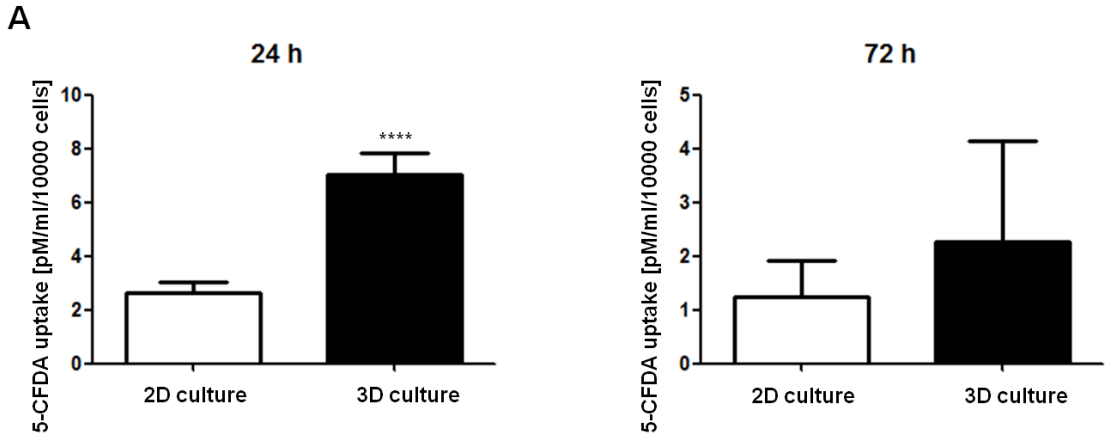

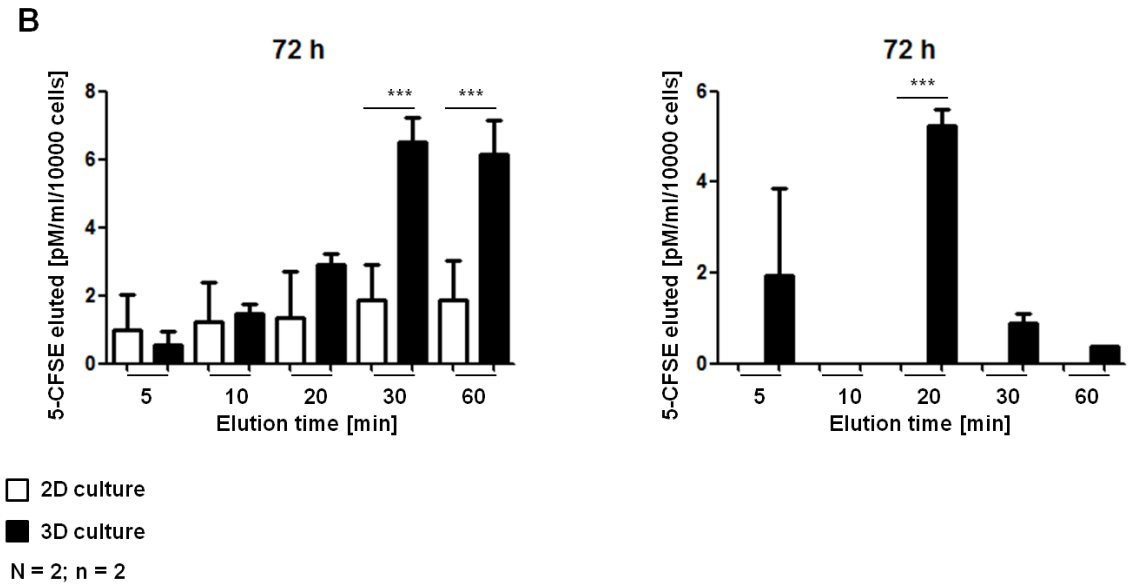

Figure 3. 6 Comparison of the transport activity of PHH in 2D and 3D cultures. **(A)** 5-CFDA taken up and metabolized into 5-CFSE by human primary hepatocytes in monolayer culture and in collagen gel after 24 h and 72 h. Unpaired t test; ****p < 0.0001; **(B)** 5-CFSE eluted by human primary hepatocytes in monolayer culture and in collagen gel through MRP1 after 24 h and 72 h. One-way ANOVA; *p < 0.5, ***p < 0.001. Data are expressed as mean ± SD [105].

3.1.1.7. Metabolism of APA

The formation rate of the toxic acetaminophen metabolite NAPQI was analyzed by LC/MS. However, as NAPQI is a highly unstable compound, it rapidly disintegrated into the measuring solution. In the hepatocyte samples, NAPQI not only disintegrated but it was also trapped by proteins and other structures, such as GSH [107]. However, NAPQI could not be measured by LC/MS. Therefore, although not a direct marker, the loss of acetaminophen was used as a marker for metabolite formation. A representative study on the kinetic metabolic turnover of acetaminophen in 2D and 3D was carried out (Fig. 3.7). PHH in culture were incubated with acetaminophen (0.25 mM, 0.5 mM, 1 mM, 5 mM and 10 mM) for 24, 48 and 72 h. The metabolic turnover of acetaminophen at 10 mM was higher in 3D cultures until the end of the incubation. This resulted in lower concentrations of acetaminophen remaining in the cultures (51.79 nM vs. 73.48 nM after 24 h, 44.84 nM vs. 62.81 nM after 48 h and 39.46 nM vs. 50.31 nM after 72 h). At the lower concentrations of acetaminophen incubation (0.25-5 mM), the remaining acetaminophen concentrations were in the same range in 2D and 3D cultures after 48 hours (5 mM) and after 72 h (0.25-1 mM).

Next, an independent experiment with 4 donors and incubation with acetaminophen for 72 h was performed. Differences between 2D and 3D cultures were only detected at high concentrations (10 mM).

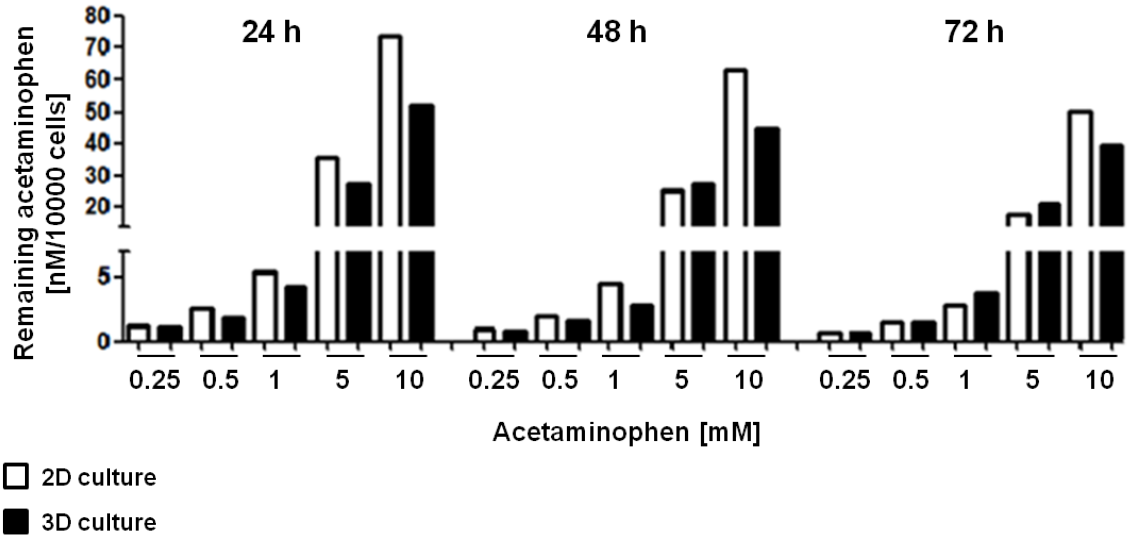

Figure 3. 7 Remaining acetaminophen after 24, 48 and 72 hours after the incubation with PHH in 2D culture compared to 3D culture. The concentrations are expressed as mM acetaminophen and were measured by LC/MS [105].

3.1.2. Collagen gel

3.1.2.1. Optimization of the number of PHH in 3D

The cell number in collagen gel cultures was optimized by resazurin conversion and by optical study of the cell distribution in the μ-slide channel. Due to the lack of availability of PHH and due to the similar size with PHH, Huh7 cells were used for the optimization of the cell number.

The highest mitochondrial activity, which was measured by resazurin conversion per cell, was observed at a cell density of $5*10^3$ cells per μl of collagen gel (Figure 3.8). This cell density seems to ensure an optimal exchange of substances in the nutrient medium, as the cells are located in the linear range of the reaction. In addition, transmitted light micrographs were taken at low magnification (x 40) in order to investigate the cell distribution in the μ-slide channel, as at this magnification the total width of the μ-slide channel was visible in the micrograph. Cultures below $5*10^3$ cells/μl did not present a

homogenous distribution of the cells in the channel, whereas cultures with higher numbers of cells form localized aggregations (Figure 3.9).

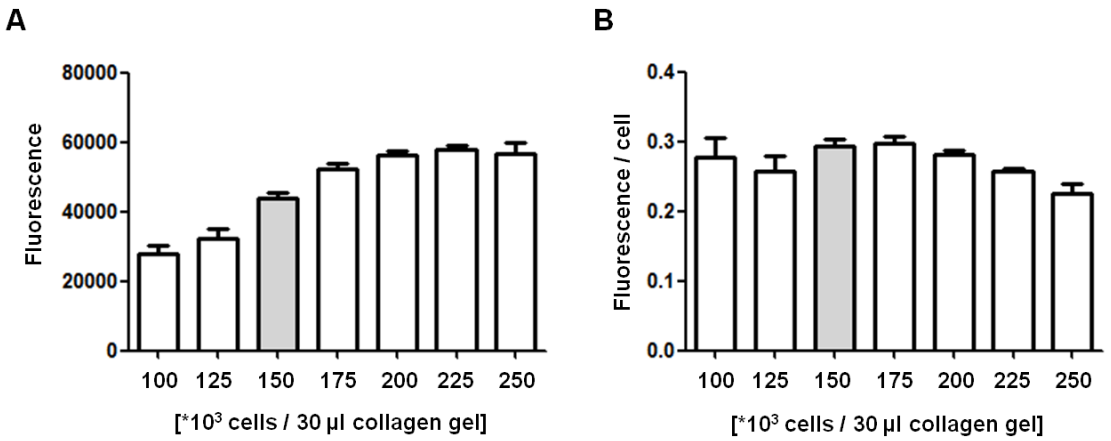

Figure 3. 8 Resazurin conversion of the collagen gel cultures **(A)** and per cell **(B)**. Fluorescence was measured by plate reader. Data are showed as mean ± SD.

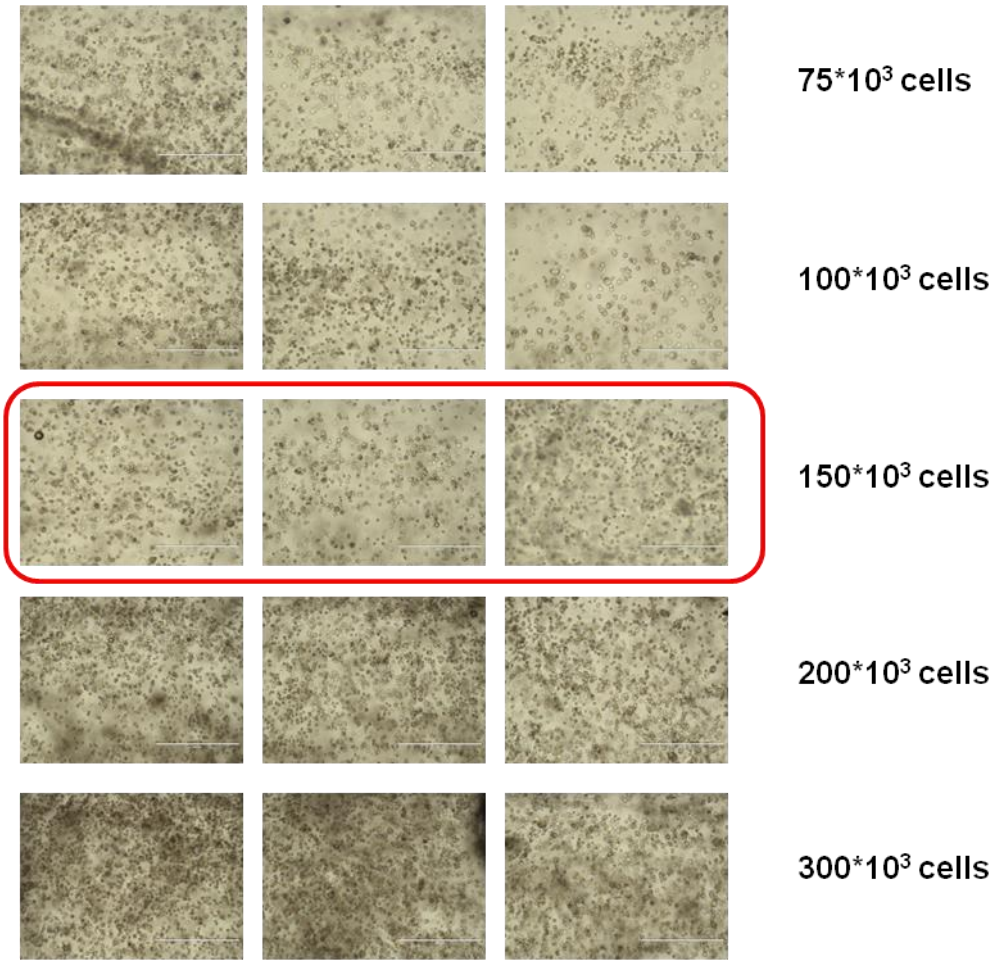

Figure 3. 9 Transmitted light micrograph of Huh-7 cells entrapped in collagen gels among the µ-slide channel with different cell dilutions (x 40 magnification). Scale bar 1000 µm.

3.1.2.2. Cell morphology studies

PHH morphology was investigated by observing the cells under the light microscope (Fig. 3.10). PHH that were cultured with the 3D collagen gels technique maintained a round shape and formed aggregates, whereas cells in 2D cultures rapidly gained a planar and fibroblast-like appearance after being cultured for several days. In addition, after 14 days of culture, hepatocytes in 2D died and detached from the plate.

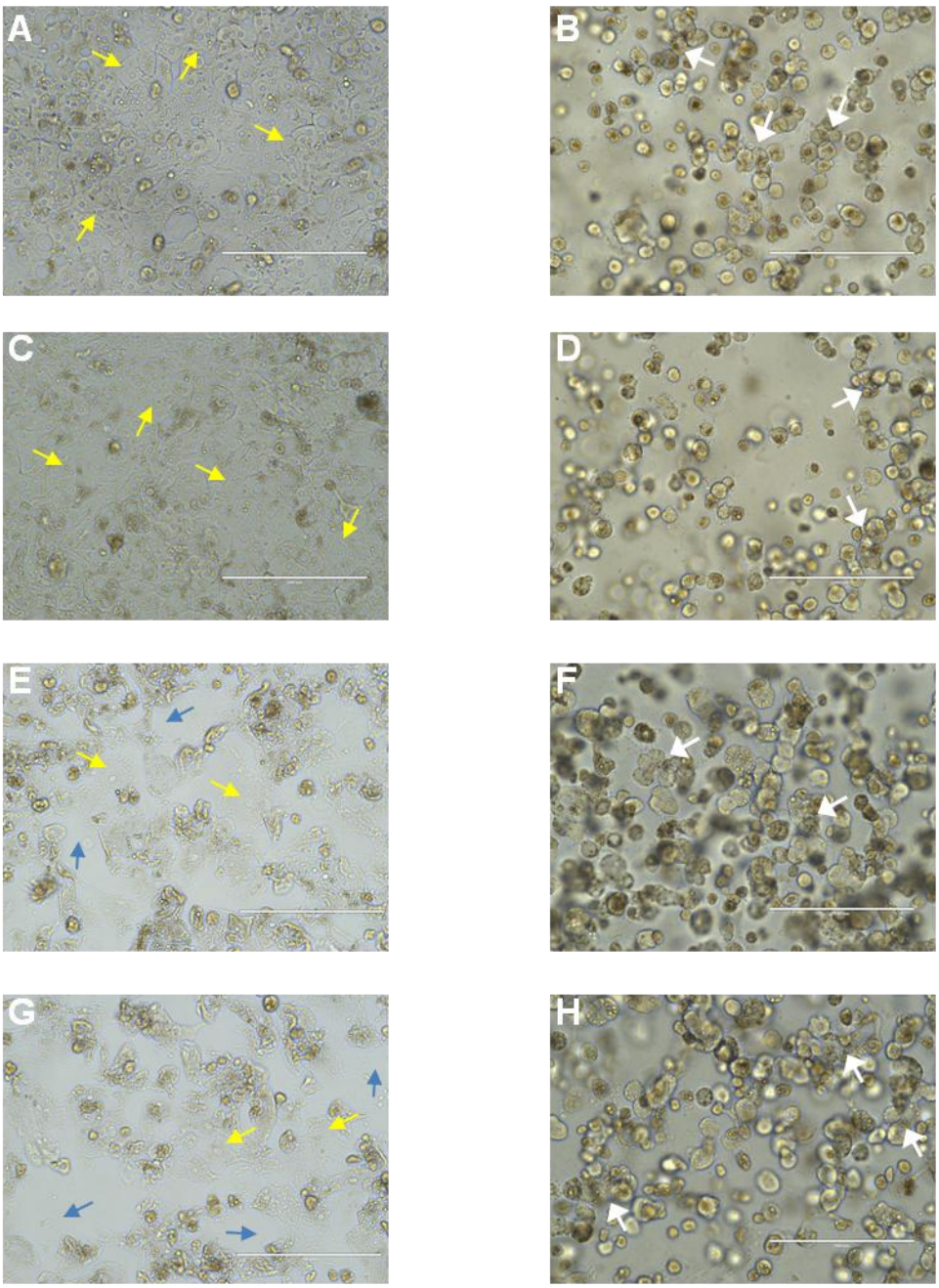

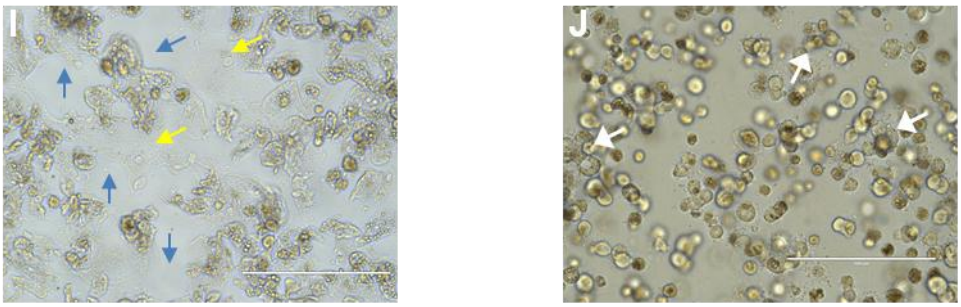

Figure 3. 10 Transmitted light micrograph of PHH on monolayer and entrapped in collagen gels: day 1 **(A)** 2D, **(B)** 3D; day 7 **(C)** 2D, **(D)** 3D; day 14 **(E)** 2D, **(F)** 3D; day 21 **(G)** 2D, **(H)** 3D; day 28 **(I)** 2D, **(J)** 3D (x 200 magnification). PHH in 2D cultures are indicated by yellow arrows while blue arrows are indicated the plate areas left by the detached PHH. PHH aggregates are indicated by white arrows. Scale bar 200 µm.

3.1.2.2. Cell Viability

PHH viability was investigated by live/dead staining (Fig. 3.11). However, in collagen gel cultures, it was impossible to perform cell quantification as, in collagen gel, cells are entrapped a different levels. Therefore, we measured mitochondrial activity by resazurin conversion, which allows for the indirect determination of cell viability (Fig 3.12).

3.1.2.2.1. Live/Dead staining

In the framework of a live/dead staining of PHH, stained living cells, green fluorescence (Calcein-AM, 2µM) and dead cells, red fluorescence (Ethidium homodimer, 4 µM). Figure 3.11, showed an increase of the number of dead cells in 2D in comparison to 3D cultures over 28 days.

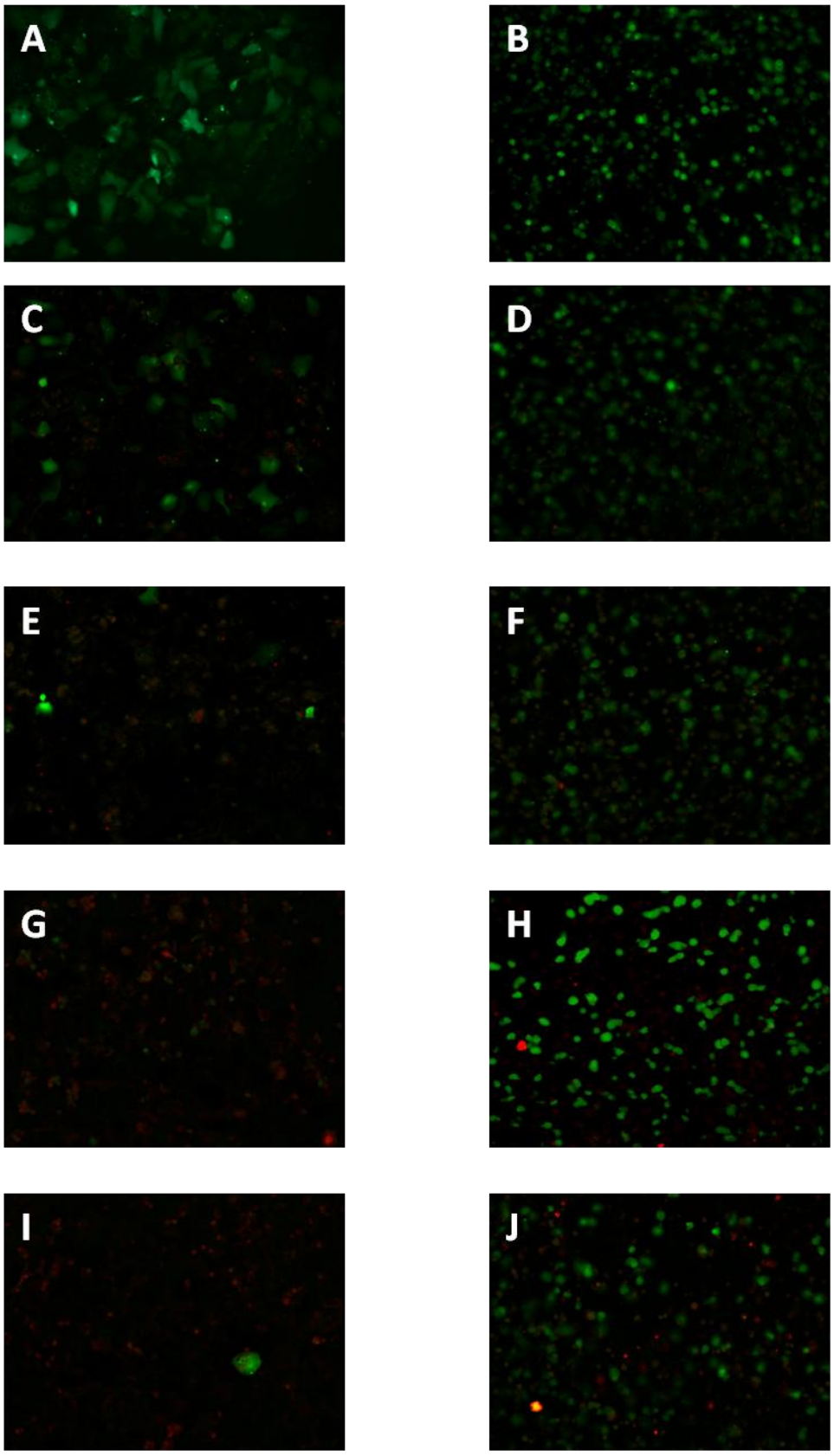

Figure 3. 11 Survival of PHH cultured on collagen monolayer and embedded in collagen gels (x 100 magnification): day 1 **(A)** 2D, **(B)** 3D; day 7 **(C)** 2D, **(D)** 3D; day 14 **(E)** 2D, **(F)** 3D; day 21 **(G)** 2D, **(H)** 3D; day 28 **(I)** 2D, **(J)** 3D.

3.1.2.3.2. Resazurin conversion

Mitochondrial activity was assessed by a measurement of the intracellular conversion of resazurin to resorufin (Fig. 3.12). A significant statistical difference (*p < 0.05) was observed after 21 and 28 days of culture. This observation, prove that PHH entrapped in collagen gel maintain higher mitochondrial activity during the time of culture.

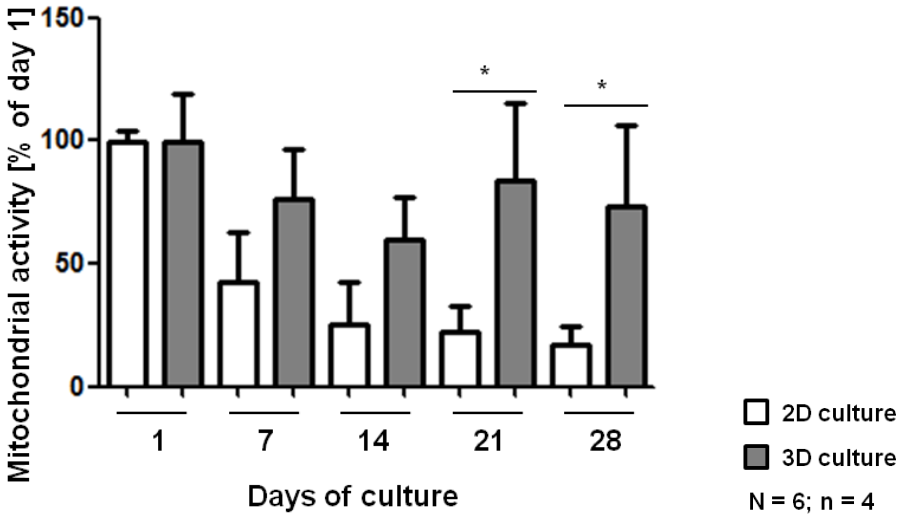

Figure 3. 12 Mitochondrial activity was assessed by resazurin conversion. Fluorescence was normalized to % of day 1 and 2D and 3D cultures were compared. Fluorescence was measured by plate reader. Data are expressed as mean ± SD; one-way ANOVA, *p < 0.05 [46].

3.1.2.4. Glucose production

Glucose production (glucogenolysis) exhibited a significant statistical difference (*p < 0.05, ***p < 0.001) over the 28 days of culture (Fig. 3.13). PHH seem to maintain this functional parameter for 28 days with collagen gel but not in monolayer culture.

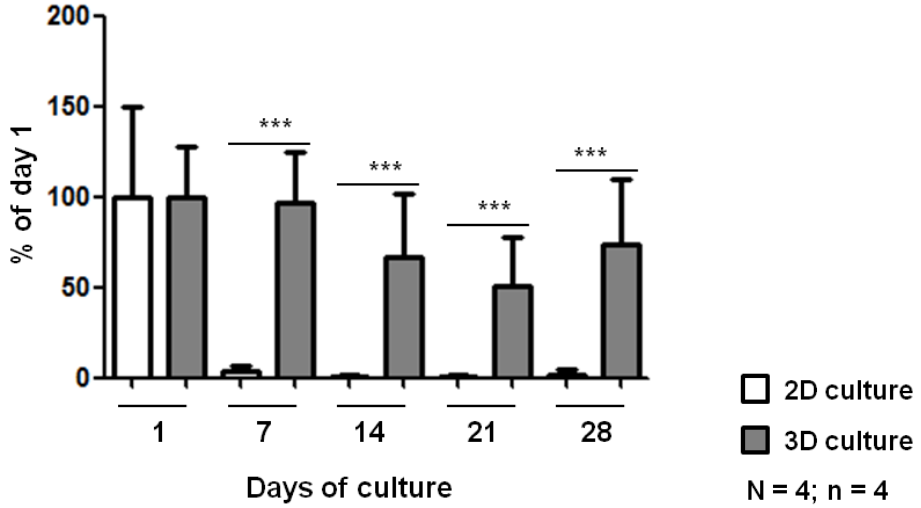

Figure 3. 13 Glucose production (glucogenolysis) over 28 days was compared in 2D and 3D cultures. Absorbance was measured by plate reader. Data are expressed as mean ± SD; one-way ANOVA, *p < 0.05, ***p < 0.001 [46].

3.1.2.5. Ammonia detoxifiation

Ammonia detoxification capacity exhibited a decrease over 28 days (Fig. 3.14). No statistical difference was observed between 2D and 3D cultures. However, 3D cultures maintained a low detoxification capacity, while the detoxification capacity of 2D cultures decreased.

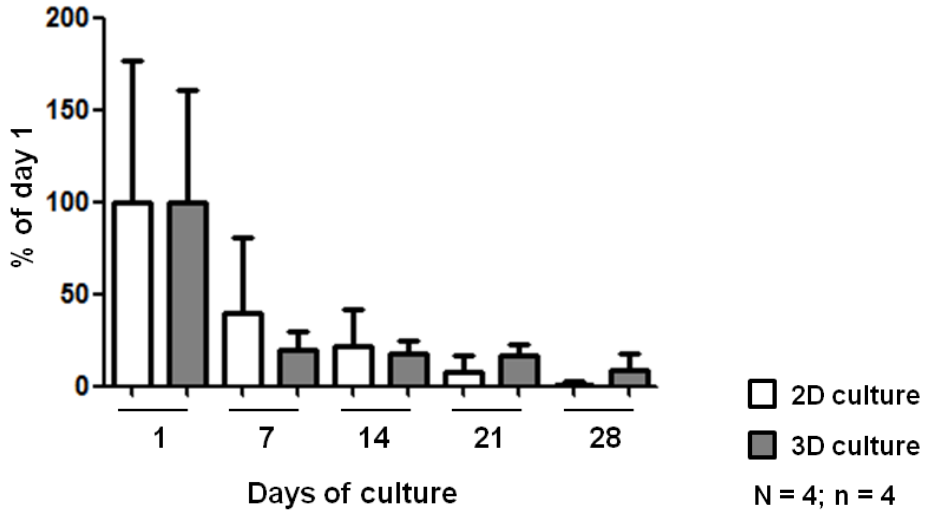

Figure 3. 14 De-toxification of ammonia over 28 days was compared in 2D and 3D cultures. Absorbance was measured by plate reader. Data are showed as mean ± SD [46].

3.1.2.6. Enzymatic activity of CYP450

3.1.2.6.1. Gene expression

CYPs are enzymes which are responsible for the major metabolism processes in the liver. Therefore, gene expression was investigated in order to determine the differences between 2D and 3D cultures over the time of culture. No significant statistical difference in the gene expression of the CYPs was observed between 2D and 3D cultures. Representative blots from the different CYPs are presented in figure 3.15.

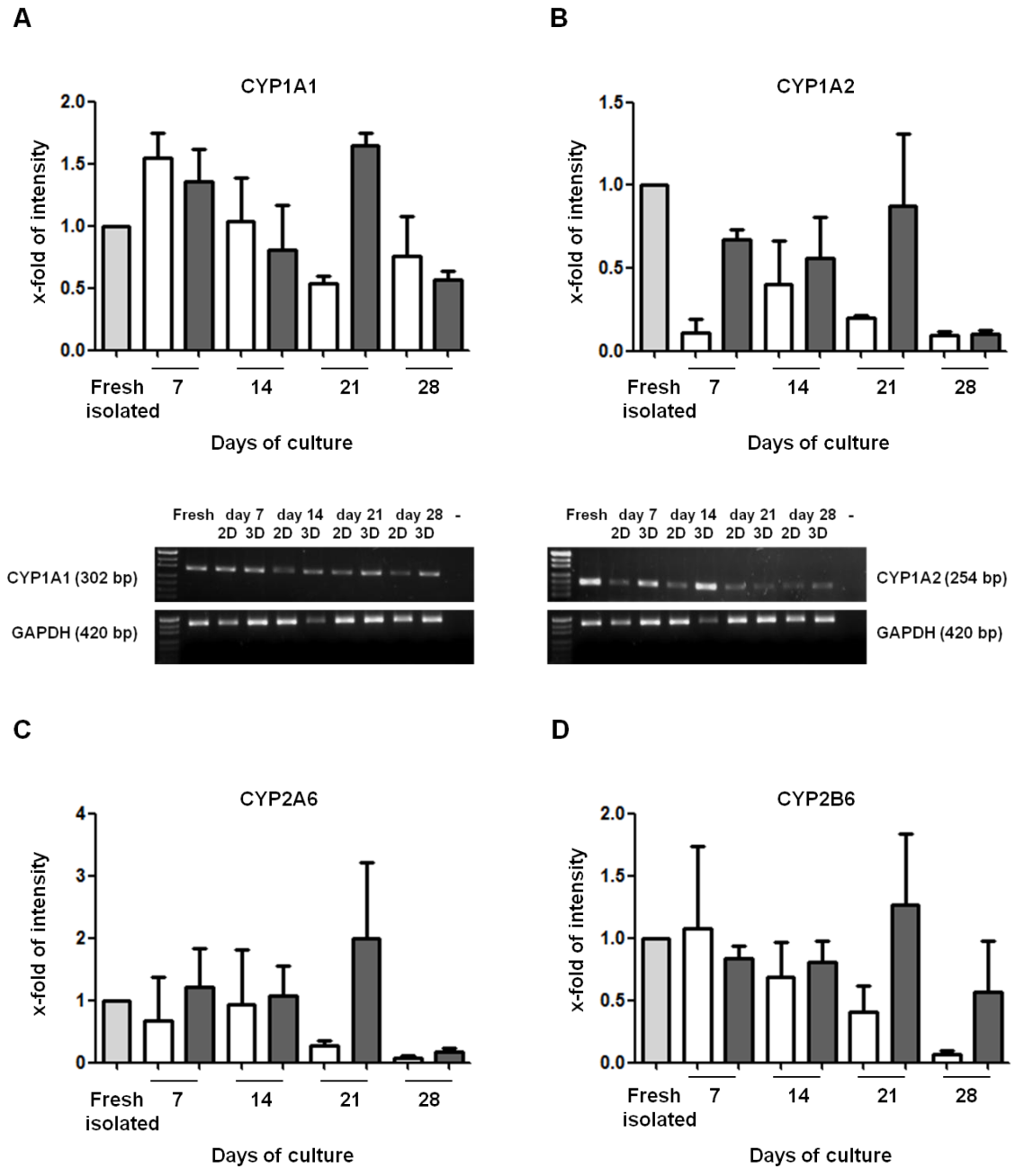

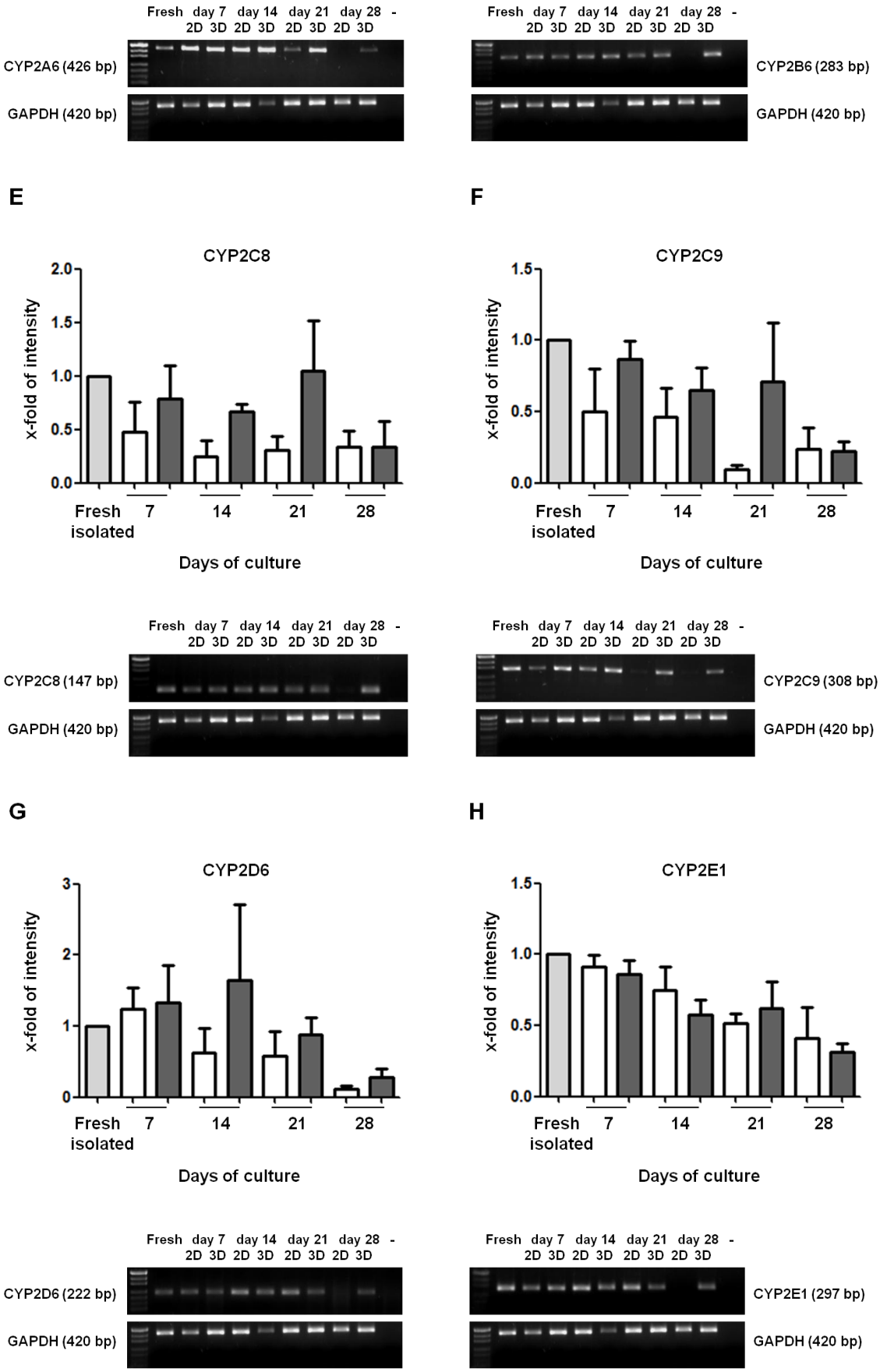
Fresh day 7 day 14 day 21 day 28 -
2D 3D 2D 3D 2D 3D 2D 3D
CYP2A6 (426 bp)
GAPDH (420 bp)
CYP2B6 (283 bp)
E
CYP2C8
x-fold of intensity
Fresh isolated
7
14
21
28
Days of culture
CYP2C8 (147 bp)
F
CYP2C9
CYP2C9 (308 bp)
G
CYP2D6
CYP2D6 (222 bp)
H
CYP2E1
CYP2E1 (297 bp)

I

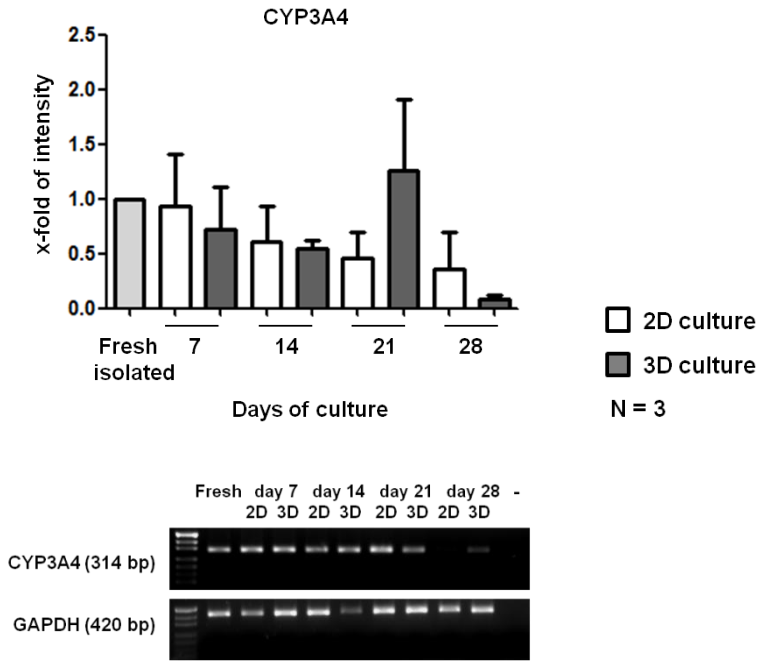

Figure 3. 15 Semi-quantitative PCR blots of different CYPs **(A-I)** were compared to their respective control in 2D and 3D cultures for 28 days. Values are expressed as x-fold of control. Gene levels were quantified by using the ImageJ software and were normalized to GAPDH; one-way ANOVA, *p < 0.05.

3.1.2.6.2. Phase I (CYPs) and phase II enzymatic activity

3.1.2.6.2.1. Phase I

Phase I enzymatic activity was investigated by a fluoresce-based assay. At day 1 (Fig. 3.16 A), only CYP1A1/2 and CYP2D6 showed a significant statistical difference (*p < 0.05, **p < 0.001, ***p < 0.0001). During the rest of the time of culture, PHH showed a similar pattern maintaining higher activity in 3D cultures with the exception of CYP2C8/9. CYP1A1/2, CYP2A6, CYP2C8/9, and CYP2D6 exhibited significant statistical differences.

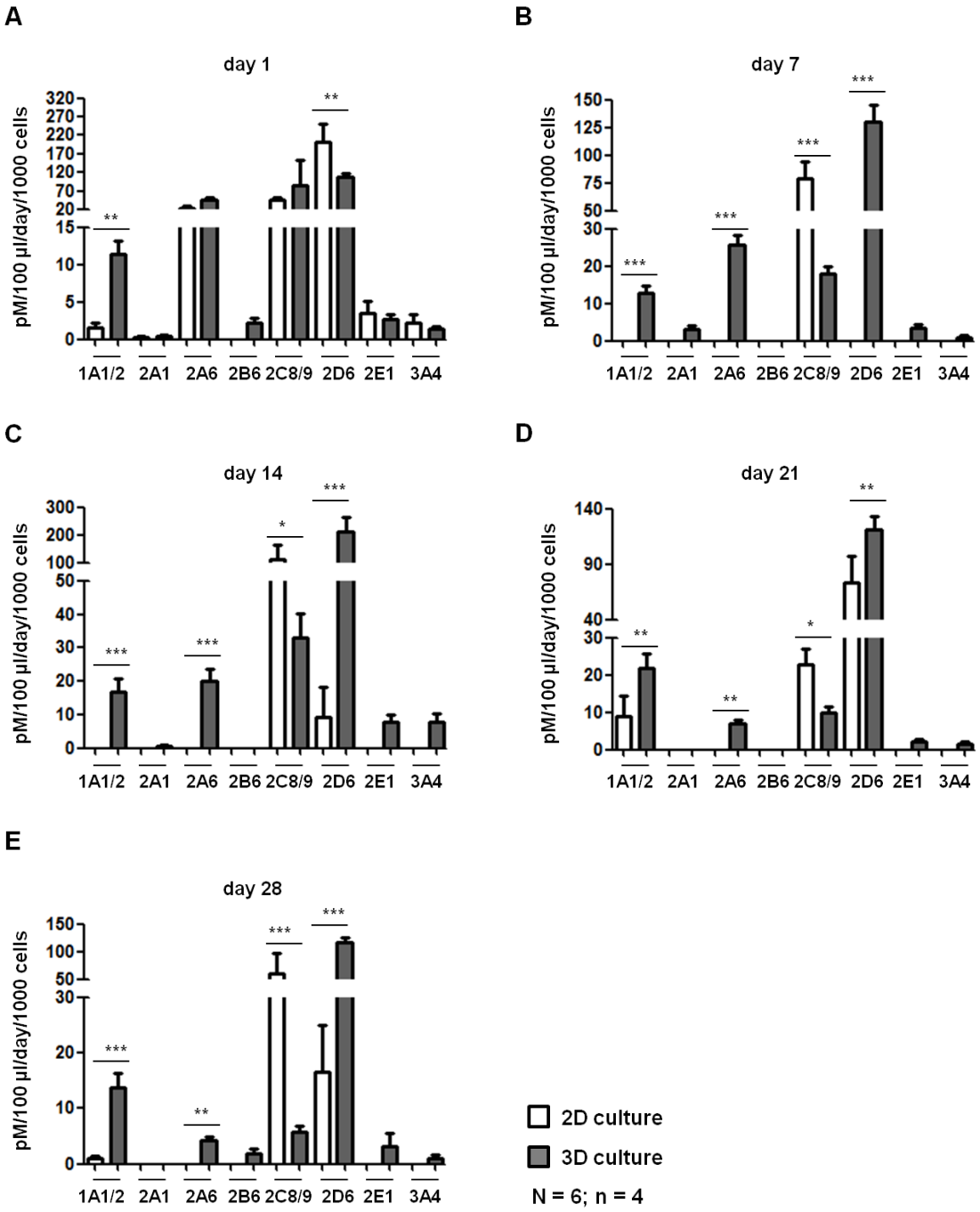

Figure 3. 16 Phase I activity of CYP 1A1/2, 2A1, 2A6, 2B6, 2C8/9, 2D6, 2E1, 3A4 in PHH. **(A)** Day 1, **(B)** day 7, **(C)** day 14, **(D)** day 21 and **(E)** day 28 in monolayer and collagen gel. Data are showed as mean ± SD; one-way ANOVA, *p < 0.05, **p < 0.001, ***p < 0.0001.

3.1.2.6.2.2. Phase II

Phase II enzymatic activity was studied in the same way as the phase I activity, by a fluoresce-based assay. At day 1 (Fig. 3.17 A) and 7 (Fig. 3.17 B), 2D cultures exhibited higher enzymatic activity than 3D cultures. Significant statistical differences were observed in GSH and CHC. After 14 days of culture (Fig. 3.17 C), the enzymatic activity in 2D and 3D cultures became similar and the tide turned. GSH and HC exhibited significant statistical differences. At day 21 (Fig. 3.17 D) and 28 (Fig. 3.17 E), 3D cultures maintained higher enzymatic activity than 2D cultures. Significant statistical differences were observed in GSH and HC at day 28.

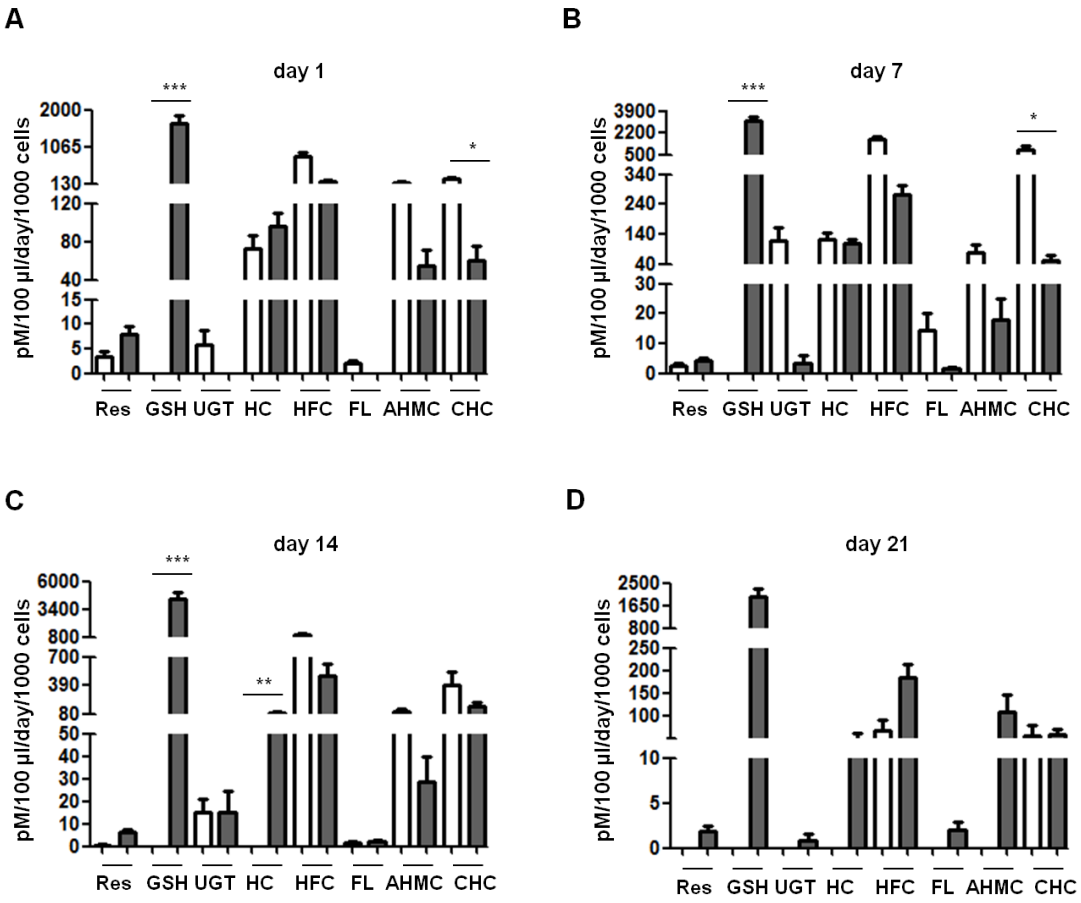

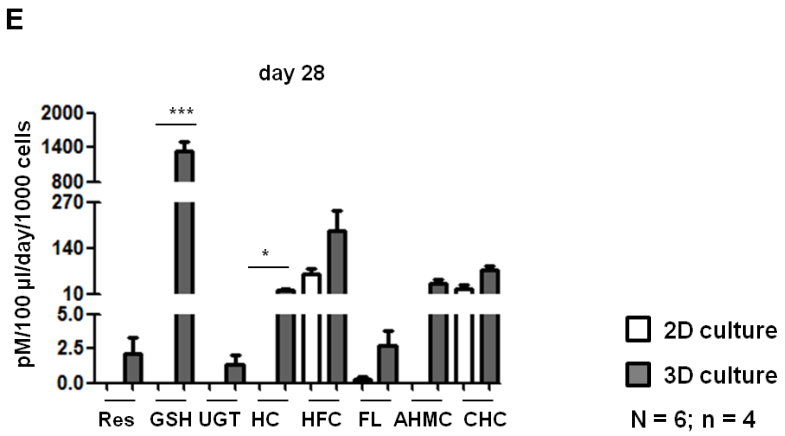

Figure 3. 17 Phase II activity of different conjugation reactions of resorufin (Res), glutathione (GSH), uridine (UGT), 7-hydroxy coumarin (HC), 7-hydroxy-4(trifluoromethyl) coumarin (HFC), fluorescein (FL), 3-(2-(N,N-diethylamino)ethyl)-7-hydroxy-4-methyl-coumarin (AHMC), and 3-cyano-7-hydroxycoumarin (CHC). **(A)** Day 1, **(B)** day 7, **(C)** day 14, **(D)** day 21, and **(E)** day 28 in PHH in monolayer and collagen gel. Data are expressed as mean ± SD; one-way ANOVA, *p < 0.05, **p < 0.001, ***p < 0.0001.

3.1.2.7. Efflux assays

3.1.2.7.1. Transporter channel gene expression

Transporter channels are proteins which are located at the apical and at the basolateral membranes and which are responsible for the major transporter processes in hepatocytes. Therefore, gene expression was investigated in order to determine differences between 2D cultures and 3D cultures during the time of culture. With the exception of OCT1 and MRP6 in monolayer cultures at day 28, no differences in the gene expression of the transporter channels were observed between 2D and 3D cultures. Representative blots from the different transporters are shown in figure 3.18.

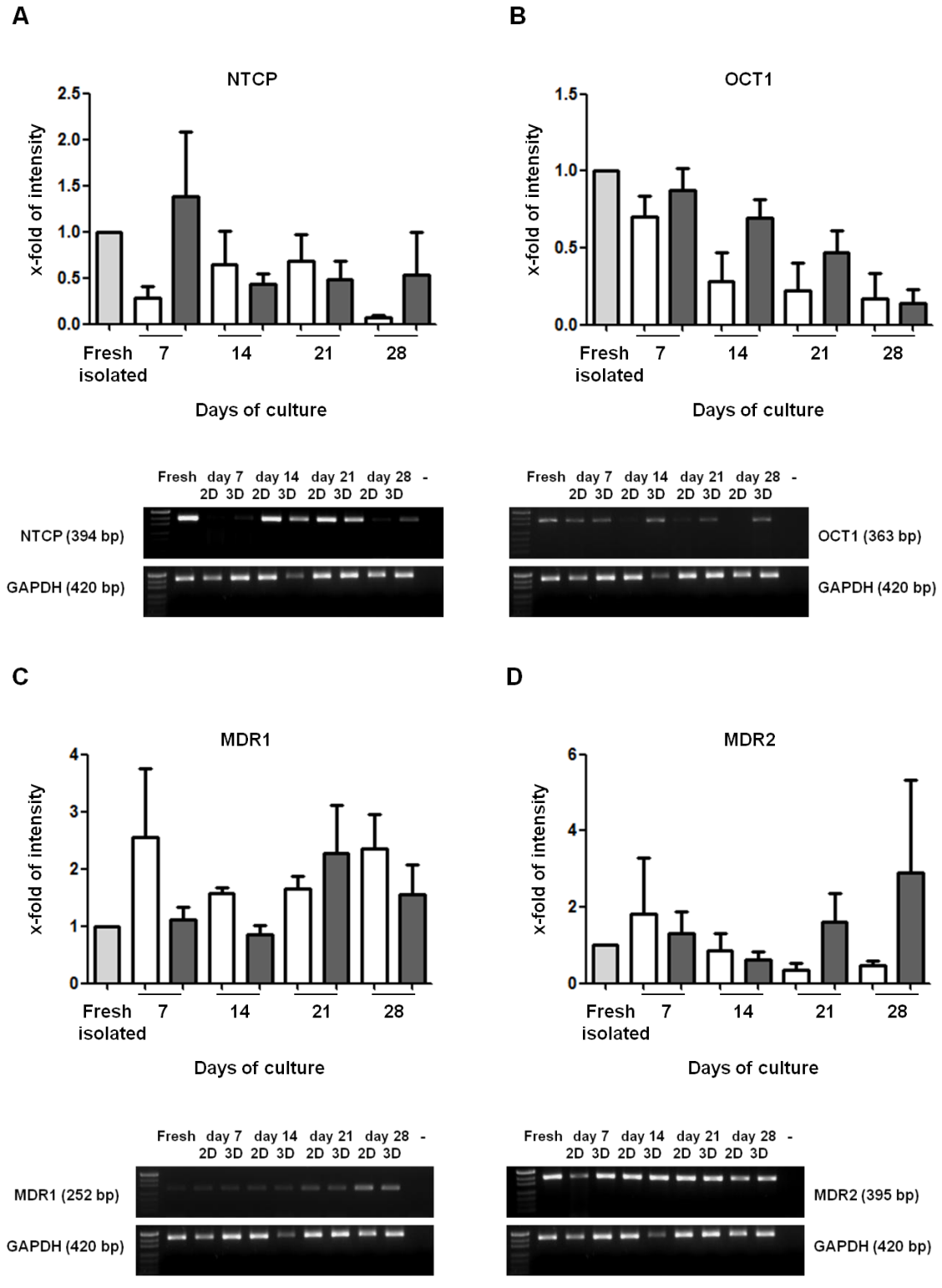
A
NTCP
x-fold of intensity
2.5
2.0
1.5
1.0
0.5
0.0
Fresh isolated
7
14
21
28
Days of culture
Fresh day 7 day 14 day 21 day 28 -
2D 3D 2D 3D 2D 3D 2D 3D
NTCP (394 bp)
GAPDH (420 bp)
B
OCT1
x-fold of intensity
1.5
1.0
0.5
0.0
Fresh isolated
7
14
21
28
Days of culture
Fresh day 7 day 14 day 21 day 28 -
2D 3D 2D 3D 2D 3D 2D 3D
OCT1 (363 bp)
GAPDH (420 bp)
C
MDR1
x-fold of intensity
4
3
2
1
0
Fresh isolated
7
14
21
28
Days of culture
Fresh day 7 day 14 day 21 day 28 -
2D 3D 2D 3D 2D 3D 2D 3D
MDR1 (252 bp)
GAPDH (420 bp)
D
MDR2
x-fold of intensity
6
4
2
0
Fresh isolated
7
14
21
28
Days of culture
Fresh day 7 day 14 day 21 day 28 -
2D 3D 2D 3D 2D 3D 2D 3D
MDR2 (395 bp)
GAPDH (420 bp)

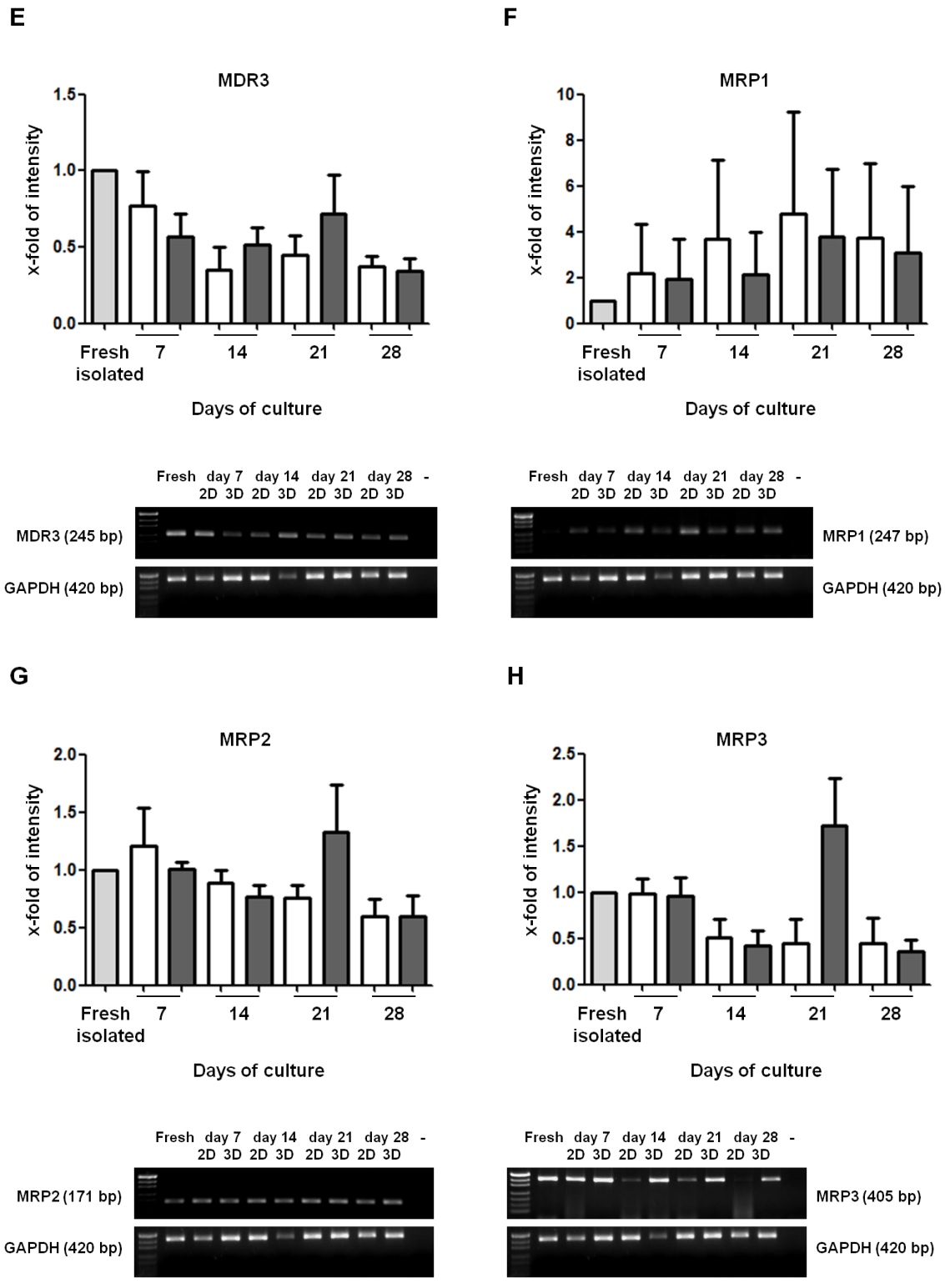
E
MDR3
x-fold of intensity
1.5
1.0
0.5
0.0
Fresh isolated
7
14
21
28
Days of culture
Fresh day 7 day 14 day 21 day 28 -
2D 3D 2D 3D 2D 3D 2D 3D
MDR3 (245 bp)
GAPDH (420 bp)
F
MRP1
x-fold of intensity
10
8
6
4
2
0
Fresh isolated
7
14
21
28
Days of culture
Fresh day 7 day 14 day 21 day 28 -
2D 3D 2D 3D 2D 3D 2D 3D
MRP1 (247 bp)
GAPDH (420 bp)
G
MRP2
x-fold of intensity
2.0
1.5
1.0
0.5
0.0
Fresh isolated
7
14
21
28
Days of culture
Fresh day 7 day 14 day 21 day 28 -
2D 3D 2D 3D 2D 3D 2D 3D
MRP2 (171 bp)
GAPDH (420 bp)
H
MRP3
x-fold of intensity
2.5
2.0
1.5
1.0
0.5
0.0
Fresh isolated
7
14
21
28
Days of culture
Fresh day 7 day 14 day 21 day 28 -
2D 3D 2D 3D 2D 3D 2D 3D
MRP3 (405 bp)
GAPDH (420 bp)

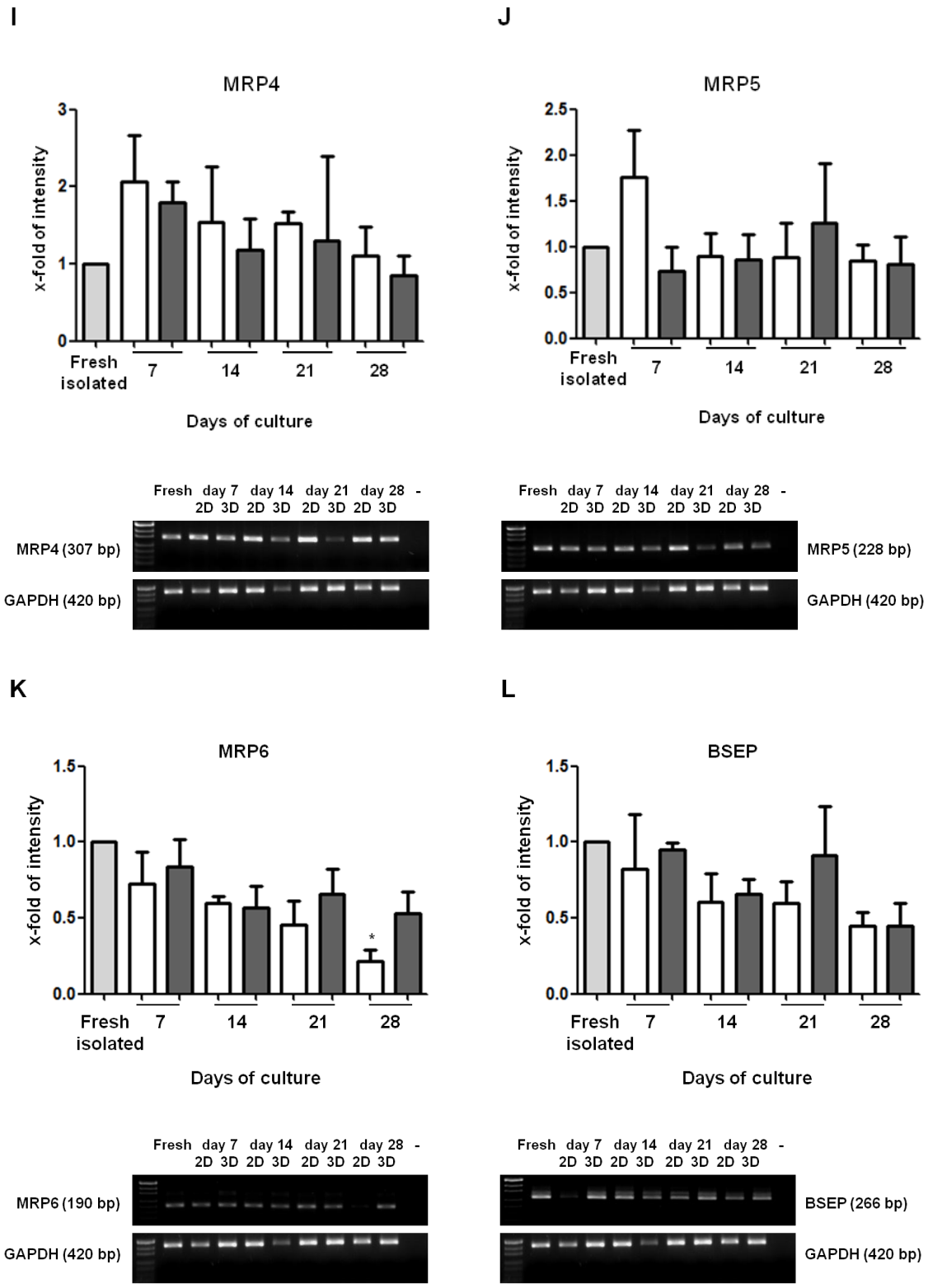
I
MRP4
x-fold of intensity
Fresh isolated
7
14
21
28
Days of culture
Fresh day 7 day 14 day 21 day 28 -
2D 3D 2D 3D 2D 3D 2D 3D
MRP4 (307 bp)
GAPDH (420 bp)
J
MRP5
x-fold of intensity
Fresh isolated
7
14
21
28
Days of culture
Fresh day 7 day 14 day 21 day 28 -
2D 3D 2D 3D 2D 3D 2D 3D
MRP5 (228 bp)
GAPDH (420 bp)
K
MRP6
x-fold of intensity
Fresh isolated
7
14
21
28
Days of culture
Fresh day 7 day 14 day 21 day 28 -
2D 3D 2D 3D 2D 3D 2D 3D
MRP6 (190 bp)
GAPDH (420 bp)
L
BSEP
x-fold of intensity
Fresh isolated
7
14
21
28
Days of culture
Fresh day 7 day 14 day 21 day 28 -
2D 3D 2D 3D 2D 3D 2D 3D
BSEP (266 bp)
GAPDH (420 bp)

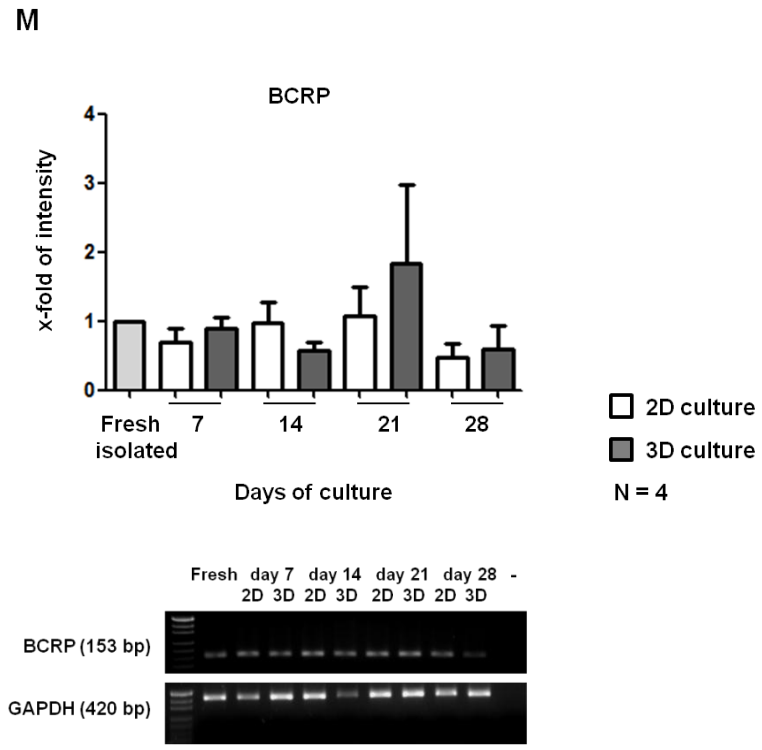

Figure 3. 18 Semi-quantitative PCR blots of different hepatic transporter channels **(A-M)** were compared to their respective control in 2D and 3D cultures for 28 days. Gene expressions were detected by semi-quantitative PCR. Values are expressed as x-fold of control. Gene levels were quantified by using the ImageJ software and were normalized to GAPDH. One-way ANOVA; *p < 0.05.

3.1.2.7.2. Transporter activity

3.1.2.7.2.1. Multidrug-resistant associated protein - 1 (MRP1)

Figure 3.19 A presents the concentrations of diffused 5-CFDA and metabolized into 5-CFSE by hepatic esterases. 2D and 3D cultures presented a decrease of the uptake of 5-CFDA over day 21. Significant statistical differences (***p < 0.0001) were observed at days 1, 7, and 14. Then, at day 28, it was possible to observe a slight increase of the uptake of 5-CFDA. Figure 3.19 B-F depict the elution of 5-CFSE in 2D and 3D cultures. 2D cultures presented elution only at day 1 and 14. However, 3D cultures maintained the transporter activity over 28 days, although it decreased during the time of culture. Significant statistical differences were observed between 2D and 3D cultures over the 28 days of culture (*p < 0.05, **p < 0.001, ***p < 0.0001).

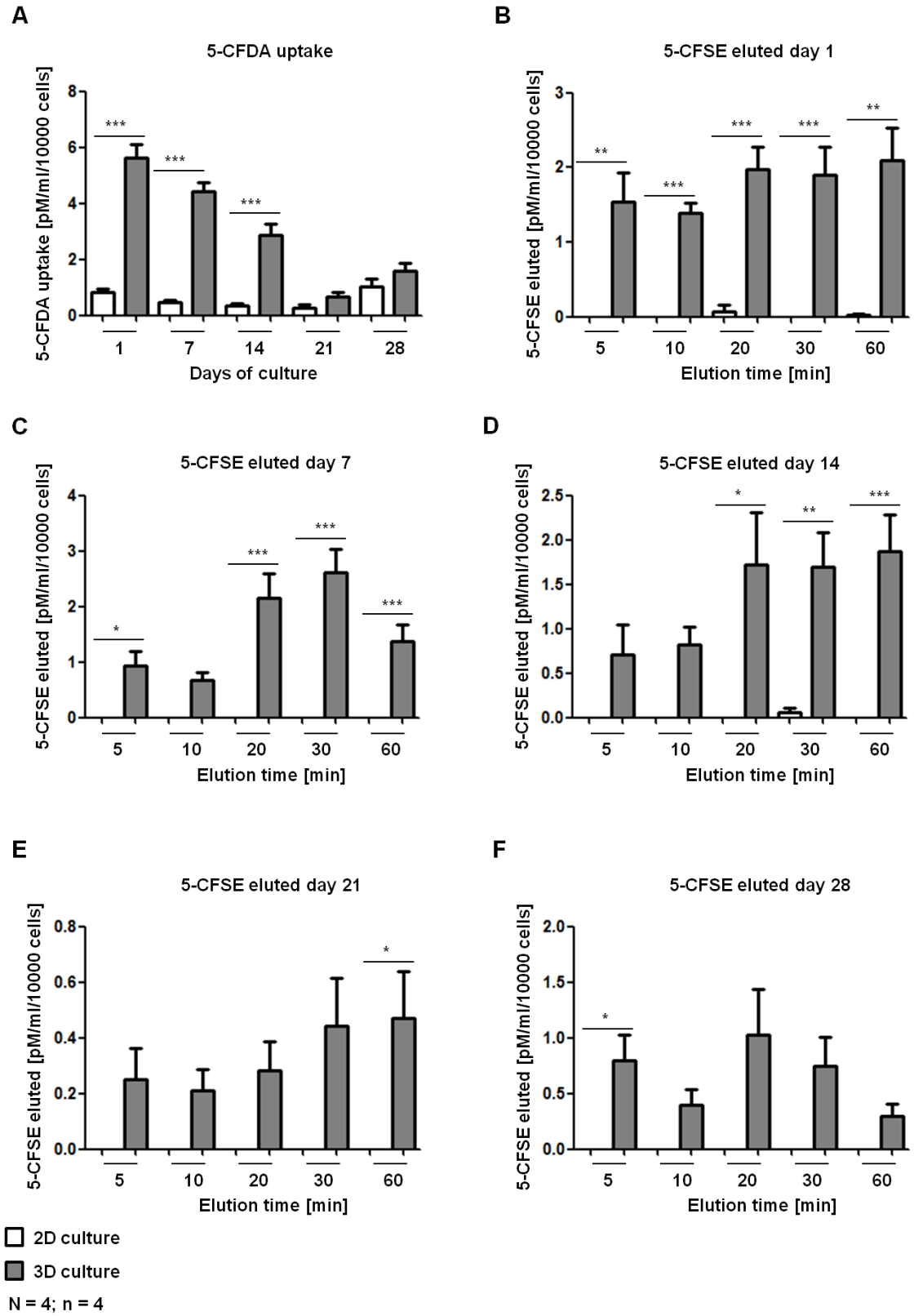

Figure 3. 19 Substrate/product efflux on MRP1 in PHH at **(A)** day 1, **(B)** day 7, **(C)** day 14, **(D)** day 21 and **(E)** day 28 in 2D and 3D cultures. Data are showed as mean ± SD. One-way ANOVA; *p < 0.05, **p < 0.001, ***p < 0.0001.

3.1.2.7.2.2. Multidrug-resistant protein 1/P-glycoprotein (MDR1/P-gp)

An elution assay was used to investigate Rhodamine 123. Hepatocytes were incubated for 30 min with 3 µM of Rhodamine 123, so that it diffuses into the cells. In hepatocytes, Rhodamine 123 is exported into the cell culture supernatant by the activity of MDR1/P-gp hepatic transporters. Finally, the elution of Rhodamine 123 was quantified by collecting the supernatants at different time points. Figure 3.20 A exhibits the concentrations of diffused Rhodamine 123 into the PHH. In 2D cultures, a decrease of the diffused Rhodamine 123 was recorded over 28 days. However, in 3D cultures, the diffused Rhodamine 123 reached a peak at day 14. Significant statistical differences (***p < 0.0001) were observed at day 1, 14 and 21. Figure 3.20 B-F depict the elution of Rhodamine 123 in 2D and 3D cultures. Both cultures exhibited a similar tendency to increase the amount of Rhodamine 123 which is eluted during the incubation time. However, 2D cultures showed an elution of Rhodamine 123 only at day 1 and 7; whereas 3D cultures maintained their transporter activity over 28 days, although it decreased during the time of culture. Significant statistical differences were observed (*p < 0.05, **p < 0.001, ***p < 0.0001).

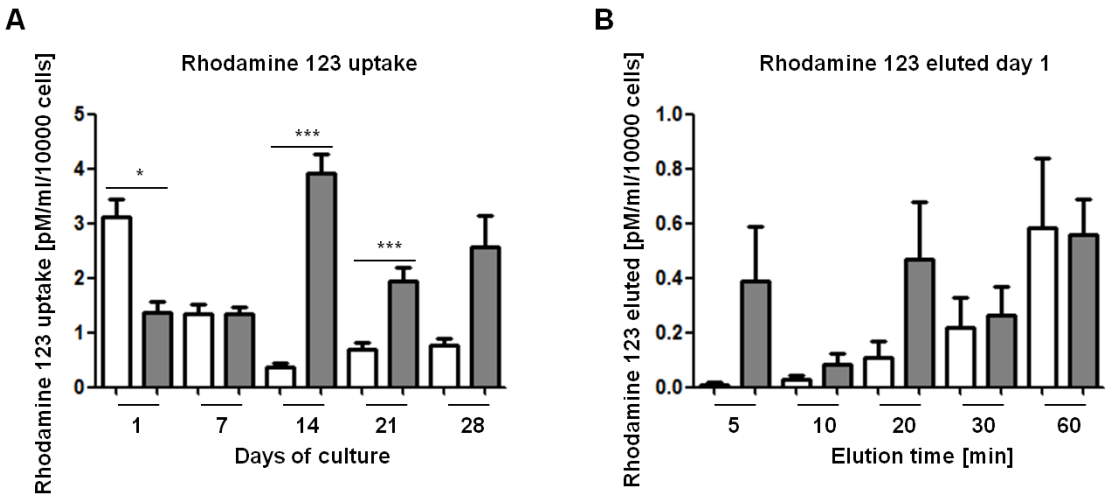

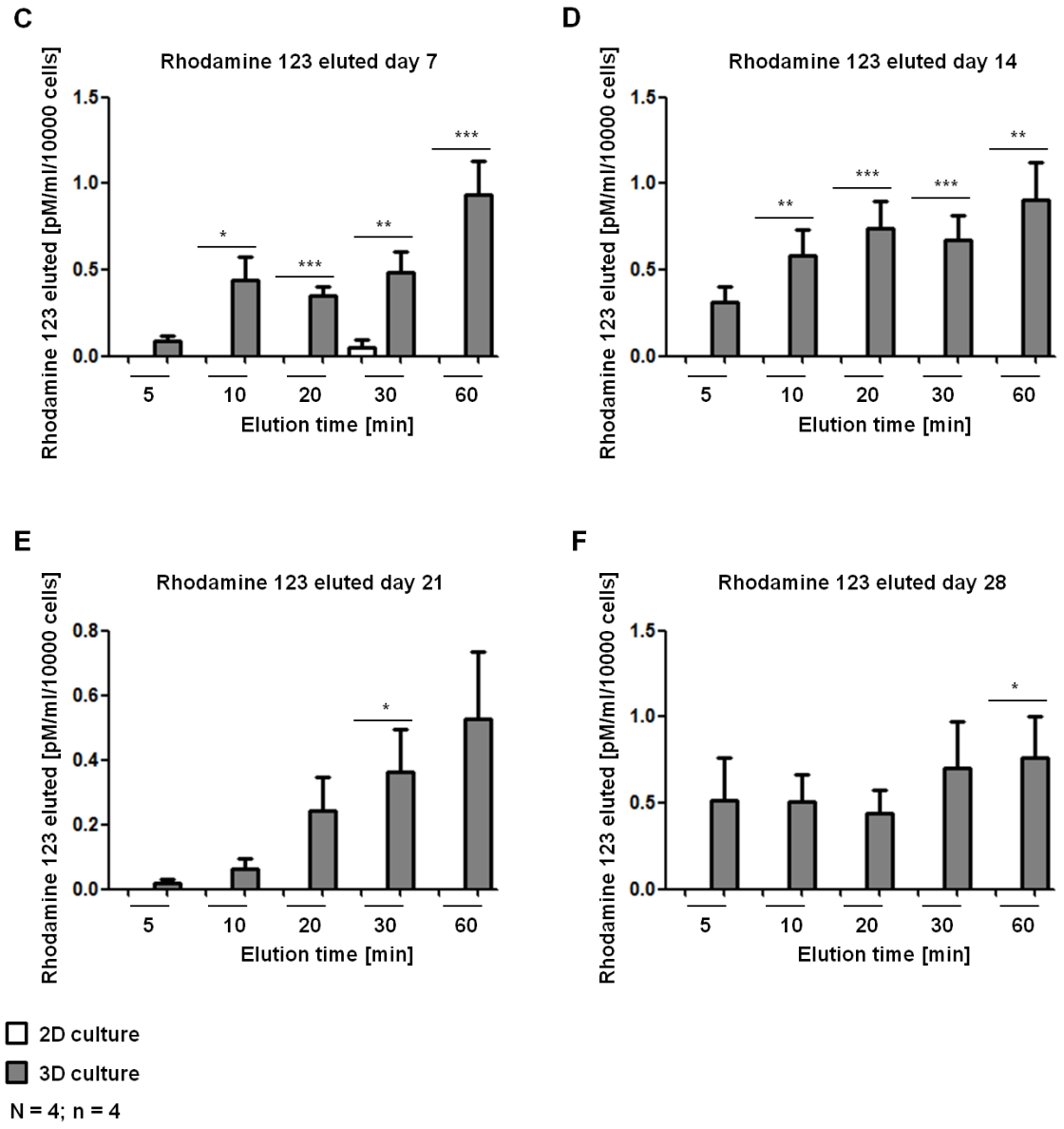

Figure 3. 20 Substrate/product efflux on MDR1/P-gp in PHH at **(A)** day 1, **(B)** day 7, **(C)** day 14, **(D)** day 21 and **(E)** day 28 in 2D and 3D cultures. Data are expressed as mean ± SD. One-way ANOVA; *p < 0.05, **p < 0.001, ***p < 0.0001.

3.1.2.8. Drug toxicity

Drug toxicity tests were performed by incubating PHH with different concentrations of acetaminophen and diclofenac. Then, cell viability was measured indirectly by resazurin conversion which measures the mitochondrial activity of the PHH.

3.1.2.8.1. Acetaminophen

At day 1 (Fig. 3.21 A), 3D cultures showed a more defined toxicity curve than 2D cultures. 2D cultures showed no variations in the drug concentration in mitochondrial activity at days 7 (Fig. 3.21 B) and 14 (Fig. 3.21 C); whereas 3D cultures maintained dose-response variations in mitochondrial activity.

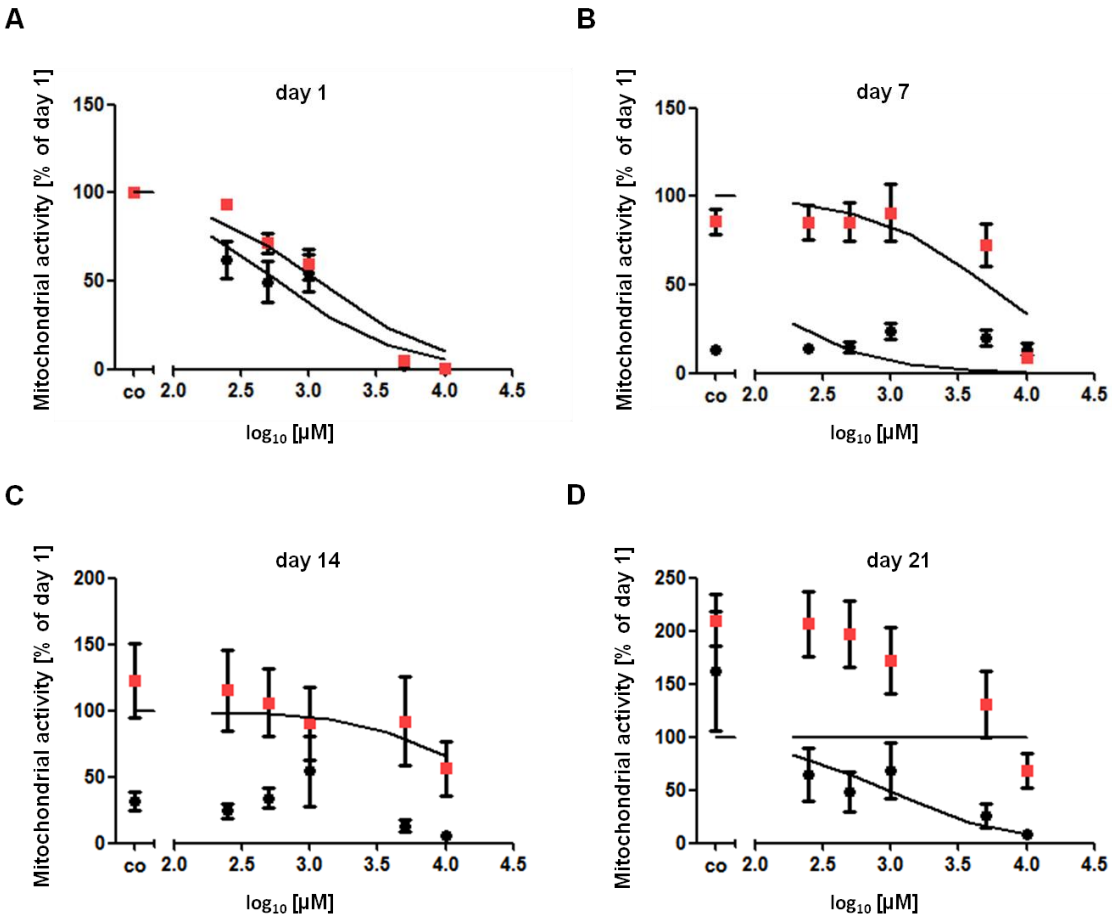

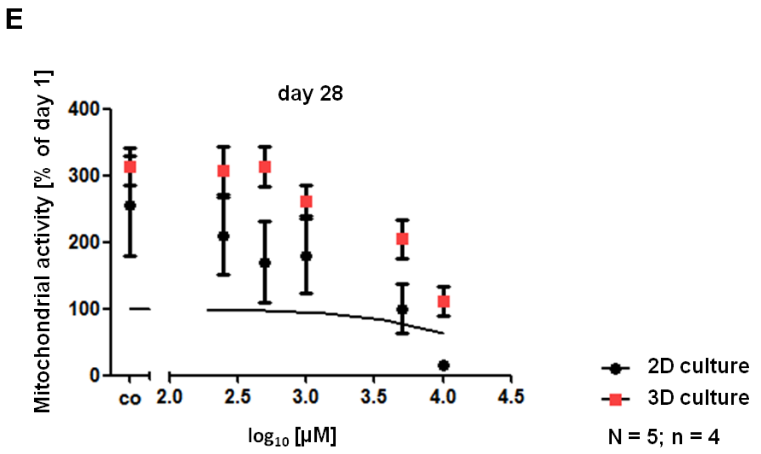

Figure 3. 21 Acetaminophen toxicity in PHH at **(A)** day 1, **(B)** day 7, **(C)** day 14, **(D)** day 21 and **(E)** day 28 in 2D and 3D cultures. Data are showed as mean ± SD.

3.1.2.8.2. Diclofenac

At day 1 (Fig. 3.22 A), 3D cultures showed a more defined toxicity curve than 2D cultures. 2D cultures showed no variations in drug concentration in mitochondrial activity at days 7 (Fig. 3.22 B) and 14 (Fig. 3.22 C); whereas 3D cultures maintained dose-response variations in mitochondrial activity.

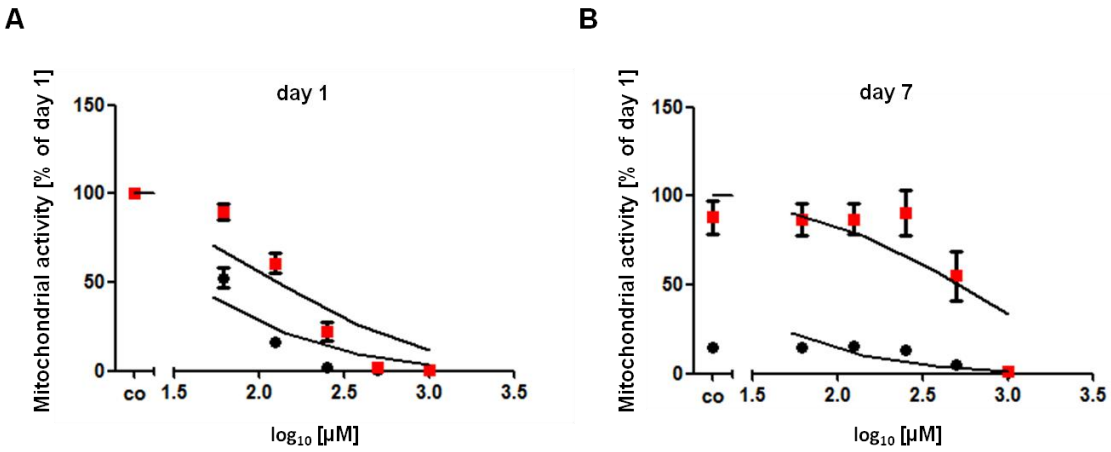

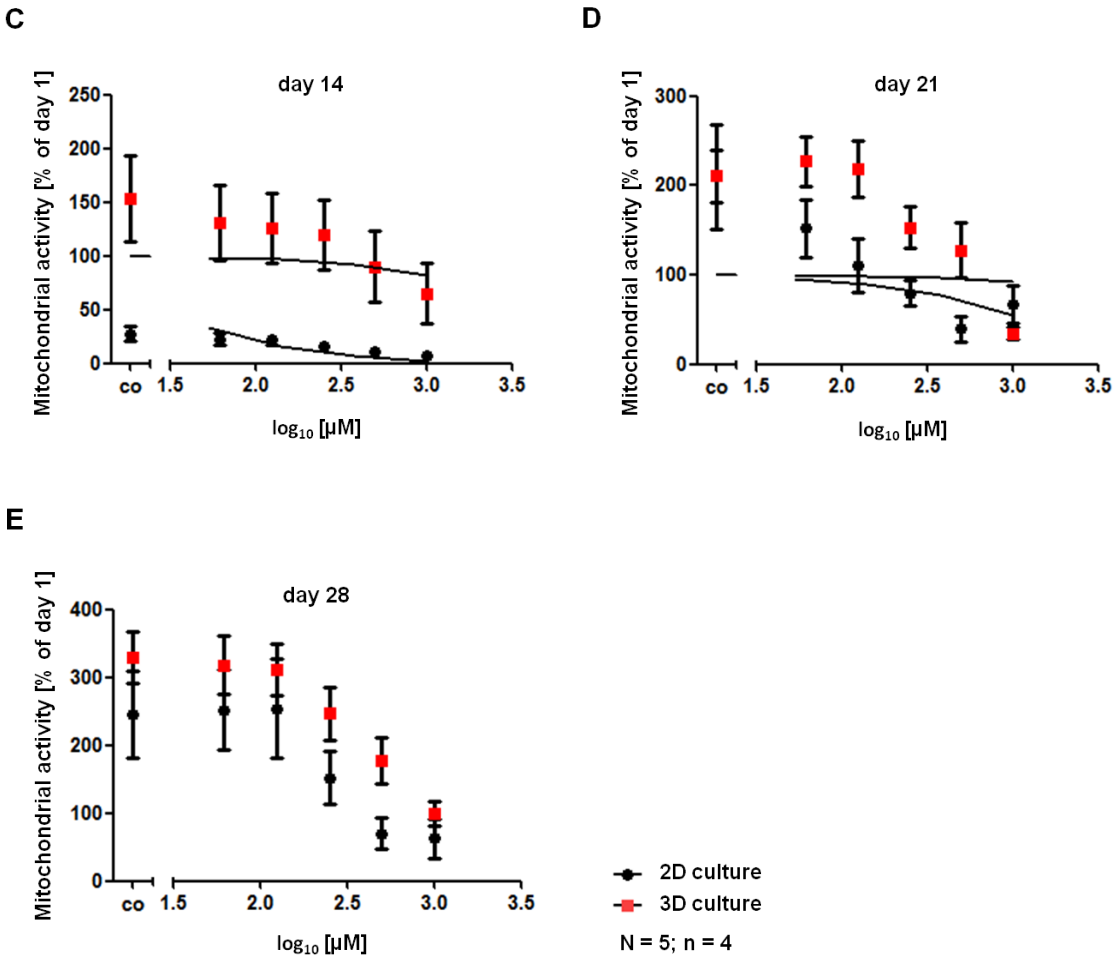

Figure 3. 22 Diclofenac toxicity in PHH at **(A)** day 1, **(B)** day 7, **(C)** day 14, **(D)** day 21 and **(E)** day 28 in 2D and 3D cultures. Data are expressed as mean ± SD.

3.2. Flow cultures

3.2.1. Perfusion assays

Collagen gel, 3D-Life hydrogel and hydrogel were loaded into µ-slide channels. Perfusion assays were performed in order to determine the adequate flow rate for the microfluidic system. Resazurin sodium salt (25%) was diluted in DPBS and used as a perfusion solution due to its dark blue color which allows for the study of the perfusion solution behavior at different flow rates (Fig. 3.23). In collagen gels, a homogeneous flow was observed only at low flow rates (Fig. 3.23 A). Moreover, collagen gel containing re-suspended cells showed no alteration of the flow rate (Fig. 3.23 C).

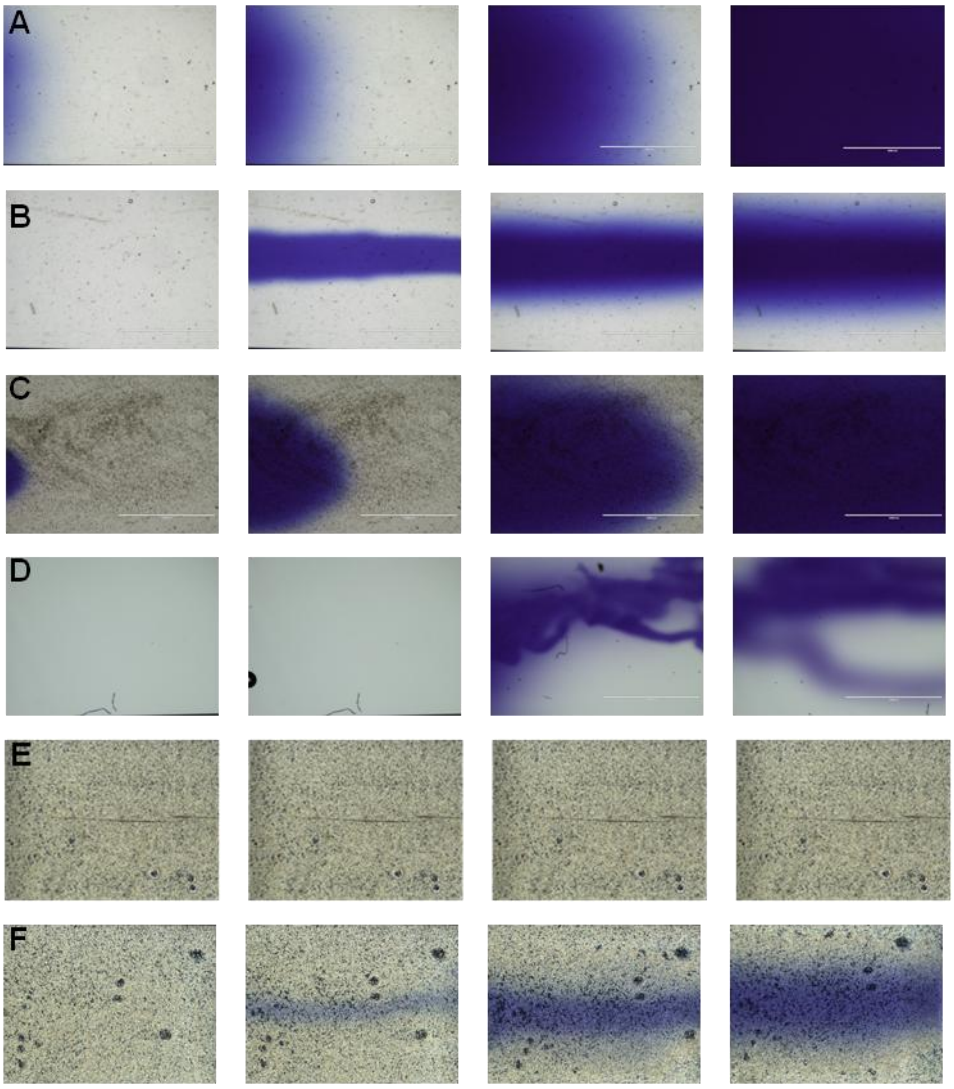

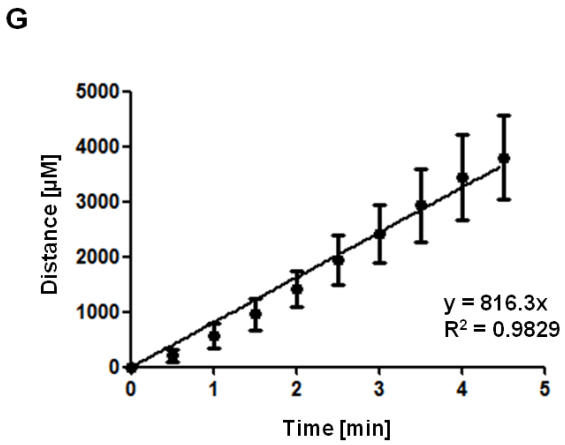

Figure 3. 23 Sequence of micrographs showing the perfusion flow through the µ-slide channels at different speeds (x40). **(A)** Collagen gel, 100 µl/h; **(B)** Collagen gel, 2 ml/h; **(C)** Collagen gel with Huh7, 100 µl/h; **(D)** 3D-Life hydrogel, 100 µl/h; **(E)** Poly(ethylene glycol) hydrogel with Huh7, 100 µl/h; **(F)** Poly(ethylene glycol) hydrogel with Huh7 2 ml/h. **(G)** Diffusion rate in collagen gels at 100 µl/h flow. Data are expressed as mean ± SD.

3.2.2. Flow in the microfluidic system

The continuous flow of 4 channels simultaneously was achieved by creating an individual medium reservoir for each channel. The syringe pump was used to pump air into the medium reservoir containers in order to increase the pressure slightly inside the falcon tubes, favoring the release of the medium (Fig. 2.12). Eluted medium from the different channels was collected in falcon tubes during 24 h. Flow rate ranged between of 80 to 100 µl/h in the four channels of the µ-slide (Fig. 3.24).

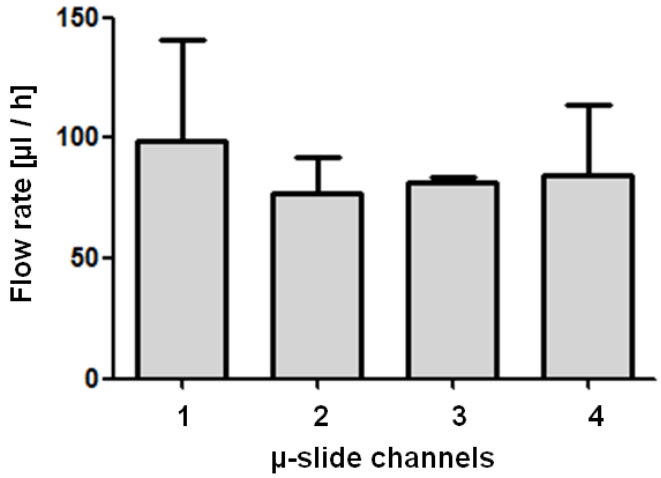

Figure 3. 24 Representation of the flow in the different channels of the µ-slide.

3.2.3. Cell morphology studies

PHH morphology was investigated by the observation of the cells under the microscope (Fig. 3.25). PHH maintained a round shape and formed aggregates which lasted over the time of culture. In static cultures, PHH were seeded in 96-well plates, whereas in flow cultures, PHH were seeded in µ-slides. As the area of the µ-slide channels is twice the area of the 96-well plates, the micrographs below present a higher concentration of cell aggregates in static than in flow cultures.

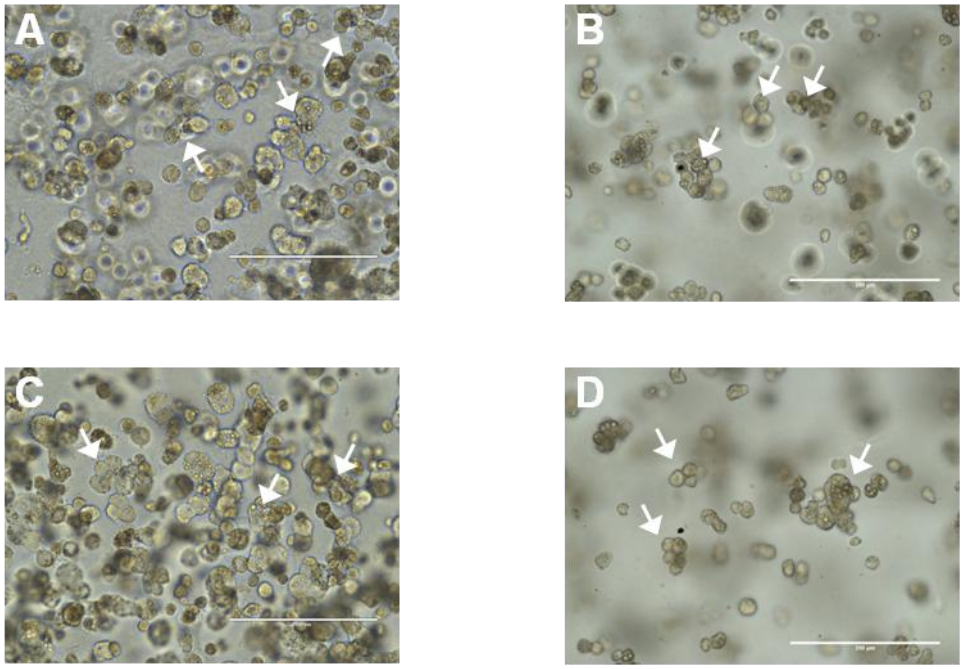

Figure 3. 25 Transmitted light micrograph of PHH entrapped in collagen gels in static and flow culture: day 1 **(A)** static, **(B)** flow; day 7 **(C)** static, **(D)** flow. (x 200 magnification). PHH aggregates are indicated by white arrows. Scale bar 200 µm.

3.2.4. Cell viability

PHH viability was investigated by live/dead staining (Fig. 3.26). However, in collagen gel cultures, cell quantification could not be performed as cells are entrapped in different levels in collagen gel. Therefore, we measured mitochondrial activity by resazurin conversion which allows for an indirect determination of cell viability (Fig. 3.27).

3.2.4.1. Live/Dead staining

In the framework of a live/dead staining of PHH, stained living cells, green fluorescence (Calcein-AM, 2µM) and dead cells, red fluorescence (Ethidium homodimer, 4 µM). Figure 3.26 shows a slightly increase of the number of dead cells in flow cultures compared to static cultures over 7 days.

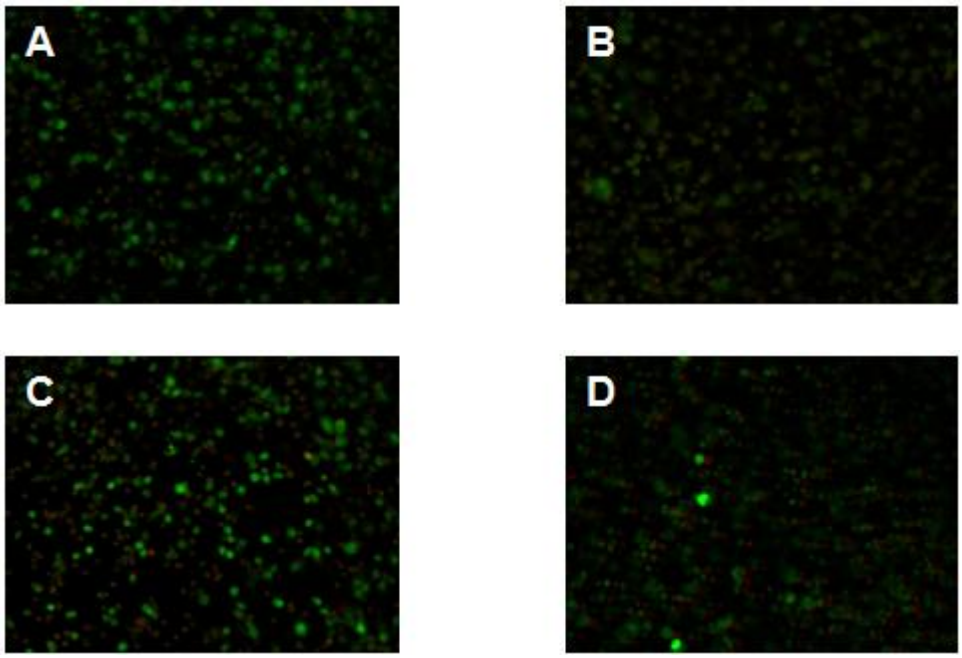

Figure 3. 26 Survival of PHH embedded into collagen gel cultured in static and flow condition (x 100 magnification): day 1 **(A)** 3D static, **(B)** 3D flow; day 7 **(C)** 3D static, **(D)** 3D flow.

3.2.4.2. Resazurin conversion

Mitochondrial activity was assessed by measuring the intracellular conversion of resazurin to resorufin. No significant statistical differences were observed after 7 days of culture. However, in static cultures, PHH maintained a higher mitochondrial activity during the time of culture.

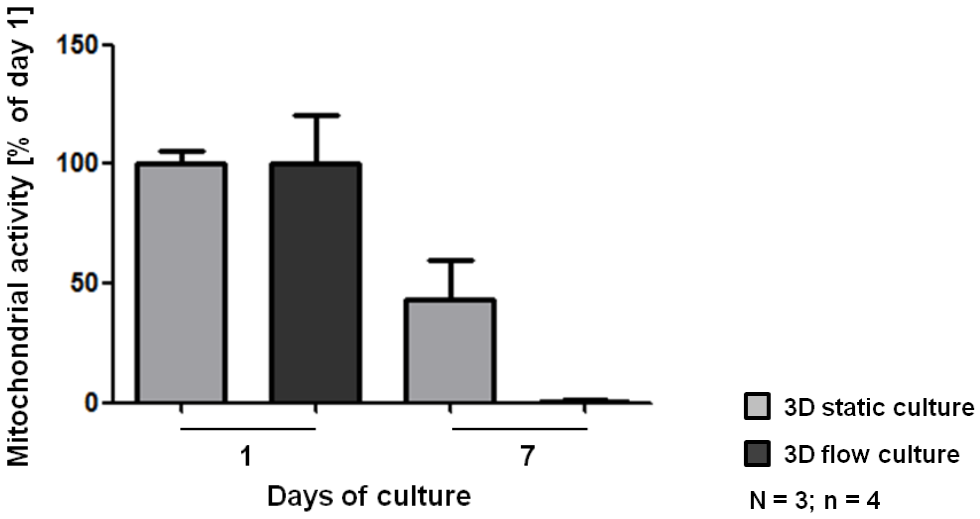

Figure 3. 27 Mitochondrial activity was assessed by resazurin conversion. Fluorescence was measured by plate reader. Data are expressed as mean ± SD.

3.2.5. Glucose production

Glucose production (glucogenolysis) exhibited significant statistical differences (*p < 0.05) over the 7 days of culture (Fig. 3.28). PHH seems to maintain this functional parameter for 7 days in static culture, but not in flow culture.

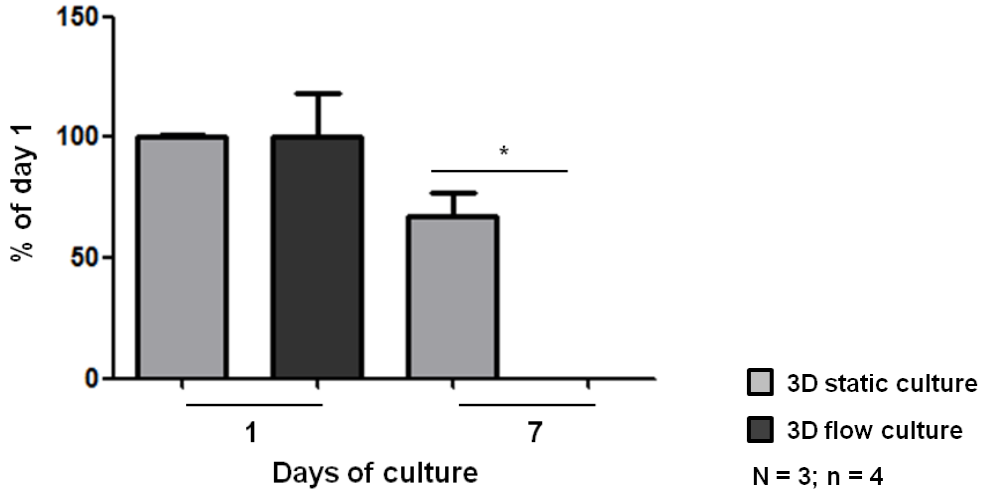

Figure 3. 28 Glucose production (glucogenolysis) in 3D static and flow cultures over 7 days. Absorbance was measured by plate reader. Data are showed as mean ± SD. One-way ANOVA; *p < 0.05.

3.2.6. Enzymatic activity of CYP2E1 and CYP3A4

Enzymatic activity of CYP2E1 and CYP3A4 were investigated by stimulating the PHH with acetaminophen (100 μM) (Fig. 3.29) and diclofenac (10 μM) (Fig. 3.30). Supernatants were collected at different time points and measured by LC/MS.

3.2.6.1. Metabolism of acetaminophen

Enzymatic activity of CYP2E1 was investigated indirectly by measuring the amount of APA-sulphate which is metabolized by PHH. No significant statistical differences were observed. APA concentration exhibited a similar decreasing tendency in static and flow cultures from day 1 to day 7 (Fig. 3.28 A-B). However, the APA-sulphate area exhibited a slight increase which correlates with the incubation time in static and flow cultures at day 1, but not at day 7 (Fig. 3.28 C-D).

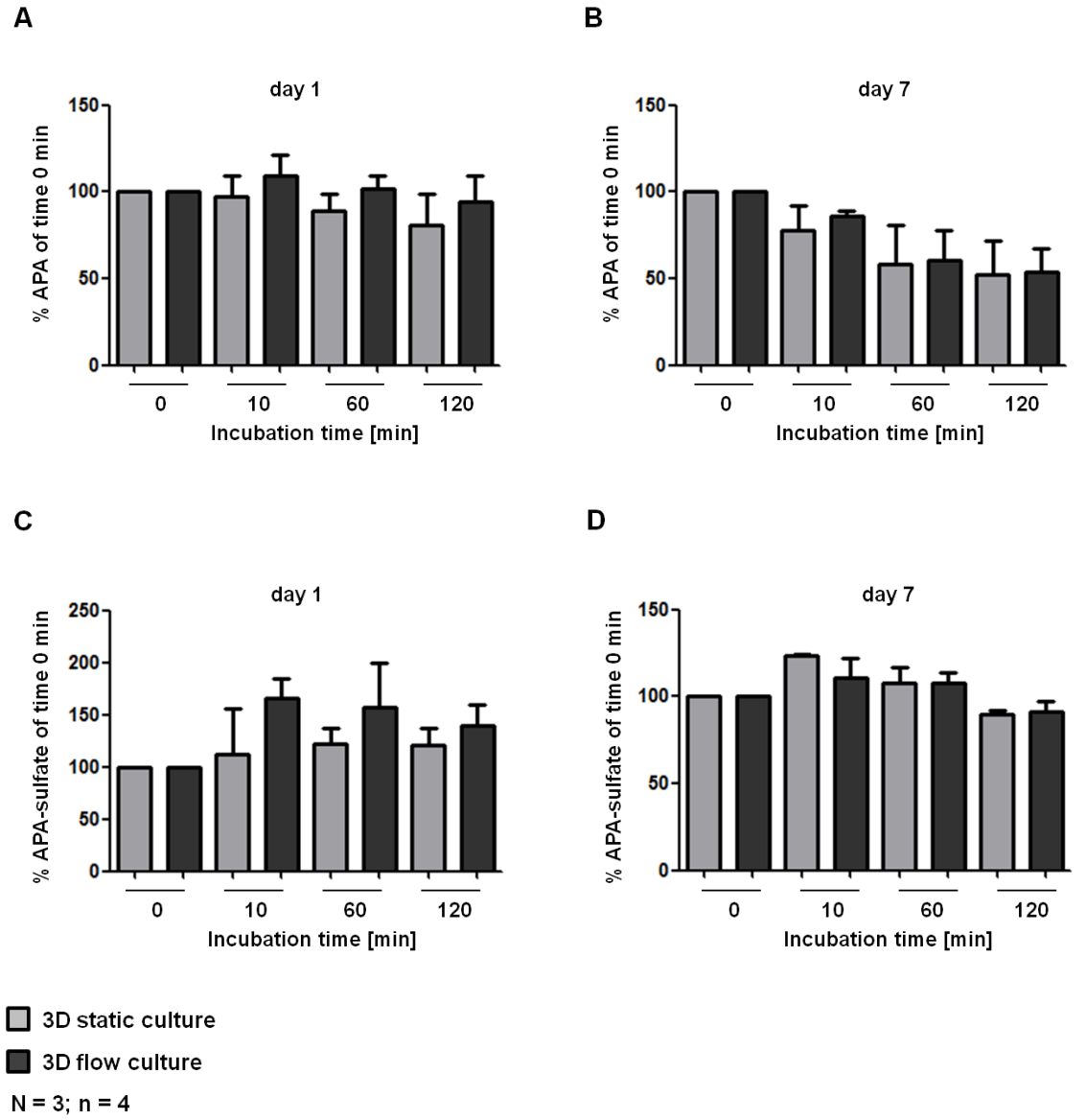

Figure 3. 29 Activity of the CYP2E1 during the metabolism of acetaminophen. **(A-B)** Remaining APA in supernatants after an incubation time of 120 min. **(C-D)** Metabolized APA-sulphate by PHH. Data are showed as mean ± SD.

3.2.6.2. Metabolism of diclofenac

The enzymatic activity of CYP3A4 was investigated indirectly by measuring the amount of 4-Hydroxydiclofenac which was metabolized by PHH. No significant statistical differences were observed. The concentration of diclofenac showed a similar decreasing tendency in static and flow cultures at days 1 and 7 when the incubation time increased (Fig. 3.29 A-B). However, 4-Hydroxydiclofenac area showed a slight increase which correlates with the incubation time in static and flow cultures at day 1 and 7 (Fig. 3.29 C-D).

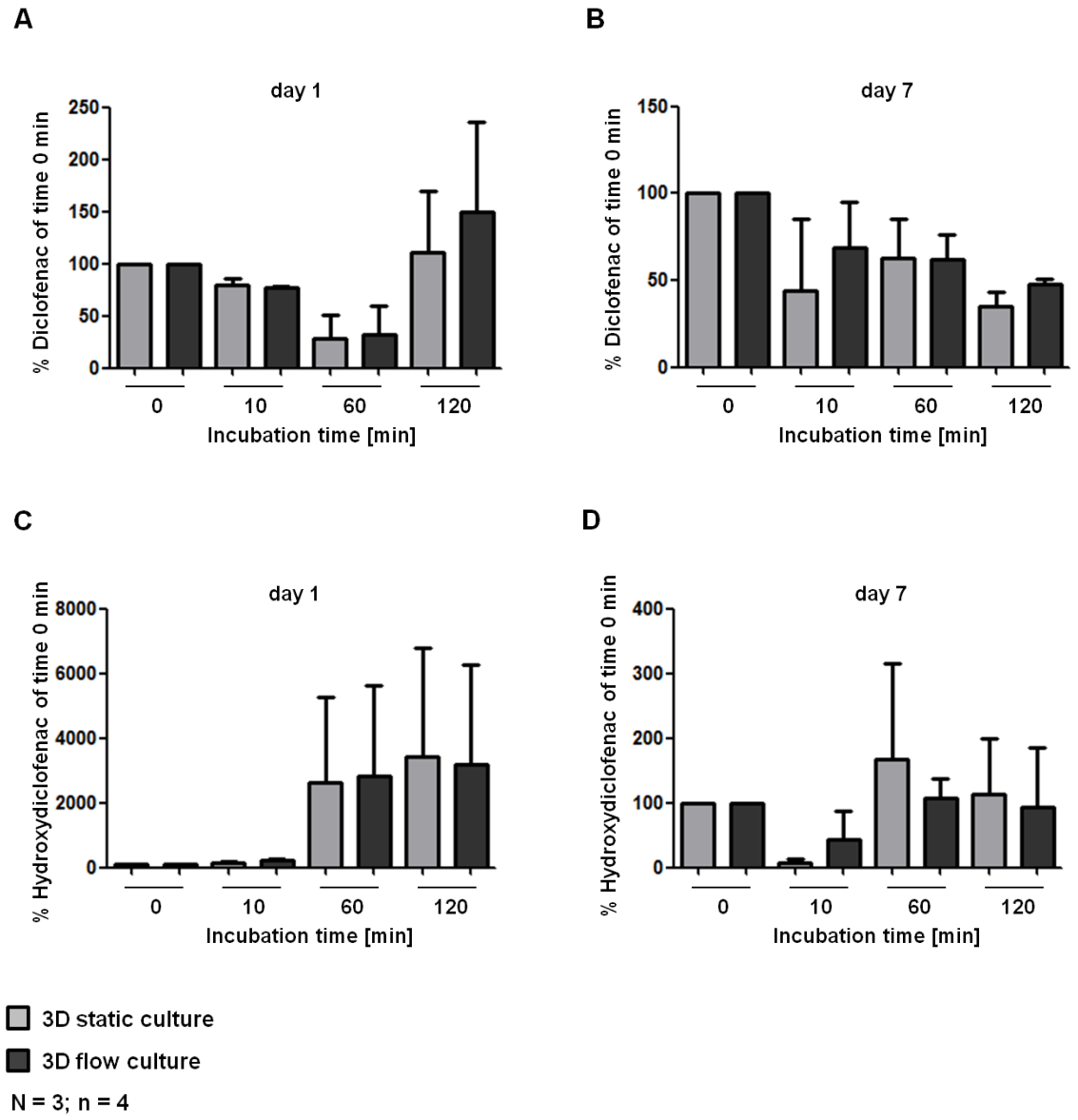

Figure 3. 30 Activity of the CYP2C9 during the metabolism of diclofenac. **(A-B)** Remaining diclofenac in supernatants after an incubation time of 120 min. **(C-D)** Metabolized 4-hydroxydiclofenac by PHH. Data are expressed as mean ± SD.

3.2.7. Drug toxicity

Drug toxicity tests were performed by incubating PHH with different concentrations of acetaminophen and diclofenac. Then, cell viability was measured indirectly by resazurin conversion which measures the mitochondrial activity of the PHH.

3.2.7.1. Acetaminophen

At day 1 (Fig. 3.31 A), 3D cultures showed a more defined toxicity curve than at day 7 in both cultures. In addition, flow cultures exhibited no drug-response the in mitochondrial activity at day 7 (Fig. 3.31 B); whereas static cultures maintained dose-response variations in mitochondrial activity.

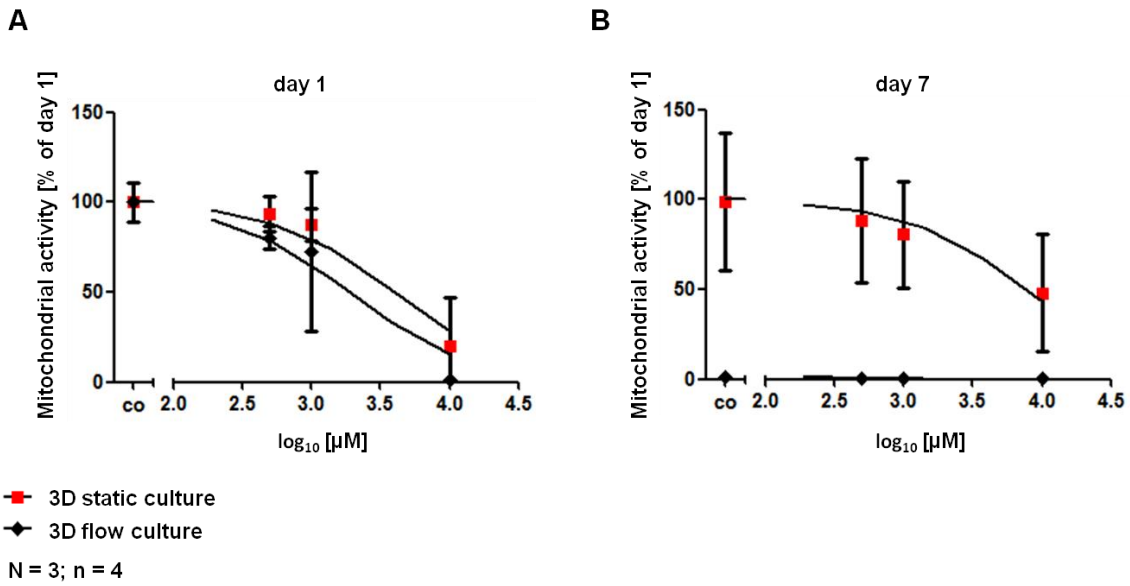

Figure 3. 31 Acetaminophen toxicity in PHH at **(A)** day 1, **(B)** day 7 in static and flow cultures. Data are showed as mean ± SD.

3.2.7.2. Diclofenac

At day 1 (Fig. 3.32 A), 3D cultures showed a more defined toxicity curve than at day 7 in both cultures. In addition, flow cultures exhibited no drug-response the in mitochondrial activity at day 7 (Fig. 3.32 B); whereas static cultures maintained dose-response variations in mitochondrial activity.

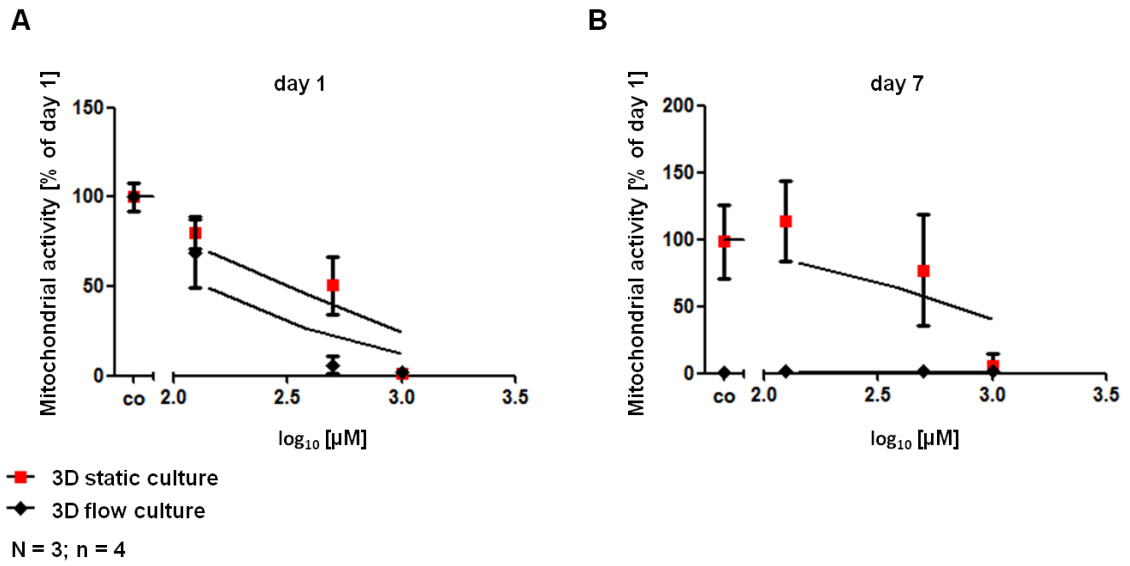

Figure 3. 32 Diclofenac toxicity in PHH at **(A)** day 1, **(B)** day 7 in static and flow cultures. Data are showed as mean ± SD.

4. Discussion

The liver is the organ which is primarily responsible for the first defense of the body against toxins and harmful substances [4, 108]. Furthermore, the liver regulates the metabolism of the body, and is responsible for glycogen storage, bile production, and plasma protein synthesis [1, 14]. Therefore, during the development of new drugs, specific toxicity tests analyse the new medicine's potential for causing liver injury. It has been proven that liver injury is the most common cause for withdrawing medicaments from the market [5]. Traditional toxicity tests, like those being performed by pharmacological companies, use laboratory animals with the intention of avoiding potential damage to humans. However, animal testing is controversial as, on the one hand, it raises ethical questions on the right to use animals, and, on the other hand, the translation of the results that have been obtained in animals to the human situation has proven to be difficult. In addition, since the approval of the Directive for the Protection of Vertebrate Animals used for Experimental and other Scientific Purposes (86/609/EEC) in 1986, the needs for laboratory animal care have increased, which, in turn, has led to higher animal maintenance costs for the pharmaceutical companies [8]. Thus, ECVAM is working on the validation of methods to assess testing safety, and drug efficiency, which reduce or replace the use of laboratory animals. Some of these methods use cells, like *e.g*. hepatoma cell lines, hepatocytes-like cells and PHH.

PHH present two main problems; the first one is the limited access to human liver tissue and the second one is their short life span [109], which refers to the rapidly loss of their phenotype and consequently loss of polarity in traditional cultures. Then, PHH spread on the culture plates generating an epithelial-mesenchymal transition during which the hepatocytes lose many liver specific functions, and decrease cell viability during the time of culture [31, 32]. Hepatocytes are very specialized cells and present an atypical polarization, apical and basolateral membranes, which is necessary to be functional [17]. ECM is crucial to keep the differentiated state of hepatocytes [110]. Thus, in order to maintain hepatocytic phenotype during the time of culture, PHH have

been cultured in different matrices which incorporate ECM proteins. The most common method used for long-term cultures is the culture of PHH sandwich conformation, being collagen and Matrigel® the most used materials [30]. Sandwich culture allows the hepatocytes to maintain their phenotype and consequently liver specific functions [53, 111, 112]. Nonetheless, *in vitro* culture of hepatocytes differs from the *in vivo* situation. In traditional 2D and 3D cultures, the medium is loaded over the cells; however, *in vivo* liver tissue presents a double blood supply, 75%-80% deoxygenated blood from the portal vein and 25%-20% oxygenated blood from the portal artery [113]. As a result, bioreactors which are 3D cultures with a continuous flow have been developed (Table 1.3). Many of these devices try to mimic the organotypic conditions of the liver which enable a more realistic study of the cell-cell and cell-environment interactions [82]. Nonetheless, the high cost of the equipment and the low throughput reduce their use in hepatotoxicity studies.

Due to the low PHH availability, hepatoma cell lines are used as an alternative in toxicity assays. Contrary to PHH, they proliferate indefinitely, and therefore provide an appropriate supply of cells. However, the low activity of metabolic enzymes in hepatoma cell lines in comparison to PHH, and the variations between the different passages restrict their use in drug testing [24, 114]. In recent years, another alternative for toxicity studies and possible future source for cell transplantation has been studied, which focuses on the generation of hepatocyte-like cells from extrahepatic cell sources. For instance, programmable cells of monocyte origin (PCMO) have been differentiated into hepatocyte-like cells with their corresponding characterization in order to be used in cell therapies and toxicological testing [104, 115-118]. Another extra-hepatic cell source for hepatic-like cells is the adipose-derived mesenchymal cells (Ad-MSCs) [119, 120]. However, low expression of hepatocytic markers, low metabolizing capacity, and difficulties of generating large reproducible hepatocyte-like cells, still limit their use in drug testing. Despite their limitations, PHH are still the “gold standard” for drug metabolism and toxicity studies [30, 39].

4.1. Choice of the matrix

Several bioreactors and microfluidic systems for PHH culture, which have already been commercialized or exist as prototypes, dispose of cavities or spaces which prevent the cells from the direct contact with the flow of the medium, so that they are protected against shear stress, and permit the 3D disposition of the cells. Two examples of this type of bioreactors are the hollow fiber bioreactor [76] and the KitChip bioreactor [79]. The μ-slide, for this part, presents 6 channels in which the cells are seeded and which are in direct contact with the flow of the medium. However, one characteristic of the μ-slide is the possibility of using different matrices which allow the study of several liver diseases as liver ECM composition changes at different stages of the disease, like *e.g.*, fibrosis and cirrhosis [4]. A first sight, solid matrices, which are also called 'scaffolds', may present the best option, as they have pores which do not disturb the flow of the medium and permit the three-dimensional culture of cells [67]. However, scaffolds were discarded in this project, because they could not be introduced in the channels. Therefore, different hydrogels were tested.

Due their reproducibility and the possibility of mimicking the ECM, two synthetic hydrogels, 3D-Life Hydrogels and poly(ethylene glycol) hydrogels, were tested [48]. Both hydrogels did not exhibit a homogenous flow. Contrary to scaffolds, hydrogels are water-swollen polymers [43] and under a continuous flow, hydrogels experience a volume change which leads to a reduction of their pore sizes [121] In addition, 3D-Life hydrogels have a small pore size (8 nm), which renders the flow difficult [92]. Because of these facts, the pressure on the gel increased during the flow time, which resulted in the damage of the gel structure, which, in turn, would explain the heterogeneous flow.

Finally, collagen a natural hydrogel and the most common ECM protein in mammals was tested as well [52]. Collagen is highly compatible and non-toxic to the PHH [48]. Interestingly, collagen gel exhibited a homogeneous flow through the μ-slide channel. Contrary to synthetic hydrogels that have a small pore size, collagen gel with a concentration of 2 mg/ml have a pore size between 1.2-1.8 μm [122] which allow homogeneous flow through the hydrogel. In addition, the collagen gel containing cells did not exhibit any alteration of the

flow at low speed (100 µl/h). Therefore, collagen gel was chosen as our matrix for the culture of PHH under continuous flow.

4.2. Collagen sandwich cultures better than monolayer cultures

Previous studies have demonstrated that PHH in collagen sandwich preserve hepatocytic functions and delay dedifferentiation during the time of culture [30, 53, 54, 111, 123]. Therefore, we have investigated the possibility of testing hepatotoxicity in sandwich cultures instead of the monolayer cultures that are currently used in the pharmaceutical industry, by using acetaminophen as a model drug. Acetaminophen is a drug which is used all over the world. It is safe at therapeutic doses [2, 89], but an over dosage can lead to acute liver failure [3]. *In vitro* monolayer cultures do not exhibit symptoms of toxicity at lower concentrations (0.5-1 mM) while *in vivo*, lower concentrations cause liver necrosis [124, 125]. Firstly, our findings corroborate that PHH in 2D cultures change their morphology, die and detach, while PHH in 3D cultures keep their structure over the time of culture. Then, PHH that had been stimulated with acetaminophen over 72 h and different aspects were studied. The exposure to acetaminophen resulted in an increase of cell death in 3D but not in 2D cultures. Similar results had been obtained in previous studies, in which rat hepatocytes cultured on a polystyrene scaffold had been incubated with acetaminophen [74].

In hepatocytes, acetaminophen is metabolized by the enzyme CYP2E1 during the phase I of the metabolism. During the metabolism, the highly toxic product N-acetyl-p-benzoquinone imine (NAPQI) is formed [126, 127]. During the treatment with acetaminophen, the level of the CYP2E1 protein increases in 3D but not in 2D cultures. Therefore, higher concentrations of NAPQI, which accumulates in the cells and induces cell necrosis, have been registered [128, 129]. On the other hand, SOD1, an antioxidant protein that protects PHH from oxidative stress [130] decreases after the stimulation with acetaminophen in 3D but not in 2D cultures. This decrease indicates a nitration of SOD1 by reactive nitrogen species which leads to an increment of toxicity in the mitochondria through the reaction of nitric oxide with the superoxide [131]. In addition, the kinetic metabolic turnover of acetaminophen was higher in 3D than in 2D cultures.

Moreover, the hepatic transporters, MRP1, MRP2, MRP3 and MRP4, have been studied at gene level after the stimulation with acetaminophen. Only the expression of MRP1 was up-regulated after the incubation with acetaminophen. Therefore, the transport activity of MRP1 was investigated in more detail: MRP1 is a transport protein located at the basolateral membrane and belongs to the ABC transporter family [132, 133]. At gene level, no statistical difference has been observed between 2D and 3D cultures. However, 3D cultures presented higher import and efflux activity than the 2D cultures. These findings indicate that the transporter activity is influenced by the culture conditions: In 2D cultures, basolateral and apical transporters are located on the cell surface which leads to a decrease of the transporter activity [134]. Another possible reason for the reduction of the transporter activity is the migration of the protein transporter from the surface of the membranes to internal sites under adverse conditions [135]. Moreover, the transport activity can be affected by the decrease of the substrate specificities due to the switch of the efflux activity between different transporter protein isoforms or due to the location of different transporters at different membranes when the PHH lose their polarity [136, 137].

Although it has been proven that sandwich cultures generate results which allow for their better comparability to the *in vivo* situation [30, 53, 54, 123], the lack of liver tissue requires a further reduction of the cell number for future hepatotoxicity prediction *in vitro*. Sandwich cultures cannot be performed in 96-well plates, as the minimal area which is necessary for sandwich cultures, corresponds to that of a 24-well plate. However, cultures in 24-well plates require a higher number of cells and reduce the throughput compared to 96-well plates. An alternative culture model to sandwich cultures is the 3D spheroid culture called hepatosphere. Hepatospheres are small aggregates of hepatocytes which their organization mimics the *in vivo* situation and maintain hepatocytic phenotype and liver specific functions for 2 weeks [138]. These spheroids can be cultured in small culture plates under static conditions but they are not suitable for our flow system as the hepatospheres will be flushed away from the μ-slide channel by the flow. Therefore, a new culture model which enables hepatocytes cultures in 96-well plates and in the ibidi® μ-slide is needed.

4.3. Culture of PHH in collagen gel

One of the restrictions of using PHH is the limited access to human liver tissue. Therefore, down scaling is necessary in order to improve the efficient use of the cells. For this reason, PHH were re-suspended in collagen gels, as they allow 3D culturing of cells in 96-well plates and in the ibidi® µ-slide. Our results have shown that the best possible viability was reached at a cell density of $5*10^3$ cells per microliter of collagen. This cell density seems to guarantee an optimal flow of substances in the culture medium. In the line with our findings, previous studies have proven that hepatocytes that are re-suspended in collagen gels with cell densities ranging from $1.5*10^6$ cells/ml to $5*10^6$ cells/ml do not alter the laminar flow, while higher cell densities (> $7*10^6$ cells/ml) do not enable any laminar flow at all [139]. In addition, PHH entrapped in 3D maintained a round shape and formed aggregates which is closer to the *in vivo* environment compared to PHH in 2D cultures [140].

The characterization of the PHH that had been re-suspended in collagen gels was carried out by measuring cell viability, hepatic specific functions and hepatotoxicity to drugs and by comparing these results to PHH cultured on collagen monolayer in order to determine any improvement due to the culture conditions. Our results exhibited that PHH entrapped in collagen gels maintain higher viability, glucose, and urea production over the time of culture than 2D cultures, which correlates with previous studies carried out with hepatocytes cultured in collagen sandwich and collagen entrapped gel cultures [53, 141, 142].

Next, the CYPs were investigated at gene expression level. Previous studies had shown that the gene expression of CYPs decreases over time in PHH cultured on collagen monolayer [24, 112]. However, our results demonstrated that the gene expression of the CYPs tested (CYP1A1, CYP1A2, CYP2A6, CYP2B6, CYP2C8, CYP2C9, CYP2D6, CYP2E1 and CYP3A4) was preserved, even though they exhibited a decreasing tendency over the time of culture in both cultures. However, there is a not strong correlation between gene expression and activity [143, 144]. Therefore, we investigated the CYP activity by a fluorescence-based assays [103]. CYP activity exhibited a decrease over

the time of culture where PHH in 3D cultures maintained higher enzymatic activity than 2D cultures with the exception of CYP2C8/9. A possible explanation to this fact is that the fluorometric substrate DBF, which was used to measure CYP2C8/9 activity, is not very selective. Thus, DBF can be metabolized by several CYPs generating larger amount of its metabolite [145]. In addition, we studied the enzymatic activity of the phase II between in both types of cultures. Contrary to the CYP activities, 2D cultures exhibited a higher activity than 3D cultures at day 1 and 7. However, after 14 days of culture, the tide turned and the enzymatic activity became higher in 3D cultures than in 2D cultures. These results showed that, in 2D cultures, PHH lose their polarized state faster, while 3D cultures slow down the depolarization of the cells, thereby maintaining enzymatic activity over a longer period of time [14, 30, 123]. Special mention needed GSH activity which increased its activity in 3D cultures during the first 14 days of cultures and then decreases over time of culture. This fact can be explain by the supplementation of the culture medium with amino acids, especially with L-proline which induces the GSH activity in 3D cultures [142].

PHH are very specialized cells and therefore, they have to be polarized in order to be functional [15]. In contrast to other epithelial cells, which dispose of only one apical membrane, hepatocytes present several apical and basolateral membranes [17]. These membranes are present in polarized PHH and are necessary for the uptake and elimination of the metabolite products through the sinusoids or through the bile canaliculi [15]. Therefore, different transporter channels, like *e.g.*, NTCP, OCT1, MDR1, MDR2, MDR3, MRP1, MRP2, MRP3, MRP4, MRP5, MRP6, BSEP, and BCRP, that are located at both membranes of the PHH, were studied. Like CYP gene expression, the majority of the transporter genes exhibited a decreasing tendency over the time of culture. The only exceptions were NTCP, MDR1, MRP1, MRP5, and BCRP, which did not follow any pattern. As no statistical differences were observed, the transport activity of MRP1 and MDR1/P-gp, which are located at the basolateral and the apical membranes respectively, were studied. MRP1 and MDR1/P-gp are transport proteins which belong to the ABC transporter family [132, 133]. The explanation for the fact that transporter activity was observed in 3D but not in 2D cultures was given in the section 4.2.

Finally, hepatotoxicity was studied by stimulating the PHH in 2D and 3D cultures with acetaminophen and diclofenac, which were used as model drugs, over 72 h. 3D cultures showed a more defined dose-response toxicity curve than monolayer cultures over 14 days of culture. Like acetaminophen, diclofenac metabolites are more toxic than the non-metabolized drug. The metabolism of diclofenac by CYP 2C9 favors the formation of 4'-hydroxydiclofenac and 5-hydroxydiclofenac which bind to hepatic proteins producing mitochondrial toxicity and consequently cell death [146]. A possible reason for this finding is that, in monolayer cultures, PHH are exposed to a higher alteration of the environment, which increases cell stress, hepatic dedifferentiation, and consequent cell death. The explanation for the fact that PHH exhibited higher toxicity after stimulation with acetaminophen was given in the section 4.2.

4.4. Microfluidic system

In this study we have shown that PHH cultured in 3D preserved their hepatocytic functions for a longer time than those in 2D. However, hepatocytes are constantly irrigated by blood in the *in vivo* situation. Culturing PHH under a continuous flow mimics the organotypic environment of the liver, which improves the detoxification activity of the cells [77]. The first flow cultures were performed in bioreactors but the high demand of cells limited their uses [51, 76]. As an alternative, microfluidic systems were developed, which enable a reduction of the number of cells and an increase of the throughput. Currently, there are several publications regarding microfluidic systems for the culture of PHH. Some of them are commercialized, like *e.g.* Quasi-Vivo® [77] and LiverChip [78], but the majority exists only as prototypes, like *e.g.* KITChip [147], HepaChip® [80], and Microfluidic Array [148]. However, all of them are composed by specific platforms, chips or arrays which have been made for their respective systems. In addition, those systems include expensive and sophisticated devices which pump the medium and oxygen into the systems restricting their use in hepatotoxicity prediction [77, 78, 80, 147, 148]. As we have already demonstrated, PHH maintain their liver functions when they are cultured in 3D. Therefore, we hypothesized that if we can apply a continuous flow to our 3D cultures we will improve the hepatocytic functions over the time

of culture. The microfluidic system that we present does not require expensive devices, like *e.g.* standard syringe pump, μ-slide, falcon tubes and tubing (Section 2.2.6.2). The choice of the matrix and the optimization of the flow rate were discussed in previous section (Section 4.1).

The characterization of the PHH was carried out by measurement cell viability, hepatic specific functions and hepatotoxicity to drugs and compared to PHH culture in static conditions in order to determine any improvement due to the culture conditions. Our data demonstrated to be contradictory, for instance, live/dead staining exhibited that PHH survive in the microfluidic system, nevertheless, a standard method used to measure cell viability by quantifying the mitochondrial activity of the cells (resazurin conversion) did not show any resorufin conversion. Similar results were found during the metabolism of acetaminophen and diclofenac which correlates to the activity of CYP2E1 and CYP2C9 respectively in static and flow cultures. On the other hand, glucose production and hepatotoxicity dose-response was only maintained in static cultures. As our system does not have any extra oxygen supply, a possible reason for the no metabolization of resazurin, no glucose production, and no hepatotoxicity dose-response is that PHH embedded in collagen gels and loaded into the μ-slide channel do not receive enough oxygen supply producing cell death by hypoxia. Also, big molecules in the medium such as glucose hinder the oxygen transport [149]. Another reason could be explained by the low mass transport of the hydrogels. Under a continuous flow, hydrogels experience a volume change which leads to a reduction of their pore sizes increasing the shear stress on the cells and consequently causing cell damage [121].

In order to further improve the characterization of the PHH in the μ-slide system, new approaches have to be committed. For instance, alternative experiments have to be performed or an improvement of the methods here performed has to be accomplished so that measurements can be performed directly on the μ-slide. The μ-slide system introduced in this study involves two major problems: One difficulty is the low throughput compared to traditional cultures in 96-well plates, which is nevertheless still higher than in some of the microfluidic systems. The other difficulty is the flow rate differences between the μ-slide

channels, which could be solved through the use of a peristaltic pump with a very low flow rate (> 100 µl/h) that creates an independent flow for each µ-slide channel. In future studies, the extensive characterization of the µ-slide system has to be broadened in order to benefit from the standardization of the system in every laboratory.

5. Abstract

Traditional toxicity tests are characterized by the use of *in vitro* and *in vivo* laboratory animals with the purpose of avoiding potential damage to humans. The use of animals for drug testing raises ethical questions, and involves high costs as well as a lack of reliability. However, the use of PHH as an alternative to animal testing involves two main problems: the limited access to liver tissue and the short life span of these cells. Therefore, hepatoma cell lines and hepatocyte-like cells from extra hepatic cell sources have been investigated as an alternative in toxicity assays, but their low expression of hepatocytic markers and their low metabolization capacity limit their use in drug testing. Polarization plays a key role in drug metabolism. Therefore, the hepatotoxicity in 2D and 3D (sandwich) cultures has been investigated here by using acetaminophen as a model drug. Our data have demonstrated that cell death is higher in 3D cultures than in 2D cultures as there is a higher metabolism of acetaminophen and therefore higher concentration of toxic metabolites (NAPQI) formed after treatment with acetaminophen. During these experiments, it has been observed that the protein expression of CYP2E1 and SOD1 depends on the concentration of acetaminophen. Therefore, the increase of the concentration of acetaminophen has led to a parallel increase of the expression of CYP2E1, but to a decrease of the expression of SOD1 in 3D, but not in 2D cultures. In addition, higher import/export rates have been observed for the multidrug resistance-associated protein-1 (MRP1), which is a specific transporter protein for acetaminophen metabolite transport in 3D cultures. 3D cultures exhibited better comparability of the results to the *in vivo* situation.

However, the limited access to liver tissue and the impossibility of using sandwich culture in small culture plates restrict the use of sandwich cultures for high-throughput screening. Therefore, PHH have been re-suspended in collagen gels. In this 3D model, cell viability, glucose production, and NH_4 detoxification have been preserved at a higher level over 28 days than in 2D cultures. Similar results have been observed during the measurements of the phase I and II metabolic activity. Furthermore, PHH have exhibited higher import/export rates in two transporter proteins, MRP1 and multidrug resistance

protein-1 (MDR1/P-gp), located at the basolateral and apical membrane respectively. Finally, PHH have exhibited higher toxicity in 3D than in 2D cultures after being stimulated by acetaminophen and diclofenac.

The culture of PHH under a continuous flow has demonstrated an improvement of the detoxifying activity of the cells. However, microfluidic systems are expensive and sophisticated devices whose use is restricted in hepatotoxicity prediction. Therefore, a simple and cheap microfluidic system has been tested in this work. The data from the live/dead staining has proven the survival of PHH in the microfluidic system. Similar results have been found during the metabolism of acetaminophen and diclofenac which correlates with the activity of CYP2E1 and CYP2C9 respectively in static and flow cultures. However, these findings could not be corroborated by the use of fluorescence and absorbance assays measured by a plate reader. In order to improve the characterization of the PHH in the µ-slide system, new approaches have to be developed, along with alternative experiments and an improvement of methods.

In this thesis, the behaviour of PHH on natural collagen gels in different culture conditions has been studied. However, the liver ECM is not only composed of collagen, but also contains proteins and proteoglycans. In addition, non-parenchymal cells are involved in the inflammatory response. Therefore, future studies should focus on testing hepatotoxicity in co-cultures of PHH and non-parenchymal cells in microfluidic systems with a matrix comprising several ECM proteins in order to achieve *in vitro* results which are highly comparable to the *in vivo* situation.

6. References

1. Sendensky, A. and J.F. Dufour, *Liver Physiology*, in *Chronic Liver Failure*, P. Ginès, P.S. Kamath, and V. Arroyo, Editors. 2011. p. 608.
2. Espinosa Bosch, M., et al., *Determination of paracetamol: historical evolution.* J Pharm Biomed Anal, 2006. **42**(3): p. 291-321.
3. Larson, A.M., et al., *Acetaminophen-induced acute liver failure: results of a United States multicenter, prospective study.* Hepatology, 2005. **42**(6): p. 1364-72.
4. Ishibashi, H., et al., *Liver architecture, cell function, and disease.* Semin Immunopathol, 2009. **31**(3): p. 399-409.
5. Abbond, G. and N. Kaplowitz, *Drug-induced liver injury.* Drug safety, 2007. **30**(4): p. 277-294.
6. Chapman, K.L., et al., *Pharmaceutical toxicology: Designing studies to reduce animal use, while maximizing human translation.* Regulatory Toxicology and Pharmacology, 2013. **66**(1): p. 88-103.
7. Bhardwaj, S. and D. Gupta, *Study of acute, Sub acute and chronic toxicity test.* International Journal of Advanced Research in Pharmaceutical & Bio Sciences, 2012. **2**(2): p. 103-129.
8. Baumans, V., *Use of animals in experimental research: an ethical dilemma?* Gene Therapy, 2004. **11**: p. S64 - S66.
9. Workman, P., et al., *Guidelines for the welfare and use of animals in cancer research.* British Journal of Cancer, 2010. **102**(11): p. 1555-1577.
10. Combes, R., M. Barratt, and M. Balls, *An overall strategy for the testing of chemicals for human hazard and risk assessment under the EU REACH system.* Altern Lab Anim, 2003. **31**(1): p. 7-19.
11. Adler, S., et al., *Alternative (non-animal) methods for cosmetics testing: current status and future prospects-2010.* Arch Toxicol, 2011. **85**(5): p. 367-485.
12. Lilienblum, W., et al., *Alternative methods to safety studies in experimental animals: role in the risk assessment of chemicals under the new European Chemicals Legislation (REACH).* Arch Toxicol, 2008. **82**(4): p. 211-36.
13. *Towards the replacement of in vivo repeated dose systemic toxicity testing*. Vol. 3. 2013, France.
14. Runge, D., et al., *Serum-Free, Long-Term Cultures of Human Hepatocytes: Maintenance of Cell Morphology, Transcription Factors, and Liver-Specific Functions.* Biochemical and Biophysical Research Communications, 2000. **269**: p. 46 - 53.
15. LeCluyse, E.L., et al., *Organotypic liver culture models: meeting current challenges in toxicity testing.* Crit Rev Toxicol, 2012. **42**(6): p. 501-48.
16. Fausto, N. and J.S. Campbell, *The role of hepatocytes and oval cells in liver regeneration and repopulation.* Mech Dev, 2003. **120**(1): p. 117-30.
17. Decaens, C., et al., *Which in vitro models could be best used to study hepatocyte polarity?* Biology of the cell, 2008. **100**: p. 387 - 398.
18. Clemens, D.L., *Use of cultured cells to study alcohol metabolism.* Alcohol Res Health, 2006. **29**(4): p. 291-5.
19. Oh, K.J., et al., *CREB and FoxO1: two transcription factors for the regulation of hepatic gluconeogenesis.* BMB Rep, 2013.
20. Robinson, B.H., *Transport of phosphoenolpyruvate by the tricarboxylate transporting system in mammalian mitochondria.* FEBS Lett, 1971. **14**(5): p. 309-312.
21. Alberts, B., et al., *Molecular biology of the cell*. 5th ed2007. 1392.
22. Soria, L.R., et al., *Ammonia detoxification via ureagenesis in rat hepatocytes involves mitochondrial aquaporin-8 channels.* Hepatology, 2013. **57**(5): p. 2061-71.

23. Inoue, Y., et al., *Defective ureagenesis in mice carrying a liver-specific disruption of hepatocyte nuclear factor 4alpha (HNF4alpha). HNF4alpha regulates ornithine transcarbamylase in vivo.* J Biol Chem, 2002. **277**(28): p. 25257-65.
24. Lin, J., et al., *Comparative analysis of phase I and II enzyme activities in 5 hepatic cell lines identifies Huh-7 and HCC-T cells with the highest potential to study drug metabolism.* Arch Toxicol, 2012. **86**(1): p. 87-95.
25. Miners, J.O. and D.J. Birkett, *Cytochrome P4502C9: an enzyme of major importance in human drug metabolism.* Br J Clin Pharmacol, 1998. **45**(6): p. 525-38.
26. Zuber, R., E. Anzenbacherová, and P. Anzenbacher, *Cytochromes P450 and experimental models of drug metabolism.* Journal of Cellular and Mollecular Medicine, 2007. **6**(2): p. 189-198.
27. McCarver, D.G. and R.N. Hines, *The Ontogeny of Human Drug-Metabolizing Enzymes: Phase II Conjugation Enzymes and Regulatory Mechanisms.* THE JOURNAL OF PHARMACOLOGY AND EXPERIMENTAL THERAPEUTICS, 2001. **300**(2): p. 361-366.
28. Glavinas, H., et al., *The role of ABC transporters in drug resistance, metabolism and toxicity.* Curr Drug Deliv, 2004. **1**(1): p. 27-42.
29. Hirano, M., et al., *Bile Salt Export Pump (BSEP/ABCB11) can transport a nonbile acid substrate, Pravastatin.* The journal of Pharmacology and Experimental Therapeutics, 2005. **314**: p. 876-882.
30. Hewitt, N.J., et al., *Primary hepatocytes: current understanding of the regulation of metabolic enzymes and transporter proteins, and pharmaceutical practice for the use of hepatocytes in metabolism, enzyme induction, transporter, clearance, and hepatotoxicity studies.* Drug Metab Rev, 2007. **39**(1): p. 159-234.
31. LeCluyse, E.L., P.L. Bullock, and A. Parkinson, *Strategies for restoration and maintenance of normal hepatic structure and function in long-term cultures of rat hepatocytes.* Adv Drug Deliv Rev, 1996. **22**(1-2): p. 133-186.
32. Godoy, P., et al., *Extracellular Matrix Modulates Sensitivity of Hepatocytes to Fibroblastoid Dedifferentiation and Transforming Growth Factor beta-induced Apoptosis.* Hepatology, 2009. **49**(6): p. 2031-2043.
33. Sanchez, A., et al., *Fibronectin regulates morphology, cell organization and gene expression of rat fetal hepatocytes in primary culture.* J Hepatol, 2000. **32**(2): p. 242-50.
34. Knobeloch, D., et al., *Human hepatocytes: isolation, culture, and quality procedures.* Methods Mol Biol, 2012. **806**: p. 99-120.
35. Diallo, A., et al., *Acute and Sub-chronic (28-day) Oral Toxicity Studies of Hydroalcohol Leaf Extract of Ageratum conyzoides L (Asteraceae).* Tropical Journal of Pharmaceutical Research, 2010. **9**(5): p. 463-467.
36. *Goodbye, flat biology?* Nature, 2003. **424**(6951): p. 861.
37. Godoy, P., et al., *Reversible manipulation of apoptosis sensitivity in cultured hepatocytes by matrix-mediated manipulation of signaling activities.* Methods Mol Biol, 2010. **640**: p. 139-55.
38. De Colli M, et al., *A biomimetic porous hydrogel of gelatin and glycosaminoglycans cross-linked with transglutaminase and its application in the culture of hepatocytes.* Biomedical Materials, 2012. **7**(5).
39. LeCluyse, E.L., *Human hepatocyte culture systems for the in vitro evaluation of cytochrome P450 expression and regulation.* European Journal of Pharmaceutical Sciences, 2001. **13**(4): p. 343-368.
40. Langer, R. and J.P. Vacanti, *Tissue Engineering.* Science, 1993. **260**: p. 920 - 926.
41. Stock, U.A. and J.P. Vacanti, *Tissue engineering: current state and prospects.* Annu Rev Med, 2001. **52**: p. 443-51.
42. Yang, S.F., et al., *The design of scaffolds for use in tissue engineering. Part 1. Traditional factors.* Tissue Engineering, 2001. **7**(6): p. 679-689.

43. Buenger, D., F. Topuz, and J. Groll, *Hydrogels in sensing applications.* Progress in Polymer Science, 2012. **37**(12): p. 1678-1719.
44. Lee, K.Y. and D.J. Mooney, *Hydrogels for tissue enginnering.* Chemical Reviews, 2001. **101**(7): p. 1869 - 1879.
45. Lee, J., M.J. Cuddihy, and N.A. Kotov, *Three-dimensional cell culture matrices: State of the art.* Tissue Engineering Part B-Reviews, 2008. **14**(1): p. 61-86.
46. Burkhardt, B., et al., *Long-term culture of primary hepatocytes – new matrices and microfluidic devices.* Hepatology International, 2013.
47. Bissell, D.M., et al., *Support of cultured hepatocytes by a laminin-rich gel. Evidence for a functionally significant subendothelial matrix in normal rat liver.* J Clin Invest, 1987. **79**(3): p. 801-12.
48. Tibbitt, M.W. and K.S. Anseth, *Hydrogels as Extracellular Matrix Mimics for 3D Cell Culture.* Biotechnology and Bioengineering, 2009. **103**(4): p. 655-663.
49. Moghe, P.V., et al., *Culture matrix configuration and composition in the maintenance of hepatocyte polarity and function.* Biomaterials, 1996. **17**(3): p. 373-385.
50. Sgroi, A., et al., *Transplantation of Encapsulated Hepatocytes During Acute Liver Failure Improves Survival Without Stimulating Native Liver Regeneration.* Cell Transplantation, 2011. **20**(11-12): p. 1791-1803.
51. Miranda, J.P., et al., *Extending hepatocyte functionality for drug-testing applications using high-viscosity alginate-encapsulated three-dimensional cultures in bioreactors.* Tissue Eng Part C Methods, 2010. **16**(6): p. 1223-32.
52. Glowacki, J. and S. Mizuno, *Collagen scaffolds for tissue engineering.* Biopolymers, 2007. **89**(5): p. 338 - 344.
53. Dunn, J.C.Y., R.G. Tompkins, and M.L. Yarmush, *Long-term in vitro function of adult hepatocytes in a collagen sandwich configuration.* Biotechnology Progress, 1991. **7**(3): p. 237 - 245.
54. LeCluyse, E.L., K.L. Audus, and J.H. Hochman, *Formation of extensive canalicular networks by rat hepatocytes cultured in collagen-sandwich configuration.* Am J Physiol, 1994. **266**(6 Pt 1): p. C1764-74.
55. Shen, C., et al., *Acetaminophen-induced hepatotoxicity of gel entrapped rat hepatocytes in hollow fibers.* Chemico-Biological Interactions, 2006. **162**(1): p. 53-61.
56. Meng, Q., et al., *Sensitivities of gel entrapped hepatocytes in hollow fibers to hepatotoxic drug.* Toxicology Letters, 2006. **166**(1): p. 19-26.
57. Jauregui, H.O., et al., *Attachment and long term survival of adult rat hepatocytes in primary monolayer cultures: comparison of different substrata and tissue culture media formulations.* In Vitro Cellular and Development Biology, 1986. **22**(1): p. 13 - 22.
58. Scott, J.E., *Proteoglycan-fibrillar collagen interactions.* Biochem J, 1988. **252**(2): p. 313-23.
59. Raub, C.B., et al., *Noninvasive assessment of collagen gel microstructure and mechanics using multiphoton microscopy.* Biophys J, 2007. **92**(6): p. 2212-22.
60. Underhill, G.H., et al., *Assessment of hepatocellular function within PEG hydrogels.* Biomaterials 2007. **28**: p. 256 - 270.
61. Tsang, V.L., et al., *Fabrication of 3D hepatic tissues by additive photopatterning of cellular hydrogels.* The FASEB Journal, 2007. **21**: p. 790 -801.
62. Lee, W., et al., *Hydrophobic nanoparticles improve permeability of cell-encapsulating poly(ethylene glycol) hydrogels while maintaining patternability.* Proc Natl Acad Sci U S A, 2010. **107**(48): p. 20709-14.
63. Kim, M., et al., *Heparin-based hydrogel as a matrix for encapsulation and cultivation of primary hepatocytes.* Biomaterials 2010. **31**: p. 3596 - 3603.
64. Lin, C.C. and K.S. Anseth, *PEG hydrogels for the controlled release of biomolecules in regenerative medicine.* Pharm Res, 2009. **26**(3): p. 631-43.

65. Genove, E., et al., *Functionalized self-assembling peptide hydrogel enhance maintenance of hepatocyte activity in vitro.* J Cell Mol Med, 2009. **13**(9B): p. 3387-97.
66. Wang, S., et al., *Three-dimensional primary hepatocyte culture in synthetic self-assembling peptide hydrogel.* Tissue Eng Part A, 2008. **14**(2): p. 227-36.
67. Dhandayuthapani, B., et al., *Polymeric Scaffolds in Tissue Engineering Application: A Review.* International Journal of Polymer Science, 2011.
68. Li, J.L., et al., *Culture of primary rat hepatocytes within porous chitosan scaffolds.* Journal of Biomedical Materials Research Part A, 2003. **67A**(3): p. 938-943.
69. Dvir-Ginzberg, M., et al., *Liver tissue engineering within alginate scaffolds: Effects of cell-seeding density on hepatocyte viability, morphology, and function.* Tissue Engineering, 2003. **9**(4): p. 757-766.
70. Li, K.G., et al., *Chitosan/gelatin composite microcarrier for hepatocyte culture.* Biotechnology Letters, 2004. **26**(11): p. 879-883.
71. Li, Y. and S.T. Yang, *Effects of three-dimensional scaffolds on cell organization and tissue development.* Biotechnology and Bioprocess Engineering, 2001. **6**: p. 311 - 325.
72. Saavedra, Y.G.L., et al., *Polyvinylalcohol threedimensional matrices for improved long-term dynamic cultureof hepatocytes.* Journal of Biomedical Materials Research Part A, 2002. **66**: p. 562 - 570.
73. Wang, T., et al., *Nanoporous fibers of type-I collagen coated poly(L-lactic acid) for enhancing primary hepatocyte growth and function.* Journal of Materials Chemistry B, 2013. **1**(3): p. 339-346.
74. Schutte, M., et al., *Rat Primary Hepatocytes Show Enhanced Performance and Sensitivity to Acetaminophen During Three-Dimensional Culture on a Polystyrene Scaffold Designed for Routine Use.* Assay and Drug Development Technologies, 2011. **9**(5): p. 475-486.
75. Godoy, P., et al., *Recent advances in 2d and 3D in vitro systems using primary hepatocytes, alternative hepatocyte sources and non-parenchymal liver cells and their use in investigating mechanisms of hepatotoxicity, cell signaling and ADME.* Archives of Toxicology, 2013. **87**: p. 1315 - 1530.
76. Mueller, D., et al., *In-depth physiological characterization of primary human hepatocytes in a 3D hollow-fiber bioreactor.* J Tissue Eng Regen Med, 2011. **5**(8): p. e207-18.
77. Vinci, B., et al., *Modular bioreactor for primary human hepatocyte culture: medium flow stimulates expression and activity of detoxification genes.* Biotechnol J, 2011. **6**(5): p. 554-64.
78. Sivaraman, A., et al., *A microscale in vitro physiological model of the liver: predictive screens for drug metabolism and enzyme induction.* Curr Drug Metab, 2005. **6**(6): p. 569-91.
79. Gottwald, E., et al., *Characterization of a chip-based bioreactor for three-dimensional cell cultivation via magnetic resonance imaging.* Zeitschrift für Medizinische Physik, 2013.
80. Schutte, J., et al., *"Artificial micro organs"--a microfluidic device for dielectrophoretic assembly of liver sinusoids.* Biomed Microdevices, 2011. **13**(3): p. 493-501.
81. Martin, I., D. Wendt, and M. Heberer, *The role of bioreactors in tissue engineering.* Trends Biotechnol, 2004. **22**(2): p. 80-6.
82. Griffith, L.G. and G. Naughton, *Tissue engineering--current challenges and expanding opportunities.* Science, 2002. **295**(5557): p. 1009-14.
83. Skett, P., *Problems in Using Isolated and Cultured-Hepatocytes for Xenobiotic Metabolism/Metabolism-Based Toxicity Testing--Solutions.* Toxicology in Vitro, 1994. **8**(3): p. 491-504.
84. Nussler, A.K., et al., *The Holy Grail of Hepatocyte Culturing and Therapeutic Use*, in *Strategies in Regenerative Medicine*, S. M., Editor 2009, Springer New York. p. 1 - 38.

85. Strom, S.C., et al., *Large scale isolation and culture of human hepatocytes.* Ilots de Langerhans et hepatocytes, 2005: p. 195 - 205.
86. Lowry, O.H., et al., *Protein measurement with the Folin phenol reagent.* J Biol Chem, 1951. **193**(1): p. 265-75.
87. Nussler, A.K., et al., *Hepatocyte Inducible Nitric-Oxide Synthesis Is Influenced in-Vitro by Cell-Density.* American Journal of Physiology, 1994. **267**(2): p. C394-C401.
88. Rajan, N., et al., *Preparation of ready-to-use, storable and reconstituted type I collagen from rat tail tendon for tissue engineering applications.* Nat Protoc, 2006. **1**(6): p. 2753-8.
89. Hinson, J.A., D.W. Roberts, and L.P. James, *Mechanisms of acetaminophen-induced liver necrosis.* Handb Exp Pharmacol, 2010(196): p. 369-405.
90. Bratosin, D., et al., *Novel fluorescence assay using calcein-AM for the determination of human erythrocyte viability and aging.* Cytometry Part A, 2005. **66A**(1): p. 78-84.
91. Lund, K.C., L.L. Peterson, and K.B. Wallace, *Absence of a universal mechanism of mitochondrial toxicity by nucleoside analogs.* Antimicrob Agents Chemother, 2007. **51**(7): p. 2531-9.
92. Choksakulnimitr, S., et al., *In-Vitro Cytotoxicity of Macromolecules in Different Cell-Culture Systems.* Journal of Controlled Release, 1995. **34**(3): p. 233-241.
93. Whitehead, M.W., et al., *A prospective study of the causes of notably raised aspartate aminotransferase of liver origin.* Gut, 1999. **45**(1): p. 129-133.
94. Schindhelm, R.K., et al., *Alanine aminotransferase as a marker of non-alcoholic fatty liver disease in relation to type 2 diabetes mellitus and cardiovascular disease.* Diabetes-Metabolism Research and Reviews, 2006. **22**(6): p. 437-443.
95. Rychlik, W., W.J. Spencer, and R.E. Rhoads, *Optimization of the annealing temperature for DNA amplification in vitro.* Nucleic Acids Res, 1990. **18**(21): p. 6409-12.
96. Laupeze, B., et al., *Multidrug resistance protein (MRP) activity in normal mature leukocytes and CD34-positive hematopoietic cells from peripheral blood.* Life Sci, 2001. **68**(11): p. 1323-31.
97. Nakayama, G.R., et al., *Assessment of the Alamar Blue assay for cellular growth and viability in vitro.* J Immunol Methods, 1997. **204**(2): p. 205-8.
98. Nociari, M.M., et al., *A novel one-step, highly sensitive fluorometric assay to evaluate cell-mediated cytotoxicity.* J Immunol Methods, 1998. **213**(2): p. 157-67.
99. McMillian, M.K., et al., *An improved resazurin-based cytotoxicity assay for hepatic cells.* Cell Biol Toxicol, 2002. **18**(3): p. 157-73.
100. Guidotti, G., J.P. Colombo, and P.P. Foa, *Enzymatic determination of glucose. Stabilization of color developed by oxidation of o-Dianisidine.* Analytical Chemistry, 1961. **33**(1): p. 151 - 153.
101. Jung, D., et al., *New Colorimetric reaction for end-point, continuous-flow, and kinetic measurement of urea.* Clin Chem, 1975. **21**(8): p. 1136-40.
102. Zawada, R.J., et al., *Quantitative determination of urea concentrations in cell culture medium.* Biochem Cell Biol, 2009. **87**(3): p. 541-4.
103. Donato, M.T., et al., *Fluorescence-based assays for screening nine cytochrome P450 (P450) activities in intact cells expressing individual human P450 enzymes.* Drug Metabolism and Disposition, 2004. **32**(7): p. 699 - 706.
104. Ehnert, S., et al., *Blood monocyte-derived NeoHepatocytes as in vitro test system for drug metabolism.* Drug Metabolism and Disposition, 2008. **36**: p. 708 - 718.
105. Schyschka, L., et al., *Hepatic 3D cultures but not 2D cultures preserve specific transporter activity for acetaminophen-induced hepatotoxicity.* Archives in Toxicology, 2013. **87**: p. 1581 - 1593.
106. Li, F.C., et al., *In vivo dynamic metabolic imaging of obstructive cholestasis in mice.* American Journal of Physiology Gastrointestinal and Liver Physiology, 2009. **296**(5): p. G1091-G1097.

107. Madsen, K.G., et al., *Development and Evaluation of an Electrochemical Method for Studying Reactive Phase-I Metabolites: Correlation to in Vitro Drug Metabolism.* Chemical Research in Toxicology, 2007. **20**(5): p. 821-831.
108. Mohutsky, M.A., et al., *Hepatic drug-metabolizing enzyme induction and implications for preclinical and clinical risk assessment.* Toxicol Pathol, 2010. **38**(5): p. 799-809.
109. Guillouzo, A., et al., *Use of Human Hepatocyte Cultures for Drug-Metabolism Studies.* Toxicology, 1993. **82**(1-3): p. 209-219.
110. Schuppan, D., et al., *Matrix as a modulator of hepatic fibrogenesis.* Seminar in Liver Diseases, 2001. **21**(3): p. 351-372.
111. Weiss, T.S., et al., *Collagen sandwich culture affects intracellular polyamine levels of human hepatocytes.* Cell Prolif, 2002. **35**(5): p. 257-67.
112. Kern, A., et al., *Drug metabolism in hepatocyte sandwich cultures of rats and humans.* Biochem Pharmacol, 1997. **54**(7): p. 761-72.
113. Eipel, C., K. Abshagen, and B. Vollmar, *Regulation of hepatic blood flow: the hepatic arterial buffer response revisited.* World J Gastroenterol, 2010. **16**(48): p. 6046-57.
114. Wilkenin, S. and A. Basder, *Influence of culture time on the expression of drug-metabolizing enzymes in primary human hepatocytes and hepatoma cell line HepG2*Journal of Biochemical and Molecular Toxicology, 2003. **17**: p. 207–213.
115. Hengstler, J.G., et al., *Generation of human hepatocytes by stem cell technology: definition of the hepatocyte.* Expert Opin Drug Metab Toxicol, 2005. **1**(1): p. 61-74.
116. Ruhnke, M., et al., *Human monocyte-derived neohepatocytes: a promising alternative to primary human hepatocytes for autologous cell therapy.* Transplantation, 2005. **79**(9): p. 1097-103.
117. Ruhnke, M., et al., *Differentiation of in vitro-modified human peripheral blood monocytes into hepatocyte-like and pancreatic islet-like cells.* Gastroenterology, 2005. **128**: p. 1774 - 1786.
118. Nussler, A.K., et al., *Present status and perspectives of cell-based therapies for liver diseases.* Journal of Hepatology, 2006. **45**(1): p. 144 -159.
119. Zemel, R., et al., *Expression of liver-specific markers in naive adipose-derived mesenchymal stem cells.* Liver Int, 2009. **29**(9): p. 1326-37.
120. Seeliger, C., et al., *Decrease of Global Methylation Improves Significantly Hepatic Differentiation of Ad-MSCs: Possible Future Application for Urea Detoxification.* Cell Transplantation, 2013. **22**(1): p. 119-131.
121. Eddington, D.T. and D.J. Beebe, *Flow control with hydrogels.* Adv Drug Deliv Rev, 2004. **56**(2): p. 199-210.
122. Mickel, W., et al., *Robust pore size analysis of filamentous networks from three-dimensional confocal microscopy.* Biophys J, 2008. **95**(12): p. 6072-80.
123. Godoy, P., et al., *Recent advances in 2D and 3D in vitro systems using primary hepatocytes, alternative hepatocyte sources and non-parenchymal liver cells and their use in investigating mechanisms of hepatotoxicity, cell signaling and ADME.* Arch Toxicol, 2013. **87**(8): p. 1315-530.
124. Prot, J.M., et al., *Integrated Proteomic and Transcriptomic Investigation of the Acetaminophen Toxicity in Liver Microfluidic Biochip.* Plos One, 2011. **6**(8).
125. Bruschi, S.A., *Methods and Aproaches to Study Metabolism and Toxicity of Acetaminophen. In: Drug Metabolism and Transport*, 2004: Totowa, NJ. p. 197-232.
126. Yamaura, K., et al., *Protective effects of goldenseal (Hydrastis canadensis L.) on acetaminophen-induced hepatotoxicity through inhibition of CYP2E1 in rats.* Pharmacognosy Res, 2011. **3**(4): p. 250-5.
127. Li, J., et al., *Molecular dynamics simulations of CYP2E1.* Med Chem, 2012. **8**(2): p. 208-21.
128. Zaher, H., et al., *Protection against acetaminophen toxicity in CYP1A2 and CYP2E1 double-null mice.* Toxicol Appl Pharmacol, 1998. **152**(1): p. 193-9.

129. Fontana, R.J., *Acute liver failure including acetaminophen overdose.* Med Clin North Am, 2008. **92**(4): p. 761-94, viii.
130. Ramachandran, A., et al., *The impact of partial manganese superoxide dismutase (SOD2)-deficiency on mitochondrial oxidant stress, DNA fragmentation and liver injury during acetaminophen hepatotoxicity.* Toxicol Appl Pharmacol, 2011. **251**(3): p. 226-33.
131. Agarwal, R., et al., *Acetaminophen-induced hepatotoxicity in mice occurs with inhibition of activity and nitration of mitochondrial manganese superoxide dismutase.* J Pharmacol Exp Ther, 2011. **337**(1): p. 110-6.
132. Aleksunes, L.M., et al., *Influence of acetaminophen vehicle on regulation of transporter gene expression during hepatotoxicity.* J Toxicol Environ Health A, 2007. **70**(21): p. 1870-2.
133. Leslie, E.M., R.G. Deeley, and S.P. Cole, *Toxicological relevance of the multidrug resistance protein 1, MRP1 (ABCC1) and related transporters.* Toxicology, 2001. **167**(1): p. 3-23.
134. Jemmitz, K., Z. Veres, and L. Vereczkey, *Contribution of high basolateral bile salt efflux to the lack of hepatotoxicity in rat in response to drugs inducing cholestasis in human.* Toxicologcal Sciences, 2010. **115**(1): p. 80-88.
135. Rost, D., J. Kartenbeck, and D. Keppler, *Changes in the localization of the rat canalicular conjugate export pump Mrp2 in phalloidin-induced cholestasis.* Hepatology, 1999. **29**(3): p. 814-821.
136. Roelofsen, H., et al., *Glutathione S-conjugate transport in hepatocytes entering the cell cycle is preserved by a switch in expression from the apical MRP2 to the basolateral MRP1 transporting protein.* J Cell Sci, 1999. **112 (Pt 9)**: p. 1395-404.
137. Kullak-Ublick, G.A., et al., *Hepatic transport of bile salts.* Semin Liver Dis, 2000. **20**(3): p. 273-92.
138. van Zijl, F. and W. Mikulits, *Hepatospheres: Three dimensional cell cultures resemble physiological conditions of the liver.* World J Hepatol, 2010. **2**(1): p. 1-7.
139. Toh, Y.C., et al., *A configurable three-dimensional microenvironment in a microfluidic channel for primary hepatocyte culture.* Assay Drug Dev Technol, 2005. **3**(2): p. 169-76.
140. Wang, Y.J., et al., *Primary hepatocyte culture in collagen gel mixture and collagen sandwich.* World J Gastroenterol, 2004. **10**(5): p. 699-702.
141. Lazar, A., et al., *Extended liver-specific functions of porcine hepatocyte spheroids entrapped in collagen gel.* In Vitro Cellular and Development biology, 1994. **31**: p. 340-346.
142. Beken, S., et al., *Cell morphology, albumin secretion and glutathione S-Transferase expression in collagen gel sandwich and immobilization cultures of rat hepatocytes.* Toxicology in Vitro, 1997. **11**(5): p. 409-16.
143. Schwanhausser, B., et al., *Global quantification of mammalian gene expression control.* Nature, 2011. **473**(7347): p. 337-42.
144. Greenbaum, D., et al., *Comparing protein abundance and mRNA expression levels on a genomic scale.* Genome Biology, 2003. **4**: p. 117.1-117.8.
145. Stresser, D.M., et al., *Cytochrome P450 fluorometric substrates: identification of isoform-selective probes for rat CYP2D2 and human 3A4.* Drug Metabolism and Disposition, 2002. **30**(7): p. 845-852.
146. Bort, R., et al., *Diclofenac Toxicity to Hepatocytes: A Role for Drug Metabolism in Cell Toxicity.* The Journal of Pharmacology and Experimental Therapeutics, 1998. **288**(1): p. 65-72.
147. Eschbach, E., et al., *Microstructured scaffolds for liver tissue cultures of high cell density: Morphological and biochemical characterization of tissue aggregates.* Journal of Cellular Biochemistry, 2005. **95**(2): p. 243-255.
148. Kane, B.J., et al., *Liver-specific functional studies in a microfluidic array of primary mammalian hepatocytes.* Analytical Chemistry, 2006. **78**(13): p. 4291-4298.

149. Malda, J., T.J. Klein, and Z. Upton, *The roles of hypoxia in the in vitro engineering of tissues.* Tissue Engineering, 2007. **13**(9): p. 2153-62.

7. Zusammenfassung

In traditionellen Toxizitätstests werden *in vitro* und *in vivo* Versuchstiere verwendet. Auf diese Weise sollen mögliche Schäden am Menschen verhindert werden. Die Verwendung von Versuchstieren zur Medikamentenprüfung wirft jedoch ethische Fragen auf und ist darüber hinaus mit hohen Kosten und einem Mangel an Reliabilität verbunden. Die Verwendung primärer Hepatozyten stellt zwar eine mögliche Alternative zu Tierversuchen dar, sieht sich allerdings mit zwei zentralen Problemen konfrontiert: der begrenzten Verfügbarkeit von Lebergewebe sowie der kurzen Lebensdauer dieser Zellen. Daher wurden Hepatom-Zelllinien und von hepatozytenähnlichen Zellen aus extrahepatischen Zellquellen in Toxizitäts-Assays als mögliche Alternativen untersucht. Jedoch ist ihre Verwendung in der Medikamentenprüfung aufgrund ihrer niedrigen Expression hepatozytärer Marker und ihrer niedrigen Metabolisierungskapazität eingeschränkt. Die Polarisierung spielt eine Schlüsselrolle beim Medikamentenstoffwechsel. Deshalb wurde die Hepatotoxizität in 2D und 3D (Sandwich)-Kulturen untersucht, wobei Acetaminophen als Modellsubstanz verwendet wurde. Unsere Daten zeigten, dass nach der Behandlung mit Acetaminophen in 3D-Kulturen mehr Zellen sterben als in 2D-Kulturen, da der Metabolismus von Acetaminophen höher ist und sich deshalb eine höhere Konzentration von toxischen Metaboliten (NAPQI) bildet. Darüber hinaus wurde festgestellt, dass die Proteinexpression von CYP2E1 und SOD1 von der Acetaminophen-Konzentration abhängig ist. Daher führte eine Erhöhung der Acetaminophen-Konzentration in 3D-Kulturen zu einer gleichzeitigen Erhöhung der Expression von CYP2E1 sowie zu einer Verringerung der Expression von SOD1, was jedoch in den 2D-Kulturen nicht der Fall war. Darüber hinaus wurden für das multidrug resistance-associated protein-1 (MRP1), ein spezifisches Transporterprotein für den Transport von Acetaminophen-Metaboliten, in 3D-Kulturen, höhere Import/Export-Raten festgestellt. Schließlich waren die Resultate, die in den 3D-Kulturen erzielt wurden, besser mit den Resultaten der *in vivo*-Situation vergleichbar.

Allerdings schränken die begrenzte Verfügbarkeit von Lebergewebe sowie die Tatsache, dass in kleine Kulturplatten keine Sandwich-Kulturen verwendet

werden können, den Einsatz von Sandwich-Kulturen für Hochdurchsatz-Screenings ein. Daher wurden die primären humanen Hepatozyten in Kollagen-Gels resuspendiert. Dabei blieben die Zellviabilität, die Glukoseproduktion und die NH_4-Entgiftung über 28 Tage hinweg in größerem Maße erhalten als in 2D-Kulturen. Die Messung der metabolischen Phase I- und Phase II-Aktivität zeigte ähnliche Ergebnisse. Außerdem verfügten die primären humanen Hepatozyten über höhere Import/Export-Raten der beiden Transporterproteine MRP1 und multidrug resistance protein-1 (MDR1/P-gp), die sich an der basolateralen beziehungsweise der apikalen Membran befinden. Schließlich wiesen primäre humane Hepatozyten nach ihrer Stimulation mit Acetaminophen und Diclofenac in 3D-Kulturen eine höhere Toxizität auf.

Die Durchflusskultur primärer humaner Hepatozyten zeigte eine Verbesserung der Entgiftungsaktivität. Mikrofluidische Systeme sind jedoch teure Testsysteme, deren Einsatz zur Vorhersage von Hepatoxizität nur eingeschränkt möglich ist. Daher wurde hier ein einfaches und günstiges mikrofluidisches System getestet. Die Daten der Lebend-tot-Färbung zeigten das Überleben der primären humanen Hepatozyten im mikrofluidischen System an. Der Stoffwechsel von Acetaminophen und Diclofenac, der in statischen Kulturen und in Flusskulturen mit der Aktivität von CYP2E1 beziehungsweise von CYP2C9 übereinstimmt, führte zu ähnlichen Ergebnissen. Diese Resultate konnten jedoch nicht durch Fluroeszenz- oder Absorptionsassays mit Hilfe eines Plattenreaders bestätigt werden. Zur Verbesserung der Charakterisierung primärer humaner Hepatozyten im µ-Slide-System müssen daher neben alternativen Experimenten und der Verbesserung bereits bestehender Methoden neue Herangehensweisen entwickelt werden.

In dieser Arbeit wurde das Verhalten primärer humaner Hepatozyten auf natürlichen Kollagen-Gels unter unterschiedlichen Kulturbedingungen untersucht. Die extrazelluläre Matrix (EZM) der Leber besteht nicht ausschließlich aus Kollagen. sondern enthält außerdem Proteine und Proteoglykane. Außerdem sind nicht-parenchymaler Zellen an der Entzündungsantwort beteiligt. Daher sollten sich zukünftige Studien auf Hepatotoxizitätstests in Ko-Kulturen von primären humanen Hepatozyten und nicht-parenchymaler Zellen in mikrofluidischen Systemen mit einer Matrix

welche verschiedene Komponenten der Lebermatrix enthält durchgeführt werden. Somit könnten *in vitro* Ergebnisse erzielt werden, die mit der Situation *in vivo* in hohem Maße vergleichbar sind.

8. List of Publications

- *****Schyschka, L., ***Martínez Sánchez, J.J.**, Wang, Z., Burkhardt, B., Müller-Vieira, U., Zeilinger, K., Bachmann, A., Nadalin, S., *****Damm, G., *****Nüssler, A.K. Hepatic 3D cultures but not 2D cultures preserve specific transporter activity for acetaminophen-induced hepatotoxicity. Archives of Toxicology, 2013. **87**: p. 1581-1593. **IF: 4.674: *Equal contribution**

- Ehnert, S., Freude, T., Eicher, C., Burkhardt, B., **Martínez Sánchez, J.J.**, Neumann, J., Mühl-Benninghaus, R., Dooley, S., Pscherer, S., Nüssler, A.K. Darbepoetin inhibits proliferation of hepatic cancer cells in the presence of TGF-β. Archives of Toxicology, 2013. **88** (1): p. 89-96. **IF: 4.674**

- Ehnert, S. Lukoschek, T. Bachmann, A., **Martínez Sánchez, J.J.**, Damm, G., Nüssler, N.C., Pscherer, S., Stöckle, U., Dooley, S., Mueller, S., Nüssler, A.K. The right choice of antihypertensives protects primary human hepatocytes from the ethanol- and recombinant human TGF-β_1 –induced cellular damage. Hepatic Medicine: Evidence and Research, 2013. **5**: p. 1-11.

- *****Burkhardt, B., ***Martínez Sánchez, J.J.**, Bachmann, A., Ladurner, R., Nüssler, A.K. Matrices and microfluidic devices used for long-term culture of primary hepatocytes. Hepatology International, 2013. **IF: 2.645: *Equal contribution**

Deaclaration

Parts of the dissertation are published in two papers. Some figures (cited in the dissertation as taken from these publications) were elaborated with Co-Authors. In the following, my contribution to the presented data is declared:

Article: “Hepatic 3D cultures but not 2D cultures preserve specific transporter activity for acetaminophen-induced hepatotoxicity” (Reference 105)

The design of the study was carried out by **me** and Prof. Dr. Andreas K. Nüssler.

The experiments were performed by Dr. Lilianna Schyschka, Dr. Ursula Müller-Vieira and **me** with the supervision of Prof. Dr. Andreas K. Nüssler. Cell morphology studies (fig. 3.1), Live/Dead staining (fig.3.2), and protein expression of CYP2E1 and SOD1 (fig. 3.4 C, D, G and H) were performed **equally** by Dr. Lilianna Schyschka and **me**. Metabolism of acetaminophen (fig. 3.7) was performed by Dr. Ursula Müller-Vieira. LDH, AST and ALT (fig. 3.3), gene expression of CYP2E1 and SOD1 (fig. 3.4 A, B, E and F), gene expression of different MRPs (fig. 3.5), and MRP1 transport activity were **exclusively performed by me**.

Statistical analysis was performed **equally** by Dr. Lilianna Schyschka and **me**.

Article: “Long-term culture of primary hepatocytes – new matrices and microfluidic devices” (Reference 46)

The design of the study was carried out by **me** and Prof. Dr. Andreas K. Nüssler.

The experiments were performed by me with the supervision of Dr. Britta Burkhardt and Prof. Dr. Andreas K. Nüssler. Resazurin conversion (fig. 3.12), glucose production (fig. 3.13) and ammonia detoxification (fig. 3.14) were performed **exclusively by me**.

Statistical analysis was performed by **me** with the supervision of Dr. Britta Burkhardt.

I declare that I have written the manuscript under the guidance of Prof. Dr. Andreas K. Nüssler and no more than the specified sources I have used.

Tübingen, 18th December 2014

Juan José Martínez Sánchez

Acknowledgements

Special thanks go to Prof. Dr. med. Ulrich Stöckle for his willingness accepting me as a doctoral student his department. Furthermore, I like to thank my supervisor, Prof. rer. nat. Dr. Andreas K. Nüssler, for giving me the opportunity to complete my PhD thesis within his team at the Siegfried Weller Institute and for his guidance throughout the years. His constructive criticism as well as his encouragement and his motivating words were an important support for me.

Sincere thanks also go to Dr. Anastasia Bachmann for her input during the flow experiments and her assistance over the last two years. Our discussions have always been very interesting and productive.

A warm thank you to Dr. Sabrina Ehnert for her great help in the beginning of my project and also for her constant and optimistic advice throughout the years.

I would also like to thank Dr. Britta Burkhardt who assisted me with the matrices and the microfluidic system and inspired me with her positive attitude.

Particular thanks are also due to Dr. Lila Schyschka, who introduced me to the isolation and culture of hepatocytes in the MRI laboratory in Munich and who has always been willing to advice and support me.

I like to thank Prof. Königsrainer and his team (EKUT, Department of General, Visceral and Transplantation Surgery) to support my research by suppling the necessary material.

Cordial thanks go to Dr. Georg Damm for his honest criticism and friendly words as well as for the supply of hepatocytes.

A warm thank you also goes to Dr. Luc Koster for his unconditional and existential help in all matters concerning language and bureaucracy.

I would also like to thank the whole team of the Siegfried Weller Institute and of the laboratory in Munich who were always available for discussions and advice and who supported me with their strong collegiality.

Finally, I would like to thank my family for its unconditional support encouragement, and love over the last years.